2016

Evaluation of Concavity Compression Mechanism as a Possible Predictor of Shoulder Muscle Fatigue

Suman Kanti Chowdhury

Evaluation of Concavity Compression Mechanism as a Possible Predictor of Shoulder Muscle Fatigue

Suman Kanti Chowdhury

Dissertation submitted to the
Benjamin M. Statler College of Engineering and Mineral Resources at
West Virginia University

in partial fulfillment of the requirements for the degree of

Doctor of Philosophy
in
Industrial Engineering

Ashish D. Nimbarte, Ph.D., Chair
Bhaskaran Gopalakrishnan, Ph.D.
Hongwei Hsiao, Ph.D.
Majid Jaridi, Ph.D.
Xiaopeng Ning, Ph.D.

Department of Industrial and Management Systems Engineering

Morgantown, West Virginia
2016

Keywords: Musculoskeletal disorders, concavity compression mechanism, stability, muscle fatigue, shoulder joint

ABSTRACT

Evaluation of Concavity Compression Mechanism as a Possible Predictor of Shoulder Muscle Fatigue

Suman Kanti Chowdhury

The overall impact of shoulder musculoskeletal disorders (MSDs) in the workplace is enormous in terms of worker's health, and corporate economics. To recognize the risk factors for shoulder MSDs, previous studies have used questionnaires, clinical examinations, direct measurements, observational, and modeling methods. While most of the existing studies substantiate that the shoulder strain (e.g. pain/discomfort, muscle force or activity, joint loading, etc.) is affected by the stress (e.g. force, posture, repetition), the underlying mechanism that explains how the shoulder joint is strained when subjected to different levels of stress is not well understood. In this study, concavity compression, a stabilizing mechanism of the shoulder joint was evaluated as a possible underlying mechanism that can explain the stress-strain relationship for the shoulder joint during dynamic physical exertions. The study was completed in three steps.

In the first step, a shoulder strain index based on the concept of concavity compression mechanism was developed. Eight male participants performed thirty different material handling tasks in various work positions using a weight of 2 lb. A biomechanical model of the shoulder complex was used to estimate the resultant reaction forces acting on the right shoulder joint during these tasks. Based on the concept of concavity compression, the reaction forces were used to formulate the strain index. Higher value of the strain index signified higher stabilizing demand and therefore higher shoulder strain. Based on the strain index values, the tasks were categorized into low, medium and high strain tasks.

In the second step, a global muscle fatigue index that considers the anatomical characterization of the muscles and their physiological and biomechanical contributions during a physical exertion was developed. Eight participants performed fatiguing exertions under static and dynamic conditions using two different weights of 2 lb and 6 lb. The activity of eight shoulder muscles – supraspinatous, infraspinatous, teres major, middle deltoid, anterior deltoid, posterior deltoid, biceps, and triceps of the right shoulder joint were recorded using surface electromyography (SEMG). Muscle fatigue was evaluated by measuring percent change in global fatigue index between first and last repetitions. Results indicated that the global fatigue index was sensitive to the fatigue related neuromuscular changes and was able to accurately predict the shoulder joint fatigue.

In the third step, the appropriateness of concavity compression mechanism in estimating shoulder strain was evaluated by testing a central hypothesis: "tasks that put higher stabilizing demand on the shoulder muscles (estimated using strain index) would result in higher fatigue (estimated using fatigue index)". Ten male participants performed repetitive exertions using the previously identified high, medium, and low strain tasks using three different weight conditions (2, 4, and 6 lb). The SEMG data were recorded from the above-mentioned shoulder muscles. The global muscle fatigue index was calculated for the first and last three repetitive exertions of each task to estimate development of fatigue. A two-factor randomized complete block design was used to test the relationship between the strain index and global fatigue index. Results showed that tasks having higher strain index values and force levels resulted in significantly ($P<0.001$) higher percent change in global fatigue index. The highest percent

change in the global fatigue index and the highest perceived exertion score was observed for the high strain task performed at 6 lb weight condition. Similarly, the lowest percent change in the GFI value and the lowest perceived exertion score was observed for the low strain task performed at 2 lb weight condition.

Thus, the overall results of this study seem to indicate that the concavity compression mechanism can explain the stress-strain relationship for the shoulder joint during dynamic physical exertions. A shoulder strain index based on the concept of concavity compression mechanism can predict the stabilizing demand and thus the shoulder muscle fatigue during dynamic physical exertions. The strain index developed in this study could potentially have applications in the workplaces to identify the stressful exertions that may increase the risk of shoulder MSDs.

ACKNOWLEDGEMENTS

First off all, I would like to greatly acknowledge and thank my advisor and mentor, Dr. Ashish Nimbarte for his guidance and support throughout the years. He has been an invaluable resource during my time here at WVU. He kept me on track to reaching my goals better than I could have ever kept myself, and for that, I am grateful and thankful. I anticipate that we will always keep in touch as I value his opinion, respect his knowledge, and regard him as a mentor.

I would also like to express my profound gratitude to my advisory committee: Dr. Majid Jaridi, Dr. Xiaopeng Ning, Dr. Bhaskaran Gopalakrishnan and Dr. Hongwei Hsiao for their valuable feedback, comments and input throughout this process. I would also like to thank my colleagues in the Ergonomics Laboratory for their assistance in the experimental set up and data collection.

I want to express my gratitude to my beloved wife who supported me endlessly and stood beside me all the ways. My sincerest gratitude to my elder sister, my brother-in-law, and my mother-in-law, all who have always helped me along the way.

Finally, I would like to thank my parents, and all my mentors throughout my life for their constant supports and blessings.

DEDICATIONS

I would like to dedicate this dissertation to my parents for their unconditional love, support and encouragement. I appreciate their sacrifices and I would not have been able to get to this stage without them.

This dissertation is also dedicated to my wife. It has been a long trip, but never once did you give up on me. With the good, comes the bad. You have always believed in me when I did not believe in myself.

I would also like to dedicate my dissertation to my elder sister and her husband. For their inspiration, dedication and dream, I would be able to come to this stage.

Finally, this dissertation is dedicated to all those who believe in the richness of learning and the virtue of hard work.

TABLE OF CONTENTS

LIST OF FIGURES

LIST OF TABLES

CHAPTER ONE: INTRODUCTION

1.1 Background

According to the Bureau of Labor Statistics (BLS), work related MSDs accounted for 32 percent of all occupational injury and illness cases in 2014 (BLS, 2015b). The incidence rate of MSDs was 33.8 per 10,000 full time workers, with 13 median lost workdays in 2014 (BLS, 2015b). Among all work related MSDs, the shoulder MSDs were the most severe type requiring 26 median days to recover before returning to work (BLS, 2015b). In addition to lost workdays, shoulders MSDs also generate expensive medical costs. For compensation claims data spanning from 2002 to 2010, the average direct cost of a shoulder MSD was $60,298 per claim in the state of Washington (Naomi, Darrin, David, Ninica, & Barbara, 2015). It was also reported that shoulder MSD claims have the second highest average costs behind only low back MSD claims. The shoulder MSDs also cause unobvious indirect costs such as reduced health, impaired task ability, and decreased productivity (Lötters, Meerding, & Burdorf, 2005; Östör, Richards, Prevost, Speed, & Hazleman, 2005).

A wide range of workplace factors such as forceful arm exertions, awkward arm postures, repetitive motions, and vibration are known to contribute to the risk of developing occupational MSDs (Gallagher & Heberger, 2013; Putz-Anderson et al., 1997; Wang, Dai, & Ning, 2015). Strong evidences between the shoulder MSDs and repetitive motions (Ohisson et al., 1995; Putz-Anderson et al., 1997), forceful arm exertions (Chiang et al., 1993; Stenlund, Goldie, Hagberg, & Hogstedt, 1993), and awkward arm postures (Sakakibara, Miyao, Kondo, & Yamada, 1995) have been reported in the literature. There were insufficient evidences between the shoulder MSDs and exposure to vibration (Stenlund et al., 1993).

Previous studies have used many methods for identifying shoulder MSDs risk factors. These methods are classified into a broad spectrum ranging from direct measurements, to questionnaire, and to observational methods. The use of questionnaires and interview techniques has the potential of studying cumulative exposure over time, which is an important parameter usually not available with other methods (Kilbom, 1994). Due to the subjectivity, these methods have low reliability (Wiktorin, Karlqvist, & Winkel, 1993). Many epidemiological studies have used observational methods such as Ovako working posture analyzing system (OWAS) (Karhu, Kansi, & Kuorinka, 1977), rapid upper limb assessment (RULA) (Lynn McAtamney & Corlett, 1993), hand-arm-movement analysis (HAMA) (Christmansson, 1994), rapid entire body assessment (REBA) (L McAtamney & Hignett, 1995), and quick exposure check (QEC) (Li & Buckle, 1998) systems for workplace risk assessment. Most of these observational methods mainly contemplate on the duration or frequency of certain postures. All these methods have drawbacks and they have been used to a limited extent in the industrial populations. According to Burdorf et al. (1992), the observational methods lack precision and are less reproducible in dynamic work situations. They are also subject to intra – and inter – observer variability.

On contrary, direct measurements such as electromyography and postural recordings are quantitative and more reliable. The electromyography has been widely used to measure muscle physiological activity, whereas the postural recordings using optical motion capture, goniometric, and accelerometric devices have been commonly used to trace the movements and working postures. They have been mostly used in a laboratory, but occasionally in a real setting since they require extensive technical supports (e.g. markers or sensors are placed on appropriate landmarks of human body) (Wang et al., 2015). Moreover, equipment used in direct measurements are expensive. Direct measurement methods can also be intrusive and may affect workers' natural work style due to sensors mounting on their body for data collection.

Many previous studies have used both electromyography and postural recordings to evaluate the risk factors of shoulder MSDs (Anton et al., 2001; Cutlip, 2014; Dubowsky, Rasmussen, Sisto, & Langrana, 2008; Ebaugh, McClure, & Karduna, 2006; Luger, Bosch, Hoozemans, Veeger, & de Looze, 2016; Moon et al., 2013; Nimbarte, Sun, Jaridi, & Hsiao, 2013; Rashedi & Nussbaum, 2016). In these studies, the concepts of muscle fatigue and shoulder posture were used to identify the MSD risk factors. In majority of these studies, simple stress-strain relationship were used to identify the MSD risk factors. Stress is due to the work-related factors such as force, posture, repetition and strain is the resulting response of the shoulder complex (pain/discomfort, muscle force or activity, joint loading, etc.). For example, awkward postures characterized by non-neutral postures and high moment arms, is one of the risk factors. The main shoulder joint, glenohumeral joint, has a range of motion covering nearly 65% of a sphere (Engin & Chen, 1986). The three rotational degrees of freedom of the glenohumeral joint with the ability to exert forces of varying magnitude in nearly any direction provides infinite functional degrees of freedom to this joint. The workers can adopt multitude of working postures and one awkward posture may be more strenuous than another awkward posture. Thus, performing ergonomic risk assessment using traditional stress-strain analysis would be challenging as evaluation of each and every postures, which is not feasible, may be necessary for the comprehensive understanding risk of the shoulder MSDs.

A better and more feasible and efficient alternative is to research an underlying physiological mechanism that relates stress with strain. To our knowledge, no such mechanism has been studied or proposed in the literature. We proposed that concavity compression, a shoulder stabilizing mechanism, might provide a physiological basis to understand relationship between stress and strain during dynamic physical exertions. The shoulder muscles work concurrently during shoulder movements and exertions and the concavity compression mechanism explains how the forces generated by the muscles stabilize the

shoulder joint. Our central hypothesis is that the tasks that put higher stabilizing demand on the shoulder muscles would result in higher strain. Three specific aims were used to test this hypothesis.

1.2 Specific Aims

Specific Aim # 1: Task classification based on the muscular effort required to achieve concavity compression: Human participants performed material handling tasks in various work positions. A biomechanical model of the shoulder complex was used to estimate the resultant reaction forces acting on the shoulder joint during these tasks. Based on the concept of concavity compression mechanism, the reaction forces were used to formulate a strain index. The tasks were classified into high, medium and low strain tasks based on the strain index values.

Specific Aim # 2: Formulation of a global fatigue index: To estimate the true physiological strain on the shoulder joint during the material handling tasks, a global fatigue index was developed using the surface electromyography (SEMG) data. The global fatigue index considered level of muscle activation, frequency shift, anatomical characterization of individual muscle, and coactivation between the agonist and antagonistic muscle groups.

Specific Aim # 3: Evaluation of relationship between strain index (Aim # 1) and global fatigue index (Aim # 2): A two-factor randomized complete block design was used to test the relationship between the strain index and global fatigue index. Human participants performed three material handling tasks using three weight conditions (2, 4, and 6 lb). The tasks were selected based on the findings of Aim#1 (high, medium and low strain).

1.3 Significance

The socioeconomic impact of shoulder MSDs is huge in terms of lost productivity, lost workdays, and healthcare costs. Shoulder MSDs are prevalent among several industries including, but not limited

to, manufacturing, transportation, healthcare, and service. Despite the high socioeconomic impact and widespread occurrence of shoulder MSDs, currently no workplace assessment/evaluation tool exists that can predict the risk of developing these MSDs. Such a tool is extremely valuable and beneficial for preventing work-related shoulder MSDs. For example, NIOSH lifting index is a well-established tool that has proven to be beneficial to several occupations in assessing and preventing risk of low back injury due to lifting tasks.

The long-term goal of the research proposed in this study is to develop a shoulder MSD workplace assessment/evaluation tool. However, development of a workplace assessment/evaluation tool is a long, multi-step process, especially considering the type and nature of exertions workers can perform at workplaces using shoulder complex. The work completed in this study address a few preliminary but important questions (or completes a few preliminary and important steps) towards developing such tool. In our opinion, there are three significant contributions of the work completed in this study:

1) A strain index was formulated based on the concept of concavity compression. This strain index is expected to facilitate evaluation of shoulder strain during repetitive submaximal exertions. Repetitive dynamic exertions are very common in various industries such as metal, packaging, warehousing, automobile, garments, and transportation.

2) A global fatigue index that considers the anatomical characterization of the muscles and their physiological and biomechanical contributions during a physical exertion was developed. This fatigue index is expected to facilitate accurate measurement of internal shoulder strain based on the direct measurement of shoulder muscle activity.

3) Using the stain index and global fatigue index, the appropriateness of concavity compression mechanism in estimating shoulder strain during workplace exertions was scientifically tested.

CHAPTER TWO: LITERATURE REVIEW

Previous studies have used different assessment methods to identify work related risk factors associated with shoulder MSDs. In this chapter, these studies are presented in four different sections. In the first section, the risk factors of the shoulder complex are discussed. In the second section, different ergonomic assessment techniques are presented. In the third sections, studies investigated biomechanical loading of the shoulder joint using different biomechanical models are reviewed. In the fourth section, different muscle fatigue assessment techniques are presented.

2.1 Risk Factors of Shoulder MSDs

Harkness et al. (2003) conducted a two year prospective study of newly employed workers from twelve diverse occupational workplaces. At the beginning, 1081 participants provided information on work related risk factors and shoulder pain status. Among these participants, 803 (74%) subjects were free from shoulder pain at the beginning. 638 responded of shoulder pain at 12 months and 476 at 24 months. New onset shoulder pain was reported by 93 (15%) and 73 (15%) subjects respectively. An increased risk of symptom onset was found in subjects reporting workplace exposures involving heavy weights including lifting with one or two hands, carrying on one shoulder, lifting at or above shoulder level, and pushing or pulling. Working with hands above shoulder level was also predictive of new onset shoulder pain. Those individuals with any other previous pain also had an increased risk of new onset shoulder pain at follow up. In multivariate analysis, lifting heavy weights with one or two hands, pushing or pulling heavy weights, working with hands above shoulder level, and monotonous work were independently associated with new onset shoulder pain.

Grooten et al. (2007) had studied the association between shoulder complaints and work place risk factors during manual material handling tasks. They conducted a prospective cohort study on 803 working

subjects who reported neck/shoulder pain at baseline. They have measured the proportion of subjects who 5–6 years later were symptom-free. The work-related biomechanical and organizational exposures were collected at baseline. The Cox regression analyses were used to calculate the relative chances (RC) of being symptom-free at the end of the study for single exposures, and for up to three simultaneous work-related exposures. In a heterogeneous population with moderate nonspecific shoulder pain, sedentary work enhanced the chance of being symptom free 5–6 years later, whereas simultaneous exposures to at least two of manual handling – working with hands above shoulder level and working with vibrating tools were associated with a lower chance of being symptom-free at the end of the study.

Leclerc et al. (2004) assessed the likelihood of occupational factors for the onset of shoulder pain in occupations requiring repetitive work. They conducted a prospective cohort study among 598 workers in five activity sectors. A self-administered questionnaire was used to collect the physical work load and shoulder complaints. The incidence of shoulder pain was associated with work related biomechanical constraints. For men, repetitive use of a tool was a strong predictor, while the two most important biomechanical risk factors for women were use of vibrating tools and working with arms above shoulder level.

Lin et al. (2015) assessed functional dynamic stability and shoulder musculature performance for three shoulder positions, namely shoulder abduction of 45°, 70°, and 90° in the scapular plane. They studied twenty one college baseball players and nineteen age-matched non-players. They observed the maximum external and internal rotational torques both occurred at shoulder abduction of 70°. The study concluded that shoulder joint positioning affect torque production and selecting a position for training or rehabilitation based upon the degree of difficulty could have a positive effect on training.

Chiang et al. (1993) found that highly repetitive upper extremity movements were associated with shoulder girdle pain (OR 1.6, 95% CI 1.1–2.5). They have used multiple logistic regression analysis with

age, gender, and force as covariates. When tested in the same model with force and repetition, the interaction term for force and repetition was also significant (odds ratio 1.4, 95% CI 1.0–2.0). The major limitation of this study was that the exposure assessment was not specific to movement at the shoulder joint and may therefore have either over- or underestimated repetition at the shoulder. In some cases the exposure assessment may have been a measure of repetitive upper arm movements, but it may also have been a measure of repetitive hand and distal upper extremity activity occurring in the context of a static load on the shoulder muscles.

Miranda et al. (2008) conducted a comprehensive national survey among a representative sample (n=909) of the Finnish adult population. After excluding those with diagnosed shoulder disorders at baseline, 883 subjects were available for the analyses. A standardized protocol was used to diagnose chronic shoulder disorders in 63 subjects (7%). Work exposure to repetitive movements and vibration at baseline increased the risk of shoulder disorder: adjusted ORs 2.3 (95% CI 1.3 to 4.1) and 2.5 (1.2 to 5.2), respectively. Exposure to several physical factors increased the risk further, the adjusted OR was nearly 4 for at least three exposures. The adverse effects of physical work were seen even among those older than 75 years at follow-up. The statistically significant risk factors differed between genders: for men vibration and repetitive movements, and for women lifting heavy loads and working in awkward postures. The study summarized that occupational physical loading increases the risk of a subsequent clinical shoulder disorder and the effects seem to be long-term.

Cardozo et al (2011) studied the fatigue development during isometric fatiguing contractions. Twenty male subjects performed the isometric contractions while the force level was set at 30%, 40%, 50% and 60% of MVC. They continued these sustained contractions until fatigued. The endurance time was recorded if the force level fell by 5% with respect to the target force or the trunk was noticeably lowered during the test. Each force level trial was performed on a different day with a minimum of 24h

between them. SEMG signals were recorded throughout the sustained contractions from both right and left longissimus thoracis muscles. Fatigue was evaluated by calculating percent change in each frequency band, and percent change in MDF. Results showed that endurance times decreased with the increase in the exertion level. This study suggested that the muscles experience increased level of fatigue with the increase in the exertion level from 30% to 60% of MVC.

In another study by Andrzejewska et al. (2014), eleven male subjects performed isometric down-going ramp (DGR) contractions (from 100% to 0% MVC force) with the torque decreasing linearly over 7.5 s (13.3 % MVC per second) under both fatigued and non-fatigued conditions. The fatiguing exercise was the sustained isometric contraction at 50% MVC until exhaustion or could not hold the force within ±5 % of the target value. SEMG signals were collected during the isometric ramp contractions from the biceps brachii muscle. Fatigue model was developed by measuring MPF, RMS, Borg's CR 10 scale, and spike shape analysis (SSA) of SEMG signals. The SSA parameters were mean spike amplitude (MSA), mean spike duration (MSD), mean spike frequency (MSF), mean spike slope (MSS), and mean number of peaks per spike (MNPPS). RMS, MSA and MSS were decreased by 50 % at 90 to 60 % MVC exertion level for both fatigued and non-fatigued SEMG. The MSF was also decreased by 50 % in the 30–10 % MVC. Except the MNPPS measures, all the other estimated SEMG parameters were significantly different during fatigued compared to nonfatigued. Significantly higher RMS value and significantly lower MPF during fatigued DGR indicated muscle fatigue.

Nussbaum (2009) studied muscle fatigue while twenty four young adults performed three sustained isometric contractions at three different experimental set up. First experiment was to perform isometric endurance test involving shoulder abduction efforts of the dominant arm at 30% of MVIC until exhaustion. The second experiment involved isometric torso extension efforts at 30% of MVIC until exhaustion. In the 3rd experiment, another group of 12 participants performed isometric shoulder

abduction at 15% and 30% MVIC level. Ratings of perceived discomfort (RPD) were collected every 30 s throughout the third experiment using a modified version of Borg's CR-10 scale. SEMG signals were collected from middle deltoid muscle of the shoulder region, and torso-paraspinal muscles at the L1 and L4/L5 levels of the torso at a rate of 2048 Hz. In addition to these, alternative SEMG spectral measures were fractal analysis using dispersion analysis (DA) and detrended-fluctuation analysis (DFA) methods, logarithmic-power frequency, and Poisson-fit method. The utility of these SEMG measures were compared based on sensitivity (Omega squared, ω^2), variability (Residual error), repeatability (using ICC), and predictive ability (using ICC). The other non-SEMG measures were endurance time, perceived exertion and rate of MVIC. Results showed that rate of MVIC has declined, RPD has increased, and endurance time declined. The fatigue was more evident for 30% of MVIC than 15% of MVIC level. The study also showed appropriate fatigue indices to be appeared promising as fatigue indices for low level isometric tasks.

2.2 Previous Studies on the Ergonomic Risk Assessment Methods

2.2.1 Observational Methods

A simpler technique for posture recording, as well as for posture classification, is the Ovako Working Posture Analysing System (OWAS), as developed by the Ovako Oy Steel Co. in Finland. The system defines the movements of body segments around the lower back, shoulder and lower extremity (including the hip, knee and ankle) as four types: bending, rotation, elevation and position. The method consists of two parts. The first is an observational technique for evaluating working postures. Work-study engineers in their daily routine can use it and it gives reliable results after a short training period. The second part of the method is a set of criteria for the redesign of working methods and places. Karhu et al. (1981) applied OWAS method to develop an alternative method for the installation and maintenance of

steel mill equipment. A possible shortcoming of the system is that the posture categories are too broad to provide accurate posture description (Keyserling, 1986).

The RULA system (Rapid Upper Limb Assessment) is designed for assessing the severity of postural loading and is particularly applicable to sedentary jobs (Lynn McAtamney & Corlett, 1993). The method adopts the concept of OWAS, using numbers to represent postures with an associated coding system. The range of movement for each upper body part (head, trunk, upper and lower arm, wrist) is divided into sections that are numbered. Number 1 is given to the range of movement or working posture where risk factors causing load on the structures of the body segment are minimal, and higher numbers are given to parts of the movement range with more extreme postures. If an abduction or rotation is involved, the scoring is described beside the diagram. In addition to posture recordings, RULA also considers the load on the musculoskeletal system caused by static or repetitive muscle work and force exertion, so that an action list can be produced. This indicates the level of intervention required to reduce the risks of injury due to physical loading on the operator. The method has been tested in a laboratory situation relative to VDU operation (Lynn McAtamney & Corlett, 1993); however, further validation may still be needed for the system relative to other occupations. In addition, its sensitivity, specificity and predictive value for quantifying the actual risk for musculoskeletal injuries has not yet been assessed.

The HAMA method (Hand-Arm-Movement Analysis) was developed to analyze stress on hands and arms when tasks mainly consist of movement of the upper limbs (Christmansson, 1994). This method consists of five fundamental parts, related to different risk factors that may influence work-related stress. These include - type of basic motion; type of grasp; position of the upper limb; external load; and perceived exertion. The fundamental parts are further divided into several sub-categories, describing different types of motion, i.e. grasps, hand position and features of the external load. Information about hand/arm motion is obtained by videotaping the task, and information about force exertion is described by the observer and

augmented by the worker. One possible drawback is that there is no reference data available for the description of the exposure level, or the description of stress in body parts other than upper limbs.

REBA (Rapid Entire Body Assessment) is developed on the basis of the RULA system (Lynn McAtamney & Corlett, 1993), but it is appropriate for evaluating tasks where postures are dynamic, static or where gross changes in position take place (L McAtamney & Hignett, 1995). To use the tool, the observers select the posture or activity to be assessed and score the body alignment using the REBA diagrams. This is then combined with a load score to form the 'coupling scores', which are further processed into a single combined risk score using the table provided. Action levels are suggested to indicate necessary ergonomic interventions.

2.2.2 Interview and Questionnaire

Using direct interviews and self-administered questionnaire techniques, Harkness et al.(2003), Grooten et al. (2007), Lecterc et al. (2004) and Miranda et al. (2008) studied the association between shoulder MSDs and work place risk factors (Section 2.2.1).

2.2.3 Direct Measurements

The direct measurements involve recording the human body postures using hand-held devices or continuously with electric equipment, and muscle activity using electromyography. With manual devices, such as the goniometer or inclinometer, the device is attached to the body segment and the device indicates the angular measure of the body section. In optical motion-light scanning units, such as mirror scanners or electric image detectors, detect capture systems, light-reflecting markers are placed at specific anatomic points and the displacement of these markers. Previous studies that have used the direct measurement techniques are described below.

Nussbaum et al. (2001)studied fatigue development at the shoulder muscles during overhead dynamic tapping exertions using electromyography system. Sixteen subjects performed overhead dynamic tapping motions for a maximum of 3 hours. The target height was set at either 50% or 75% of overhead reach. Subjects performed the task at two hand orientations - pronated or supinated. The task duty cycles were 20/40s or 40/20s of task and rest. A total of 10 minutes or 10 cycles constituted a block. Each subject performed a total of maximum 18 blocks. 1 minute of task and rest was a cycle. 10 cycles was one block. Maximum duration was 3 hous or 18 blocks. The subject also performed isometric exertion at 30% of MVIC for each muscle at every 5 min during the resting period. Both SEMG raw and RMS data were recorded from middle deltoid (MD), descending trapezius (TRAP), anterior deltoid (AD), and infraspinatus (INF) muscle. Results showed that RMS value increased for almost 63%, 57%, 49%, and 59% of the SEMG data of MD, TRAP, AD, and INF muscle during dynamic exertion. Similarly, almost 50%, 61%, 58%, and 49% of the SEMG data showed decrease of MDF, and 53%, 63%, 60%, and 48% showed decrease of MPF for MD, TRAP, AD, and INF muscle during dynamic exertion, respectively.

Fuller et al. (2009) investigated the effect of arm fatigue on the whole body 3D biomechanical task characteristics by recording both shoulder postures and activities. Sixteen subjects performed repetitive reaching task (RRT) with dominant arm from one target to other while keeping the elbow at shoulder level. Task was to touch each target while matching the sounds with the metronome, one movement per second (1Hz). SEMG signals were collected from descending trapezius, anterior deltoid, biceps brachii, triceps brachii, and olecranon process muscles using bipolar Ag/AgCl surface electrodes. The RMS of SEMG data, MVIC for shoulder flexion-extension, and elbow flexion-extension, kinematics for average positions and range of motion of shoulder joint, elbow joint, wrist joint, center of mass (COM), and center of pressure (COP) were measured to evaluate muscle fatigue. Fatigue caused significant increase of heart rate, and trapezius and biceps RMS. The significant decreases of shoulder elevation and MVIC were also

observed due to fatiguing contractions. During fatigued reaching, subjects elevated their shoulder (11.7 ± 10.5 mm) and decreased their average shoulder abduction angle by 8.3 ± 4.4. COM and COP shifted towards the non-reaching side on the onset of fatigue. The ROM of shoulder and wrist joint increased during fatigue.

Ebaugh et al. (2006) determined the effects of shoulder muscle fatigue on three dimensional scapulothoracic and glenohumeral kinematics by using both electromyography and postural recordings. Twenty subjects (10 males and 10 females) performed shoulder elevation task. One cycle consists of three tasks. The first task was a static elevation of arms at 45° and manipulated small objects for 2 min. The second task was 20 repetitive arm elevations in scapular plane, and the third task was repetitive raise and lower arm through a diagonal pattern. During the repetitive shoulder elevation, the targeted force was 20% of maximum voluntary isometric contraction (MVIC). The cycle of the fatiguing tasks continued until the subject reported exhaustion or failed to correctly perform two tasks consecutively. Muscle fatigue was investigated by collecting SEMG signals from upper trapezius, lower trapezius, serratus anterior, anterior deltoid, posterior deltoid, and infraspinatus muscles while subjects performed three isometric push up exertions (60% of MVIC force) for 5 s before and after the shoulder elevation task. SEMG sampling frequency was 1024 Hz and band pass filtered at 10-500 Hz. The surface electrodes were bipolar Ag/AgCl electrodes with an inter-electrode distance of 2.5 cm. The MPF was measured for each 1s epoch of the isometric exertion of 5 s. The MPF of the 1st, 2nd, 3rd, and 4th s intervals were then averaged. A minimum reduction of 8% in the MPF value was considered as an indication of local muscle fatigue. Shoulder kinematics was also measured to observe fatigue related kinematic changes. Results showed that except lower trapezius, all other muscles demonstrated signs of local muscle fatigue (>8% reduction' in MPF). Fatigue of the shoulder girdle muscles resulted in increased amounts of scapulothoracic motion and decreased amounts of humeral external rotation.

In another study, Dingwell et al. (2008) observed the body kinematic changes with the muscle fatigue. They have measured both electromyography and range of motion using motion capture system. Seven highly trained male cyclist rode a stationary bicycle ergometer at 100% of their maximum oxygen consumption (VO2 max) until voluntary exhaustion. Participants were instructed to cycle at ~90 rev/min and were allowed to recover if their revolution per minute fell below 90. The SEMG signals were collected from vastus lateralis (VL), biceps femoris, gastrocnemius, and tibialis anterior (TA) muscles of left leg using Ag/AgCl bipolar surface electrodes spaced a distance of 10 mm. SEMG sampling rate was 1080Hz and band passed at 30-400Hz. The MDF was calculated using STFT and determined separately for each down and up stroke. Time series of MDF, mean joint angle (MA), and range of motion (ROM) were calculated and correlated between each other. MDFs started dropping almost immediately after the task began at every muscle, indicating that the muscles began to fatigue. Moreover, the change in MDF were positively correlated with kinematic fatiguing fluctuations - in mean trunk lean ($p = 0.009$) and knee splay angles ($p= 0.011$), and with trunk lean ($p= 0.002$) and ankle ($p = 0.001$) range of motion.

2.3 Shoulder Studies Based on Biomechanical Modelling

Depending on the aspect of shoulder function to be investigated, various modelling approaches can be selected. Accordingly, they have used different biomechanical models to investigate shoulder moments during physically demanding tasks.

Dickerson et al. (2007) studied load transfer tasks using two shoulder biomechanical models. A 3-D mathematical model was used to generate resultant shoulder torques as well as muscle force predictions during static hold phases of the reaches. The model integrates motion, task and subject data streams to generate temporal predictions of muscle force levels. Another regression based model was constructed to investigate the loading/perception relationship. The latter model was based primarily upon loading

metrics, which was complemented by the other factors (subject and task parameters). Two shoulder biomechanical models and experimental muscle activity data (EMG signals) were used to assess physical exposure for a series of reaching tasks using eight right handed subjects (4 males, 4 females). Effort perception was quantitatively correlated to these measures of physical loading, both at the resultant torque and muscle activity model-based muscle force predictions. Muscle data did not explain variation in effort perception more fully than torque data. The results suggested that effort perception may not be fully explained by only an image of the motor command, but is rather a complex integrative quantity that was affected by other factors, such as posture and task goals, which might be dependent on sensory feedback.

To study the shoulder moment during a range of load conditions, Hall and Dickerson (2010) developed efficacy of a moment-based training technique. Nine hand loads were set to create shoulder moments equal to 20–100% of maximum shoulder moment at 10% intervals. Thirteen right handed female participants performed nine load transferring tasks along five different angles. The maximum force measured along with the postural data, participant stature, body weight and the kinematic data were used as inputs into an external inverse dynamic biomechanical shoulder model in order to determine the maximum voluntary shoulder moment (MVM). The shoulder moments based on different loading conditions were calibrated using perceived exertion of Borg's CR – 10 scale. Both the shoulder moment data and perceived exertion data were rescaled from 0 to 100. The results showed that perceived exertion data were better related to mean shoulder moment ($r = 0.75$). The perceived exertion data were higher than the physical shoulder load.

Holscher et al. (2016) studied glenohumeral instability using AnyBody modeling system to compute joint reaction forces for several static abduction tasks with different muscle weakness. Results showed that weakness of the rotator cuff muscles (supraspinatus; infraspinatus; teres minor) leads to a deviation of the joint reaction force from the centerline.

In another study, Fischer et al. (2012) investigated whether psychophysically acceptable and maximum voluntary hand forces depended on the underlying biomechanical factor that limited the maximum voluntary hand force. They collected kinematic data from eighteen right handed males. The participants were asked to perform nine test conditions – three exertion directions (pulling in toward the body, pressing down toward the floor, pushing medially from right to left across the body) and three postural conditions (Shoulder width foot placement, free foot placement, upper body braced). Participants also performed psychophysically acceptable exertions at every half a min for 30 min. They rated discomfort at 10 and 20 min into task. They were also asked to perform two 5s MVC before and after each task. The shoulder moments were calculated using a three dimensional static linked segment model. Results showed proportional relationship between psychophysically acceptable and MVC forces. The ratio of psychophysically acceptable force to the maximal force was significantly different depending on the underlying biomechanical factor. Psychophysically acceptable hand forces were selected at 86.3 ± 19.7% of the MVC hand force when limited by balance (pulling exertions), 67.5 ± 15.2% when limited by joint strength (downward pressing), and 78 ± 23% when the limitation was undefined in the medial exertions. They concluded that magnitude of the proportionality was depended on the underlying biomechanical factor that was most likely limiting MVC capacity. Those biomechanical factors were: strength limitations (net joint moments at the elbow and shoulder), balance limitations (distance between the geometric center of the shoe–floor interface and the boundaries of the shoe–floor interface), and friction limitations (maximum available shoe–floor friction force)

Nikooyan et al. (2011) used a dynamic forward flexion motion to validate the Delft Shoulder and Elbow Model (DSEM), a musculoskeletal model of the shoulder and elbow. They collected both motion data and SEMG signals of 12 superficial muscles from a male participant. The geometrical data of the shoulder and elbow were taken from a 57-year-old muscular male cadaver. A total number of 31 muscles

of the shoulder (23 muscles) and elbow (8 muscles) were divided into 139 elements. Joint surfaces and other bony contours were digitized for modeling using geometrical forms. Patterns of the model-predicted relative muscle forces were compared with their normalized EMG-signals. Results showed relatively good agreement between forces and EMG (mean correlation coefficient of 0.66). However, for some cases, no force was predicted while EMG activity had been measured (false-negatives). A potential limitation of this study was the model was not scaled to subject's geometry.

Several other previous studies have investigated the biomechanical loading of the shoulder taking into consideration the concavity compression mechanism to understand stress-strain relationship for the shoulder complex.

Hoozemans et al., (2004) evaluated the mechanical load on the low back and shoulders during cart pushing and pulling using one or two hands, three different cart weights, and two handle heights. They found that the exerted force and handle height both had a considerable effect on the mechanical loading of the shoulder. During the initial phase of moving the cart, a large increase in the compressive force at the glenohumeral joint while pushing and pulling at hip height was observed with an increase in cart weight. This was also seen for the sustained motion phase, although to a smaller extent. Their recommendation was that cart weight should remain as low as possible and to push or pull at shoulder height with the general idea that the net shoulder moment is kept lower by keeping the shoulder joint close to the line of action of the exerted force. The study however did not evaluate the translational forces acting at the glenohumeral joint with the consideration that the compressive force on the glenohumeral joint is a suitable measure. The compressive forces are largely exerted by the rotator cuff muscles that compensate for the translational forces acting on the glenohumeral joint.

Nimbarte et al., (2013) also evaluated the effects of a dynamic cart pushing task on the biomechanical loading of the shoulder and low back. In this study, subjects performed dynamic cart

pushing tasks on a walkway of varying gradient (0°, 5°, and 10°) using three different cart weights (20, 30, and 40 kg). Peak reaction forces at the acromioclavicular and glenohumeral joints were found to be comparable to one another and were higher than the peak forces at the sternoclavicular joint. Variation on the cart weight was found to significantly affect the reaction forces at the shoulder complex joints. The peak reaction forces for all three shoulder joints increased with an increase in cart weight suggesting that higher exertion forces required to push the cart resulted in a higher joint loading. For the glenohumeral joint, reaction forces in the distraction (medial-lateral) direction were found to be substantially higher than the reaction forces in the anterior-posterior and inferior-superior directions. The reaction forces in the distraction direction stabilize the glenohumeral joint by improving the concavity compression. A significant increase in the distraction forces was observed with the increase in the cart weight and walkway gradient, indicating increased muscular demand of the shoulder stabilizers to improve the concavity compression.

Another study by De Looze et al. (2000), investigated the changes in force direction of pushing and pulling as result of changes in handle height and force level. They found that as the force exertion rises, the physical load parameters also rise. An increase in the push/pull force exertion level was reflected in an increased net shoulder torque. The variations in force exertion and physical load observed were due to variations in force direction. They suggested that besides force magnitude, force direction with respect to the body posture should also be measured in order for accurate assessment of the physical load.

As part of the shoulder complex's characteristic instability, translational forces in the inferior-superior or anterior-posterior directions destabilize the glenohumeral joint while compressive forces in the distraction direction help stabilize it. Physical exertions with a higher ratio between the translational and compressive forces may destabilize the joint and therefore pose an increased risk of MSD (S. B. Lippitt et al., 1993). Because of this, it is useful to evaluate the loading present on the shoulder joints in

order to calculate this ratio, determine whether a particular exertion poses an increased risk for joint instability, and ultimately risk for MSDs.

2.4 Neuromuscular Fatigue Assessment Methods

In the scientific literature, researchers have used the following five assessment methods to quantify neuromuscular fatigue.

1. *Changes in the maximum voluntary contraction (MVC):* MVCs are executed by instructing the participants to produce the highest possible force, in a setting where the length changes are restricted to the initial tightening up of the muscle-tendon unit (isometric exertion). The changes in recorded force before and after a bout of exertions are used to estimate muscle fatigue. A significant decrease in the force exertion during the MVC contraction indicates the sign of fatigue. In a study, Newham et al., (1991) examined the force generating capacity during the MVC exertions before and after 4 min of knee extension activities. Authors observed 80% decreases in the force exertion during the MVC exertions after 4 minutes of knee extension activities.
2. *Changes in the endurance time:* In many studies, fatigability is examined by assessing the endurance time. This approach is based on a presumption that there is an association between the decline in maximal force generating capacity and the time to exhaustion. Garg et al., (2002) studied the fatigue of shoulder girdle musculature by using isometric contraction performed at different shoulder postures under different weight conditions. The weights used by the participants were 5%, 15%, 30%, 45%, 60%, 75%, and 90% of the MVC at each of the shoulder postures. With an increase in the weight, the endurance time decreased significantly. The decrease in endurance time followed a non-linear trend and corresponded very well with the subjective assessment measures of fatigue and pain ratings.

3. *Changes in the metabolite concentration:* There are a number of metabolic changes that occur concurrently with muscular fatigue. The relationship between intracellular metabolites and the force exertion during fatigue has been examined in a number of studies (Cady, Jones, Lynn, & Newham, 1989). Most of these studies indicated that the normal participant's intracellular pH value decreases as the muscle is fatigued. Cady et al., (1989) studied the first dorsal interosseous muscle of the hand by fatiguing the muscle with three bouts of maximal voluntary contraction. The intracellular phosphorus metabolites were measured by nuclear magnetic resonance during the intervals between the fatiguing contractions. The relationships between loss of force and change in metabolite concentrations were obtained from four normal participants and one subject with myophosphorylase deficiency (MPD) who could not utilize muscle glycogen and therefore produced no hydrogen ion from glycolysis. For both the MPD and normal participants the relationship between relative force loss and inorganic phosphate concentration was found to be curvilinear.
4. *Near-infrared spectroscopy:* This technique utilizes oxygenation properties of skeletal muscle to estimate muscle fatigue. Yoshitake et al., (2001) used near-infrared spectroscopy to investigate the etiology of lower-back fatigue. They compared isometric back extensions for a period of 60 seconds performed at an angle of 15° with 0° horizontal plane. It was observed that oxygenation and the blood volume of the lower back muscles decreased significantly throughout the exertions performed at 15° compared to those performed at 0°.
5. *Electromyography (EMG):* This is probably one of the most widely used methods in fatigue quantification in the occupational settings. EMG has been extensively used to study the patterns of activation or tension developed in the muscles during a variety of occupational tasks. There are two types of EMG data recording techniques: intramuscular EMG (needle of fine-wire) and

surface EMG (SEMG). Intramuscular EMG involves inserting needle or fine-wire electrodes directly into the muscle through the skin and is invasive in nature. In SEMG, surface electrodes are placed on the muscle of interest over the skin to record the muscle activity. Surface electrodes pick up changes in the muscle activation resulting from either a changed number of active muscle fibers or excitation rates (Basmaijan & De Luca, 1985). Electrical activity picked up by the surface electrodes reflects a summary of active motor unit action potential, which reflects a chemical-electrical process in several muscles' fibers and motor units (Sommerich, Joines, Hermans, & Moon, 2000). The EMG data can be processed using time domain or frequency domain analysis. Time domain analysis typically deals with amplitude estimation, while frequency domain analysis deals with the trends in the different frequencies in the signal. The following methods are commonly used by the researchers to evaluate EMG signal for the objective assessments of fatigue:

i. Change in the EMG amplitude: There are two methods that are most commonly used to estimate changes in the amplitude of the EMG signal: mean absolute value (MAV) and root-mean-square (RMS) value. In previous studies, it was shown that EMG amplitude increases with fatigue due to additional recruitment of motor units during the exertions that are physically demanding, such as maximal or near maximal exertions (Sekulic, Medved, & Rausavljevi, 2006).

ii. Change in the Zero-crossing rate (ZCR) of the signal: Zero-crossing rate (ZCR) is defined as half the number of zero crossing of EMG signal (S(t)) per second (Inbar, Paiss, Allin, & Kranz, 1986). Inbar et al., (1986) showed that the ZCR can be used to monitor the spectral changes of EMG signal. Authors observed that zero crossing of the raw EMG signal shifts to lower values as an indicator of muscle fatigue.

iii. Changes in the frequency spectrum variables: To estimate changes in the frequency content of the EMG signal, the raw EMG signal is transformed from the time domain to the frequency domain. Fast Fourier transform (FFT) is the most frequently used method for conducting this transformation. By using FFT, the frequency spectrum of EMG signals are clarified and recognized by breaking down the signal into its corresponding sinusoidal of different frequencies (Kilby & Hosseini, 2004). Three variables based on the FFT transformed data that are often used to estimate muscle fatigue are:

(1) Mean frequency: the mathematical mean of the spectrum curve

(2) Median frequency: the parameter that divides the total power area into two equal parts

(3) Total power: The integral of the spectral curve.

A number of previous studies have used changes in the median frequencies of EMG data to evaluate muscle fatigue (Potvin, 1997). A shift in the median frequencies to lower values has been identified as the indicator of neuromuscular fatigue in most of these studies (S K Chowdhury & Nimbarte, 2015; D. K. Kumar, Pah, & Bradley, 2003). For example, in a study conducted by Potvin et al., (1997) behavior of the bicep brachii muscle was evaluated using changes in the median frequencies of the EMG signal during fatiguing contractions. The authors found that muscle fatigue resulted in the drop of median frequencies. In another study by Georgakis et al., (2003) fatiguing behavior of knee extensors was studied during the isometric knee extension. A consistent decrease in the median frequencies of knee extensor muscles, vastus medialis, vastus lateralis, and rectus femoris muscles, was reported by the authors. A drop in the mean frequency has also been used as the biomarker of fatigue in a few studies. However, a relatively lower coefficient of variation for the mean frequency was reported than the median frequency. In terms of power, an increase in the power of the low frequency components of the

EMG and a decrease in the power of high frequency components were reported by a number of authors for various muscles in the human body with the onset of fatigue (Kilby & Hosseini, 2004; R. Merletti, A. Rainoldi, & D. Farina, 2004; Potvin, 1997).

iv. Joint analysis of EMG spectrum and amplitude (JASA): In non-isometric contractions, sometimes it is very difficult to interpret changes in the spectrum and amplitude of the surface EMG signal independently (Merletti & Parker, 2004). At such instances, simultaneous consideration of amplitude and spectrum related variables of EMG signal is essential to provide information on whether EMG changes are fatigue-induced or force-related. JASA uses the following four criteria to distinguish fatigue-induced or force-related changes caused by a dynamic exertion (Hägg, Luttmann, & Jäger, 2000):

(1) If the EMG amplitude increases and EMG spectrum shifts to the right, muscle force increase is the probable cause.

(2) If the EMG amplitude decreases and EMG spectrum shifts to the left, muscle force decrease is the probable cause

(3) If the EMG amplitude increases and EMG spectrum shifts to the left, this is considered to be result of muscle fatigue

(4) If the EMG amplitude decreases and the EMG spectrum shift to the right, this is considered to be recovery from previous muscle fatigue.

v. Short-time Fourier transform: Isometric muscle contractions can be easily analyzed for muscle fatigue by using either of the above mentioned time or frequency domain analysis method. Evaluation of fatigue caused by dynamic contraction is rather problematic because of its time variant nature. For such signal, variations of the EMG signal spectrum cannot be analyzed by simply applying Fourier transform, since information about time would be lost. Also, generally

speaking, EMG signals do not conform to the stationary requirement of the Fourier transform. One way to satisfy this requirement is to apply Fourier transform only to signal segments that are short enough to fulfill this requirement. Short-time Fourier transform (STFT) provides the potential solution to this problem, where the EMG signal is divided into short time windows and Fourier transform is applied to each window. Previously, STFT was used by Sparto et al., (2000) to study fatigue of low back muscles caused by isokinetic exertions. The authors used a window size of 1 second to compute the Fourier transform. A significant decline in the median frequency was reported by the authors in this study.

2.5.1 Muscle Fatigue Measurement Using SEMG Based Traditional Indices

2.5.1.1 Isometric exertion studies that observed the expected fatigue development trend

Allison and Fujiwara (2002) performed sustained isometric elbow flexion at 60% of an individual's MVIC for as long as possible or until they reached 35% of their value. Ten subjects (5 males and 5 females) performed two trials with a 2 min recovery between trials. SEMG signals were collected throughout the contractions from biceps brachii muscle using bipolar electrodes having an inter-electrode distance of 25 mm. SEMG sampling frequency was 1024 Hz and filtered digitally using 20–500 Hz band-pass filter. Ten 1s epochs of the data were collected. Frequency analysis was performed on each epoch. For each epoch, MPF, IEMG (Integrated EMG) of low (15–45 Hz), medium (45–95 Hz), and high frequency (>95 Hz) bands, ratio of low frequency amplitude to total IEMG, and high frequency band to low frequency band amplitude ratio were calculated. Perception of effort suggested that subjects reported significant fatigue following both endurance tasks. In both endurance tasks, there was a linear increase in low frequency band amplitude with a concomitant decrease in the high frequency band. There was also an increase in amplitude and relative decrease in MNF for each trial. MNF was highly associated with both high-low amplitude ratio and with low to total IEMG ratio for both trials.

In another study, Dedering et al. (1999) studied correlation between subjective and objective assessment of muscle fatigue. Fatigue was generated using a modified Sorensen's test protocol. The protocol was an isometric contraction, and fifty subjects (25 males and 25 females) performed it until exhaustion. Moreover, when the test was concluded, 5-s contractions were performed in the modified Sorensen's test position at l-, 2-, 3- and 5-min intervals of rest to test recovery from fatigue. SEMG signals were recorded from erector spinae muscle during the test protocol as well as during the test contractions. Four pairs of surface electrodes were attached to both sides of the back and inter-electrode distance was 20 mm. Sampling frequency was 1000 Hz and filtered by 9th order Butterworth filtered with cut-off using 10–1000 Hz. Fatigue model was developed by calculating initial MDF and MPF (mean of the first 5s), end MDF and MPF (mean of the last 5s), MDF and MPF slope for the whole contraction, MDF and MPF slope for the first minute, and MDF and MPF intercept of the slope. MDF and MPF were calculated every second using FFT algorithm. Along with the SEMG measures, Borg's subjective rating scale (CR-10) and endurance time were also recorded. It was observed that, MDF and MPF and endurance time were reduced by 30% at a Borg's rating of 3, by 50% at a Borg's rating of 5, and by 60-70% at a Borg's rating of 7. This study found a significant correlation between subjective and objective assessment of muscle fatigue.

Hummel et al. (2005) studied the relationship between Borg's scale rating and objective muscle fatigue indices. Subjects performed two isometric shoulder elevation tasks at 30% of their MVIC level, separated by a rest period of 6 min. They hold the load as long as possible, however with a maximum period of 6 min. During these exercises, Both SEMG signal and perceived exertion using the Borg's scale (CR-10) at every minute were simultaneously detected from the right upper trapezius. The surface electrode was consisted of eight rectangular electrodes equally spaced at 5 mm inter-electrode distance. SEMG sampling frequency was 2048 Hz and filtered at a bandwidth of 10–400 Hz. Rate of change of normalized MPF and Borg's value were computed to evaluate muscle fatigue. Normalized MPF slopes

were calculated from the ratio between the slope of the regression line and the corresponding MPF initial value. Initial MPF values and the slopes of the normalized MPF significantly correlated with Borg's scale ratings.

Yung et al. (2012) evaluated muscle fatigue using high to low frequency ratios. In this study, fifteen males performed five isometric elbow extension protocols: 1) sustained isometric elbow extension at 15 % MVIC (15 %Sus), 2) intermittent elbow extension between 0 and 30 % MVIC (0–30 %Int), 3) intermittent contraction of 7.5–22.5 % MVIC (7.5–22.5 %Int), 4) intermittent contraction between 1 and 29 % MVIC (1–29 %Int), and 5) intermittent sinusoidal wave pattern with peaks at 0 and 30 % MVIC (0–30 %Sine). Each protocol consisted of two experimental sessions that occurred in two separate days. The first experimental session consisted of 10 min of baseline activity, 60 min of exercise or until exhaustion, and 60 min of recovery. The second session was a 24-h follow-up where baseline activity was only monitored. SEMG signals were collected continuously during 10 min of baseline activity and 60-min exercise from middle deltoid (MD), upper trapezius (UT) muscles of both sides. SEMG sampling rate was 2048 Hz, and band pass filtered at 10-1000 Hz. The surface electrodes were bipolar Ag-Cl electrodes with an inter-electrode distance of 20 mm. The signals were later analyzed every 2 min in 30-s windows. In the second session, SEMG, MMG, rating of perceived exertion and blood velocity measurements were collected during 30 s of baseline activity. The measured variables for fatigue modeling were SEMG RMS, MPF, MDF, and high frequency (130-238 Hz) to low frequency (20-40Hz) power ratio (Hi-Lo ratio). Both MPF and MDF shifted toward lower values during the 15 %Sus contraction. The RMS value was also increased, more for 15% Sus, then, 7.5%-22.5%Int, 0-30%Sine, 1-29%Int, 0-30%Int, consecutively. This study suggested that time-varying force might be a useful intervention to reduce local muscle fatigue while workers perform low-load tasks.

2.5.1.2 Isometric exertion studies that failed to observed the expected fatigue development trend

In their study, Clancy et al. (2008) failed to observe the fatiguing trend using traditional fatigue indices such as MPF and RMS parameters. Twelve subjects (6 males and 6 females) performed a constant force and a force varying isometric handgrip task. The gripping force was 50% or 40% of MVIC from 30 min to maximum 90 min. Cycle of the force varying isometric contraction was 12 s. It constituted with 1s rest, 4s contraction hill, 1s rest, 3s contraction hill, 1s rest, 2s contraction hill. The constant-force contraction pattern also had a 12 s pattern, constituted with 1-s rest, 2-s ramp increase in force, 8-s reference level contraction, and 1-s rest. The force was increased at every 15 minutes during both isometric contraction tasks. Borg's discomfort rating was collected at every 5 min during the experiments. SEMG signals were collected from fore arm muscles - flexor digitorum superficialis (FDS) and extensor carpi radialis (ECR). The sampling rate was 4096 Hz and band pass filtered at 25-1350 Hz. The RMS was calculated for each complete 12 s period of the cyclic force-varying task and for a 5 s epoch (using 500 ms window) at every 5 min period of the constant force contraction, respectively. MPF was calculated for a 500 ms segment out of 12 s cycle of the force varying task period and for the 5 s epoch of the constant force contraction using the STFT technique. The time trends of SEMG RMS and MPF showed no consistent trends during both force-varying and constant-force fatiguing contractions. The results of this study indicated limitations in the use of the traditional SEMG indices for the assessment of fatigue during long-duration, force-varying contractions.

Strimpakos et al. (2005) evaluated the traditional muscle fatigue indices during sustained isometric exertions. Thirty three healthy subjects (17 males, and 16 females) performed a 30 s of sustained isometric contraction at 60% MVIC. The test was terminated if the participant could not keep the force within 10% of the target. Borg's data (CR-10) was collected 3 times during the sustained exertion at 0, 15 and 30 s. Subjects performed the same experiment on three different days with an approximate one-week (5–9 days) interval. SEMG recording was taken from semispinalis capitis, splenious capitis, sternocleidomastoid

(SCM) and levator scapulaes muscles of neck region throughout the sustained contraction. Bipolar surface electrodes were consisted of Ag/AgCl with an inter-electrode distance of 20 mm, and placed over the four muscle groups of neck flexors, extensors, lateral flexors and right rotators. SEMG sampling rate was 1024 Hz and filtered at 8-500Hz using 2nd order Butterworth filter. Both MDF and RMS were calculated at every 1s epoch of the contraction. Both MDF and RMS were normalized against their respective initial values (mean of the first two seconds) and a linear regression line was fitted for 30s to obtain a measure of the rate of MF decrease and RMS increase. The objective measures of this study were MVIC, normalized MDF slope, RMS slope, initial MDF, and end MDF. The reliability of the fatigue measures were established by calculating intraclass correlation coefficient (ICC), the standard error of measurement (SEM), and the smallest detectable difference (SDD). The reliability of MVIC data was high with an ICC of 0.9 -0.98. Normalized MDF slope had low repeatability. Initial MDF had moderate to good reliability and small error. The RMS slope yielded also poor repeatability. The Borg assessment was more reliable than the SEMG estimate though variability between sessions was still quite high. The results revealed that there was no correlation between objective measures of normalized MDF slope, RMS slope, initial MDF, and end MDF, and subjective measure of Borg's rating.

In their study, Sogaard et al. (2003) failed to observe the fatigue trend using MPF parameters. Six male subjects performed three sessions of repetitive isometric exertion using both hands. The fatiguing exercise protocol was consisted of duty cycles with 6 s of contraction at 30% or 10% MVIC followed by 4s of relaxation and repeated for a total duration of 30 min giving a total number of 180 contractions in each session. fatiguing exercise at 10% with visual feedback and at 30% MVC with visual and proprioceptive feedback for 30 min. Subjects also performed isometric test contractions at 5% and 80% of MVIC before prolonged contraction and at 10 min and 30 min of recovery after termination of each of the three sessions of fatiguing intermittent contractions. SEMG signals were collected during

isometric test contractions for 15 s from biceps brachii muscle using Ag/AgCl surface electrodes with an inter-electrode distance of approximately 37 mm. The SEMG signal of 15 s was divided into consecutive 1-s epochs. The RMS and MPF, and the mean force and standard deviation (SD) of the force was calculated for 15 epochs. Following the fatiguing exercise MVIC decreased significantly in all three sessions. In the time domain, the significant increases in RMS after the fatiguing exercise were found only in the 5% MVIC tests. The SEMG MPF trend was not consistent for both test contractions.

Alizadehkhaiyat et al. (2011) observed muscle fatigue development sixteen subjects (7 women and 9 men) performed a controlled gripping task at 50% of MVIC contraction in a standardized sitting and arm position. Fine wire EMG were recorded from supraspinatus and infraspinatus shoulder muscle for about 70 s from which the first and last 5 s were discarded before the analysis. The EMG sampling rate was 2000 Hz, and band pass filtered at 20-1000 Hz. RMS and MDF were calculated for 60 s in 5 s intervals. Both RMS and MDF were normalized to the start value, and linear regression was fitted to calculate the rate of change (slope). A significant positive RMS slope ($p < 0.01$) was found for both supraspinatus and infraspinatus muscle, indicating that the task resulted in increasing muscle activity. Judging by the MDF slope, there was no sign of fatigue progression.

2.5.1.3 Dynamic exertion studies which failed to observe the expected fatigue development trend

El Falou et al. (2003) had studied fatigue development pattern while driving for two different types of car seats with and without vibrating platform. Eleven male subjects seated in a car seat for 150 minutes. SEMG data were collected seven times randomly spread throughout this period: 20 min, 35 min, 65 min, 85 min, 120 min, 135 min, and 150 min. Each data collection period took 5 min (3 min to assess performance and 2 min to measure subjective discomfort). SEMG signals recorded at 840 Hz sampling rate from cervical erector spinae, and external oblique muscles using Ag/AgCl bipolar surface electrodes with an inter-electrode distance of 20mm. The signals were filtered at 8th order low-pass filter with a cut

off frequency of 350 Hz. Subjective discomfort ratings (scaled from 0 to 10), and subject's performance were also assessed using two tasks - auditory stimulus at random orders, and tracking a simple two-dimensional task. SEMG data were segmented by a method of variance comparison using two windows: a sliding window with a constant length (decision window), and an adaptively growing window (observation window). The MDF was calculated for each postural SEMG segment. Results showed no significant difference in MDF throughout the trial for any of the four experimental conditions. Greater subjective discomfort and poor task performance were found for Car seat U and in the presence of vibration (El Falou et al., 2003).

Sood et al. (2007) performed two different tasks: first task was to test the reliability of SEMG measures, and the second task was to measure the effect of working height on shoulder fatigue. During the first task, ten subjects (5 males, and 5 females) performed overhead tapping task using the dominant arm, with a cycle time of 54 s (50% duty cycle - first 27s repetitive key tapping, and next 27s rest). During the 27s of rest period, subjects performed light manual work of screwing and unscrewing nuts and bolts. Pacing was controlled (36 key taps per work cycle). Subjects freely selected their postures at a fixed height. Tapping task was continued until participant reported a perceived discomfort (RPD) of 9 or greater or 1 hour elapsed. During the second task, twelve subjects (6 males and 6 females) performed same tapping task but with three working heights. Participants attended four sessions - one practice session and three experimental sessions for one at each height. The task was approximately 15-20% of MVIC. SEMG signals were obtained from three accessible shoulder muscles: anterior deltoid, medial deltoid, and upper trapezius muscle using Ag/AgCl bipolar surface electrodes having an inter-electrode distance of 2.5 cm. The SEMG signals recorded at 2048 Hz and filtered with a bandwidth of 10-500 Hz. SEMG RMS with a 110ms time constant was sampled at 128Hz. SEMG was recorded at last 6s of tapping task of each cycle and shoulder RPD collected at every 5th cycle or every 4.5 min. Three categories of response variable

were obtained: MVICs for each muscle; SEMG-based measures; and shoulder RPDs. The SEMG based measures were normalized RMS, mean frequency (MPF), and median frequency (MDF). The reliability of the measures was evaluated using intra-class correlation coefficient (ICC), standard error of measurement (SEM), and coefficient of variation (CV). Results showed that the MVICs (computed using load cells) exhibited excellent reliability, with very low error estimates. Initial values of MPF and MDF demonstrated good-excellent reliability for all muscles. However, temporal changes (slope) of the SEMG MPF and MDF exhibited lower reliability, and more variability between muscles. However, MPF and MDF were more reliable than RMS. Reliability of SEMG RMS; both initial and temporal changes (Slope) were quite variable across muscles, ranging from fair to high. On contrary, RPD measures demonstrated excellent reliability for both final reported values and temporal changes. During the second task, none of the SEMG -based measures showed any significant main or interaction effects of task height or any consistent trends

Bosch et al. (2007) studied muscle fatigue during low intensity work in temporal aspects. Subjects performed two monotonous, low-intensity arm lifting tasks. The work load during the first task was estimated to be approximately 5% of MVIC. The first task was performed for 4 weeks period of 8-h working day followed by a 4-week period of working days of 9.5 h in a manufacturing industry of medical instrument. The second task was also performed for 1 week with 9-h working days and the work load was estimated to be 15% MVIC. SEMG signals were collected while subjects performed isometric test contraction for 30 s by abducting their arms at an angle of 90 degrees at seated position. Bipolar Ag/AgCl surface electrodes with an inter-electrode distance of 25 mm were placed on trapezius muscle. Signals were recorded at 1000 Hz sampling frequency and filtered with a bandwidth of 10-400 Hz. Six frequency bands of 50 Hz (10-50, 50-100, 100-150, 150-200, 200-250, and 250-300 Hz) were used to analyse the frequency content by calculating the power of each band. The relative power of each band in relation to

the total power was determined by dividing the mean power of each band by the total power. Fatigue modeled was developed by measuring mean amplitude, MPF, relative power of each frequency band, and local perceived discomfort (0 to 10; 0 = no discomfort, 10 = extreme/maximum discomfort). Mean amplitude and MPF were normalized to the SEMG values of the start of the working day. Results showed that SEMG amplitude increased during the first part of the day while the MPF did not change significantly over time for the first task. However, an increase in amplitude of the SEMG signal was accompanied by a decrease of the MPF during the first part of the day for the second task. During the first task, the low frequency band (10–50 Hz) significantly increased before the lunch, which was accompanied by a significant decrease in higher frequencies (150–200 Hz), whereas the low frequency band (10–50 Hz) significantly increased after the lunch accompanied by a significant decrease in higher frequencies (150–200 Hz). The subjective discomfort rating showed the development of discomfort in the neck and shoulder region for both cases. However, correlation coefficients were low and not significant between subjective and objective estimates of muscle fatigue. In another study, Bosch et al (2012) investigated whether temporal movement and performance changes during 1 hour of fatiguing repetitive work and how the changes correlated with SEMG signals. Eighteen male subjects performed a 1-h repetitive arm reaching task. Six consecutive work blocks were performed, each consisting of 7 min of repetitive task and five and half minute of rest break. The repetitive task consisted of moving a 300 g manipulandum between two targets at a frequency of 0.5 Hz (cycle time 2 s), as guided by a 1 Hz metronome signal. One target at elbow height and another target were at shoulder height. Each movement was 1s duration. Before the task an isometric reference contraction was performed. The task variables were two targets - low and high, and direction of the task - up and down motion. The SEMG signals were collected from right trapezius muscle using Ag/AgCl bipolar surface electrodes having an inter-electrode distance of 20 mm. The sampling frequency was 2000Hz, and band pass filtered at 10-500 Hz. Average SEMG amplitude in terms of RMS

value and MPF was calculated for 1s window using Welch method . The RMS values were normalized (% RVE) with respect to RMS value of the isometric reference contraction. The RMS and MPF of first 30 (30s) cycles of each work block (Early) and last 30 (30s) cycles of each work block (Late) were compared. Mean absolute deviation (MAD) of cycle-to-cycle variability in SEMG were calculated. Along with SEMG parameters, subjective discomfort ratings using Borg's CR 10 scale, waiting time for W1 and W2, and timing error (performance) were estimated. The timing error was defined as the time difference in seconds between the metronome beats and the corresponding first touch of the upper (E1) and lower (E2) target connectors. Borg's CR-10 showed that fatigue significantly developed from early to late time and gradually across work blocks. The RMS values increased significantly within each block (early vs late time), showed that fatigue significantly developed from early to late time, and gradually across work blocks for both direction. No significant change of the MPF values was found across work blocks, suggesting that the overall MPF had not changed after one hour.

2.5.2 DWT as a Better Tool for Neuromuscular Fatigue Determination

Discrete wavelet transform in SEMG signal analysis lays a foundation for studying the muscle fatigue in a variety of muscle contraction modes. The quantification of the amount of neuromuscular fatigue of the back during repetitive exertions has been performed by using DWT in SEMG signal processing. For this purpose, Sparto et al., (2000) used filter banks and wavelets to determine additional insights into the fatigue process during repetitive isokinetic trunk extension tasks. They also decided which measures were more highly correlated with the decline in maximal trunk extension torque. Trunk muscle electromyograms were collected from 16 healthy men performing repetitive isokinetic trunk extension endurance tests over a four week period. The test was controlled at 35% and 70% of the participants' maximal voluntary contraction while they exerted at 5 and 10 repetitions per minute to induce different rates of fatigue. SEMG data were analyzed using the wavelet and the traditional Short Time Fourier

methods. Linear regression quantified the rate of change in Fourier and wavelet measures caused by fatigue, whereas Pearson's correlation coefficient determined their association with the decline in maximum torque. Six scales of Daubechies wavelet were selected that resulted in adequate coverage of the frequency range expected for SEMG signals (*i.e.*, 5–300 Hz). Wavelet coefficients were computed for each wavelet function and scale during each exertion. The root-mean-square value was calculated for the 1 second of data corresponding to the trunk range of motion between 25° and 10°. RMS torque in the STFT and wavelet measures were quantified using simple linear regression. The statistical analysis of regression reflected that repetition rate is a significant factor that affects the decline in maximal torque. There was a significant decrease in the scale 4 coefficients (209–349 Hz) and a significant increase in scale 32 coefficients (26–44 Hz) and scale 64 coefficients (13-22 Hz) for 10 repetitions. Only 69% of the coefficients at the same scale were significantly increased during the trials of 5 repetitions per minute. The same trends were also observed during STFT. In addition, the decline in maximal torque output was significantly affected by exertion magnitude. The correlations between the rate of change in the RMS value of Daubechies wavelet coefficient and the maximum torque output decline were positive for scale 4 (the high-frequency range) and negative for the other scales. Hence they showed that DWT is a validated tool for quantifying and detecting back muscle fatigue.

The most commonly used parameters describing the spectral content of SEMG, such as Fourier-based mean and median power frequencies, are routinely used to characterize muscle activity and fatigue in many physiologic and pathologic circumstances. The application of the Fourier transform to a data stream is only limited for stationary signal, but for the cases where repetitive or non-constant muscular activity is considered, stationary constraints are violated. Hence the researchers proposed the use of multi-resolution wavelet analysis which provides both temporal and frequency resolution of a signal (Daubechies, 1990). In order to determine the ability of this method, Vukova (2008) investigated fatigue-

induced changes in the spectral parameters of slow (SMF) and fast fatigable muscle fiber (FMF) action potentials using DWT and FFT. Intracellular potentials were recorded during repetitive stimulation of isolated muscle fibers immersed in Ca^{2+}-enriched medium, while extracellular potentials were obtained from muscle fibers pre-exposed to electromagnetic microwaves. The changes in the frequency distribution of the action potentials during the period of uninterrupted fiber activity were used as criteria for fatigue assessment. The results showed a fatigue-induced decrease of potential high frequencies (SMF: 59% vs. 96%, MMW vs. control; FMF: 30% vs. 92%, respectively), and an increase of low frequencies (SMF: 200% vs. 207%, MMW vs. control; FMF: 93% vs. 314%, respectively). They further observed that DWT provides a reliable method for estimation of muscle fatigue onset and progression from data analysis of RMS analysis of the wavelet coefficients.

The frequency characteristics of random signals like SEMG can be studied by power spectrum analysis by using wavelet transform function. These SEMG power spectrums are also varied when different wavelet functions are used and it is not clear which wavelet function offer appropriate results. In a gait analysis using various wavelet functions, Reaz et al. (2006) analyzed SEMG power spectral parameters and compared different wavelet families. In this research, SEMG were decomposed using Discrete Wavelet Transform (DWT) with various wavelet families (WFs) - Haar, Daubechies (db2, db3, db4, db5, db45) and Symlet (sym4, sym5) at Matlab environment. The authors collected 11 separate EMG data files for the 9 trial walks, muscle at rest level, and muscle at maximum contraction level. The power spectrum properties (mean frequency and median frequency) were calculated by using FFT to estimate the muscle contraction at various walking trials. The difference of mean and median frequency is used to analyze the EMG signal to understand the muscle contractions. It was observed that changes in the mean and median frequencies are most significant in db45 to indicate muscle contraction compared to the other seven wavelet functions. The results also indicate a significant increase in SEMG amplitude and mean

power frequency during with the increase in the force. On the other hand, during muscle fatigue, the power spectrum of SEMG shows a shift to lower frequencies. The power spectrum analysis of mean and median frequency verified that wavelet function db45 most significantly presents variation on the power spectrum.

2.5.3 Discrete Wavelet Transform Algorithm

Most of the time, signals are sampled at discrete time points with limited resolution and one must use a very limited number of discrete incremental scales and time translations if they are going to produce an answer in a reasonable amount of time. The discrete wavelet transform (DWT) technique was introduced by Mallat (1989). The DWT provides highly efficient wavelet representation that can be implemented with a simple recursive filter scheme, but provides no redundancy. Moreover, it only produces as many coefficients as there are sampled within the original signal, without the loss of any information at all. Consequently, the DWT permits perfect reconstruction of the original waveform by an inverse filtering operation. In general, the discrete wavelet tools have capabilities for both signal analysis and signal processing, such as noise reduction, data compression, peak detection and so on (Polikar, 2006). A number of studies employed discrete wavelet transform to study Electromyography signal (Hussain, Reaz, Mohd Yasin, & Ibrahimy, 2009; Kanoun & Ali, 2009; Khezri & Jahed, 2008; D. K. Kumar et al., 2003; Moshou, Hostens, Papaioannou, & Ramon, 2005; Phinyomark & Phukpattaranont, 2009; Ranniger & Akin, 1997).

The DWT coefficients are usually sampled on a dyadic grid. Given that the signal is a discrete time function and interchangeable sequence is denoted by X[n], where n is an integer. The DWT is computed by successive low pass and high pass filtering of the discrete time domain signal. First of all, the signal (sequence) will pass through a half band digital low pass filter with impulse response P[n] and filter the signal by convoluting the signal with the impulse response of the filter. The convolution operation in discrete time is defined as follows (Hussain et al., 2009):

$$X\,[n] * P[n] = \sum_{k=-\infty}^{\infty} X[k] * P\,[n-k] \quad (1)$$

To understand the DWT it is necessary to understand a remarkable property of wavelets. It is possible for wavelets to be *orthogonal,* meaning that a subset of a given wavelet family can be chosen from specially selected scales and translations in such a way that none of the scaled and translated wavelets in the subset correlate with each other at all. Such subsets are said to form an orthogonal *basis* for representing real functions. That is, any EMG waveform can be perfectly constructed by adding together point-for-point in time all of the orthogonal wavelets in the subset after correctly setting their individual magnitudes. Hence, the DWT algorithm consists of two phases, the decomposition phase and the reconstruction phase. In 1988, Mallat produced a fast wavelet decomposition and reconstruction algorithm (Mallat, 1989).

2.2.4.1 Discrete wavelet decomposition

The DWT analyzes the signal at different frequency bands with different resolutions by decomposing the signal into a coarse approximation and detail information. DWT employs two sets of functions, called scaling functions and wavelet functions, which are associated with low pass and high pass filters, respectively. The procedure of decomposition starts with passing the signal X [n] through a series of half band high pass filters H[n] to analyze the high frequencies, and passing through a series of half band low pass L[n] filters to analyze the low frequencies. The coefficients resulting from the high pass filter band are known as 'details coefficients' and the coefficients found in low pass filter band are known as 'approximate coefficients'. To obtain additional scales of waveform information, the first detail function is set aside and the approximate coefficients for the low resolution signal after the first filtering operation are fed back through the two filters simultaneously, giving a second set of small-scale wavelet coefficients and a new set of coefficients for the low resolution signal. This procedure can mathematically be expressed as

$$Y_{low}[k] = \sum_n X[n] * L[2k - n] \quad (2)$$

$$Y_{high}[k] = \sum_n X[n] * H[2k - n] \quad (3)$$

In Equation (2) and (3), $Y_{high}[k]$ and $Y_{low}[k]$ are the outputs of the high pass and low pass filters respectively, after down sampling by 2. The above procedure, known as the sub band coding, can be repeated for further decomposition. At every level, the filtering and sub sampling will result in half the number of samples (and hence half the time resolution) and half the frequency band spanned (and hence doubles the frequency resolution) (Hussain et al., 2009; Polikar, 2006).

To illustrate with an example, it is assumed that the signals have 'n' points and 'f' highest frequency and run through high pass filter, H_0, and low pass filter, L_0 whose filter coefficients are uniquely determined by the particular wavelet shape that is to be used in the analysis. Different wavelet shapes are associated with different filter coefficient sequences. The filtering operation can eliminate half of the samples according to Nyquist's rule. The output of each filter is a series of *n* wavelet coefficients. Every other coefficient is discarded from the series, leaving *n*/2 coefficients for each filter output. This process of discarding alternate coefficients is known as down sampling and is indicated by the downward pointing arrow and adjacent ''2'' symbol (Figure 1). The signal now has a highest frequency of f /2 radians instead of f. The low pass filter output captures all of the low frequency energy of the waveform (0 – f/2) and the high pass filter output captures all of the high frequency energy of the waveform (f/2 – f). This constitutes one level of decomposition.

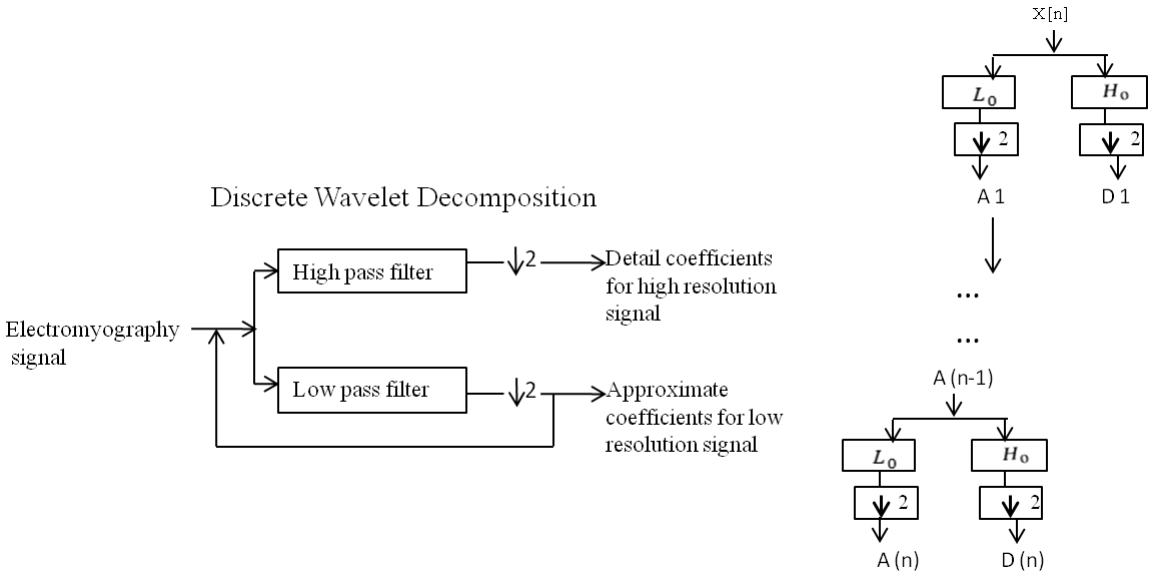

Figure 1: Discrete wavelet decomposition process (Samar, Bopardikar, Rao, & Swartz, 1999).

This signal is then passed through the same low pass and high pass filters for further decomposition. This process continues until two samples are left. The maximum level of decomposition depends on the signal length. If the signal has 'N' number of data points, the maximum level of decomposition will be

$$Q = log_2^N \tag{4}$$

Equation (4) can also be expressed as – $N = 2^Q$.

The maximum level of decomposition is also known as full decomposition. A neuro-electric signal can be decomposed at any level within the maximum level of decomposition, depending on the choice of frequency bands. Each of these wavelet levels correspond to a frequency band. The maximum frequency that can be measured is given by the Nyquist theory as:

$$f_{max} = \frac{f_s}{2} \tag{5}$$

Here f_{max} is the maximum frequency band of the signal if the sampling frequency of the signal is f_s (Parameswariah & Cox, 2002).

In Figure 1, each successive detail function– D1, D2, D3, … D (n) and approximate function – A1, A2, A3,… A (n) has a spectrum with a center frequency (f) and bandwidth (Δf) that is half those of the previous detail function and approximate function. As an example, the frequency of the first level details is $\frac{f_{max}}{2}\ to\ f_{max}$ and the frequency of the first level approximation is $0\ to\ f_{max}$. Thus, frequency resolution improves by a factor of 2 for each successively larger scale in a DWT while time resolution correspondingly decreases by a factor of 2. Conversely, time resolution improves by a factor of 2 at successively smaller scales and frequency resolution correspondingly decreases by a factor of 2. The corresponding frequency band of each level will appear as high amplitudes in that region if these are prominent frequencies in the original signal. On the contrary, the frequency bands that are not very prominent in the original signal will have very low amplitudes, and that part of the DWT signal can be discarded without any major loss of information.

2.2.4.2 Discrete wavelet reconstruction

Since the wavelet transform is a band pass filter with a known response function (the wavelet function), it is possible to reconstruct the original time series using either deconvolution or the inverse filter. This is straight-forward for the orthogonal wavelet transform (which has an orthogonal basis), but for the continuous wavelet transform it is complicated by the redundancy in time and scale. The original EMG signal can be built back up from its wavelet components by adding those wavelet components all up in the correct proportions and with the correct time translations (Torrence & Compo, 1998). The signal reconstruction procedure follows the reverse order of the signal decomposition. Figure 2 represents the schematic diagram of the signal reconstruction where the signals at every level are up-sampled by two, and passed through the synthesis filters $L'[n]$, and $H'[n]$ (low pass and high pass, respectively), and then added.

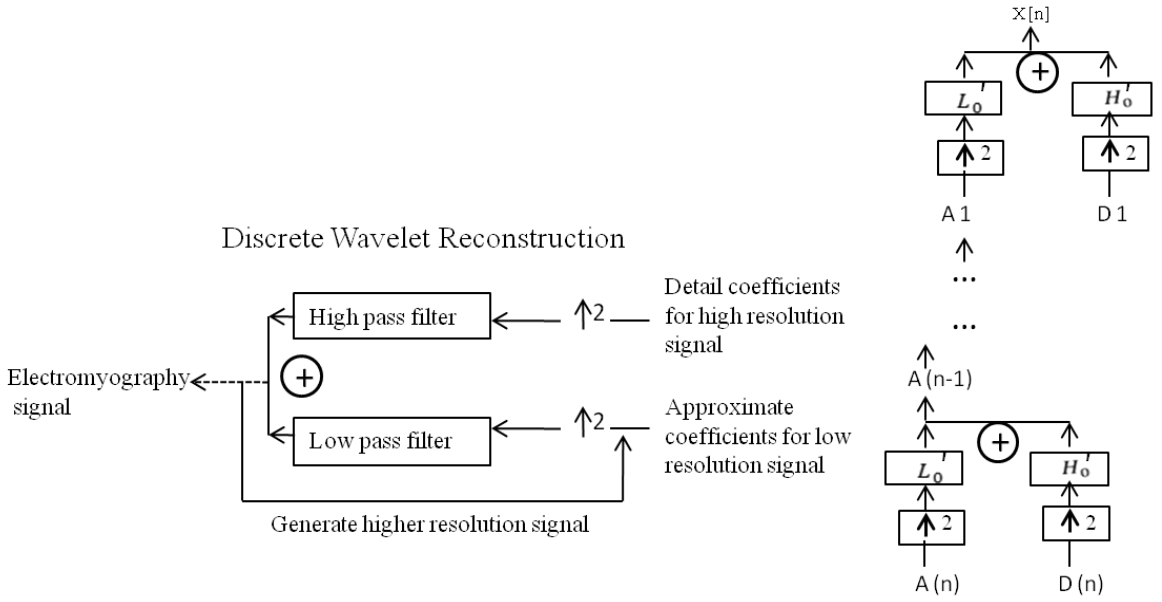

Figure 2: Discrete wavelet reconstruction process (Samar et al., 1999).

Both the analysis and synthesis filters are identical to each other, except for a time reversal. Therefore, the reconstruction formula for each level can be written as:

$$X\,[n] = \sum_{k=-\infty}^{\infty}(Y_{high}[k].\ H[-n+2k]) + (Y_{low}\,[k].L\,[-n+2k]) \quad (6)$$

Regardless of the number of detail functions generated, the total number of wavelet and scaling function coefficients necessary to exactly reconstruct the original waveform always equals the number of original waveform samples. However, if the filters are not ideal half band, then perfect reconstruction cannot be achieved. Although it is not possible to realize ideal filters, under certain conditions it is possible to find filters that provide perfect reconstruction (Samar et al., 1999). Hence, the best wavelet function selection is a very crucial issue in DWT analysis.

CHAPTER THREE: FORMULATION OF STRAIN INDEX AND TASK CATEGORIZATION (AIM 1)

3.1 Background

The shoulder complex is comprised of four major joints: glenohumeral, acromioclavicular, scapulothoracic and sternoclavicular (Figure 3a). The glehonumeral joint is a ball-and-socket joint between the humeral head and the glenoid cavity of the scapula (Figure 3b). The acromioclavicular joint is a joint between the acromial end of the clavicle and the acromion of the scapula. The sternal end of the clavicle and the manubrium of the sternum form the sternoclavicular joint. The scapulothoracic joint is a joint where the scapula meets with the ribs at the back of the chest. Along with shoulder muscles, tendons, and ligaments, these joints provide the shoulder complex its strength and mobility (Culham & Peat, 1993). Among these four joints, the glenohumeral joint is the main joint at the shoulder complex as it provides much of the shoulder mobility. This glenohumeral joint is also known as shoulder joint. It is the most mobile joint in the body, allowing a person to adopt a wide variety of arm postures and facilitating the application of forces in nearly any direction.

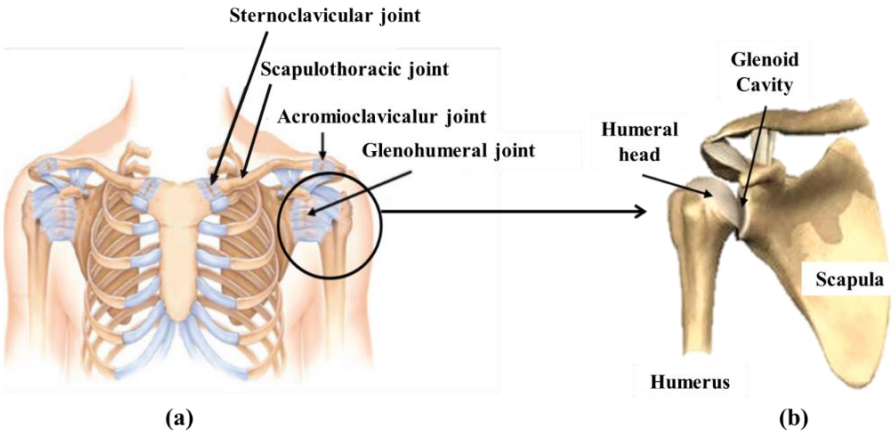

Figure 3: (a) Major anatomical joints of the shoulder complex, (b) the glenohumeral/shoulder joint. Figure is modified based on images from Cutlip (2014).

The shoulder complex is vulnerable to injuries due to high mobility and low stability of the glenohumeral joint (Andrews, Wilk, & Reinold, 2008). The range of motion of the glenohumeral joint covers almost 65% of a sphere (Engin & Chen, 1986). The humerus of the upper arm can be axially rotated at almost any orientation within this sphere (Figure 3b). However, the joint is structurally unstable because of the loose fitting (around 30%) of the humeral head into the glenoid cavity (McCluskey III & Getz, 2000). The stability of this joint is primarily ensured by the coordinated action of the surrounding muscles (S. Lippitt & Matsen, 1993). Shoulder muscles produce a net compressive force through a stabilizing mechanism called concavity compression mechanism that acts against the translational (shear) forces produced by the external loading (Konrad, Jolly, Labriola, McMahon, & Debski, 2006; S. B. Lippitt et al., 1993) (Figure 4a). The magnitude and direction (line of action) of the net compressive force depend on the muscular performance as well as relative posture of the shoulder (McMahon & Lee, 2002; Werner, Favre, & Gerber, 2007). Tasks resulted in high translational reaction forces push the humeral head away from the glenoid centerline (Figure 4b). During such tasks, shoulder muscles create compensatory compressive force and press the humeral head into the glenoid cavity (Figure 4c). A comprehensive understanding of the interplay between the resultant compressive and the translational forces to achieve the concavity compression may provide a basis to understand the contribution required by the shoulder muscles during the workplace exertions.

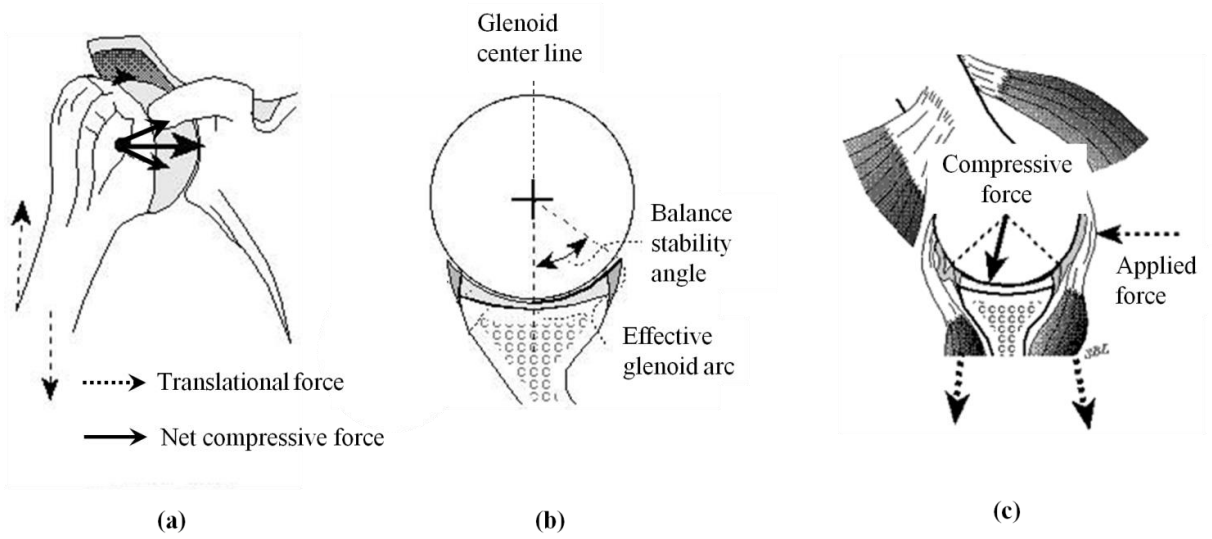

Figure 4: (a) Net compressive force created through concavity compression mechanism, (b) the effective glenoid arc, and (c) the shoulder joint will not dislocate as long as the net compressive force is directed within the net effective glenoid arc (Medicine, 2013).

A few previous studies have used the concavity compression mechanism to investigate the workload of the shoulder joint (Cutlip, 2014; De Looze et al., 2000; C. Dickerson et al., 2007; M. J. Hoozemans et al., 2004; Nimbarte et al., 2013). All of these studies have calculated the reaction forces in a biomechanical model to evaluate the shoulder joint stability. Depending on the line of action, the reaction forces can be classified as: medial-laterally directed force, superior-inferiorly directed force, and anterior-posteriorly directed force. Lippitt et al, (1993) suggested that higher translational forces (in the inferior-superior and anterior-posterior directions) destabilize the shoulder joint whereas higher compressive forces (in the medial-lateral direction) help to stabilize the shoulder joint. They have quantified the ratio between the translational forces and the compressive forces to measure the stability of the shoulder joint. Hoozemans et al., (2004) evaluated the mechanical load on the shoulders during cart pushing and pulling tasks by investigating the compressive forces at the shoulder joint. They found a large increase in the compressive force with an increase in cart weight. The study however did not evaluate the translational forces acting in the sagittal or transverse planes with the consideration that the compressive force in the

frontal plane is a suitable measure. In another study, De Looze et al., (2000) investigated the changes in force direction of pushing and pulling as result of changes in handle height and force level. They found that the shoulder loading rises as the force exertion rises. They also found that the variations in the shoulder loading were due to the variations in the force directions. Similar to ball and socket joint, Poppen and Walker (1978) suggested that the shoulder joint is most stable with compression forces directed through the center of the joint and less stable when the force has a large translational component that promotes translation of the ball within the socket. According to the theory of concavity compression mechanism, the shoulder joint requires the surrounding musculature to reduce the net translational strain (Savoie, 2015). Therefore, precise estimation of the concavity compression mechanism requires both magnitude and direction of the joint reaction forces to accurately represent the loading at the joint during physically demanding exertions.

The direction of the resultant of the compressive and the translational reaction forces can be measured using the inverse tangent function. The direction should be measured with respect to the medial-lateral direction since shoulder muscles press the humeral head to the glenoid center line to stabilize the joint (Figure 4b). Tasks result in higher angular deviations from the glenoid center line may indicate higher likelihood of shoulder instability (Figure 4c). Similarly, the magnitude of the resultant compressive force is also important to understand the amount of effort the shoulder muscles produce to stabilize the joint. Therefore, an index that combines both magnitude and angular deviation of the resultant compressive force can allow estimation of efforts by the shoulder muscle to achieve the concavity compression.

3.2 Objectives

There are two objectives in this aim:

Objective 1: To develop a strain index based on the concept of concavity compression. Resultant of the reaction forces generated by the muscles to achieve the concavity compression were used to formulate a strain index.

Objective 2: Using the strain index, several material handling tasks were analyzed to classify them into low, medium and high strain tasks.

Work exposures for the shoulder complex vary drastically between the industries from repetitive submaximal force exertion to forceful exertions (Dunning et al., 2010; Putz-Anderson et al., 1997) to confined awkward postures (Bernard, Putz-Anderson, & Burt, 1997). Confined awkward postures, especially the work exertions performed over the shoulder postures were evaluated extensively in the previous studies (Bjelle, Hagberg, & Michaelson, 1981; Ebaugh et al., 2006; Grieve & Dickerson, 2008; Haslegrave, Tracy, & Corlett, 1997; Sakakibara et al., 1995; Wiker, Chaffin, & Langolf, 1989). Working over the shoulder level has been linked to a multitude of negative physiological and biomechanical consequences, with increased intramuscular pressure, impaired circulation, and fatigue development (Bjelle et al., 1981; Chopp, O'Neill, Hurley, & Dickerson, 2010; Ebaugh et al., 2006; Grieve & Dickerson, 2008). Studies that look at the work exposures performed below the shoulder level are sparse. Submaximal exertions performed under the shoulder level are common among various industries such as construction, healthcare, pharmaceuticals, transportation, warehousing, light assembly, and packaging industries. To achieve objective 2, multiple submaximal material handling exertions performed at several vertical and horizontal work locations were evaluated using the strain index.

3.3 Methods

3.3.1 Approach

To achieve objective 1, a well-established biomechanical model of upper body was used. The model outputs such as direction and magnitude of the resultant reaction forces in three anatomical

directions were used to develop the strain index. To achieve objective 2, human participants were recruited to perform material handling tasks in the laboratory setting. Joint kinematics during the material handling tasks were measured using an optical motion capture system. The kinematic data were used as inputs to the biomechanical model. Model output were used to estimate the strain index values for the different material handling tasks.

3.3.2 Strain Index Formulation

The coordinated action of shoulder muscles compresses the humeral head into the glenoid cavity to achieve concavity compression required for the joint stabilization. The compressive force (F_c) in the medial direction improves the concavity compression. The translational forces in the inferior-superior ($F_{I/S}$) and anterior-posterior ($F_{A/P}$) directions put additional stabilizing demand on the shoulder muscles, as these forces destabilize the joint by working against the concavity compression. Figure 5 shows the schematic representation of the process. Higher the translational forces in the inferior-superior ($F_{I/S}$) and anterior-posterior ($F_{A/P}$) directions, more the humeral head is pushed away from the glenoid center line and therefore higher the demand on the shoulder muscles to produce compressive force (F_c) required for concavity compression.

Thus, to achieve the concavity compression required for the joint stabilization, the compressive forces in the medial direction are always higher than the translational forces in the inferior-superior and anterior-posterior directions. The interaction between these forces was used to develop a strain index. Magnitudes and directions of these forces were used in the computation of the strain index based on two assumptions: (1) higher stress (due to external force, awkward posture) would result in higher magnitudes of the internal forces; (2) higher stress (due to external force, awkward posture) would result in higher decentralization of the resultant force vectors, i.e., higher deviation from the medial direction in the frontal and transverse planes.

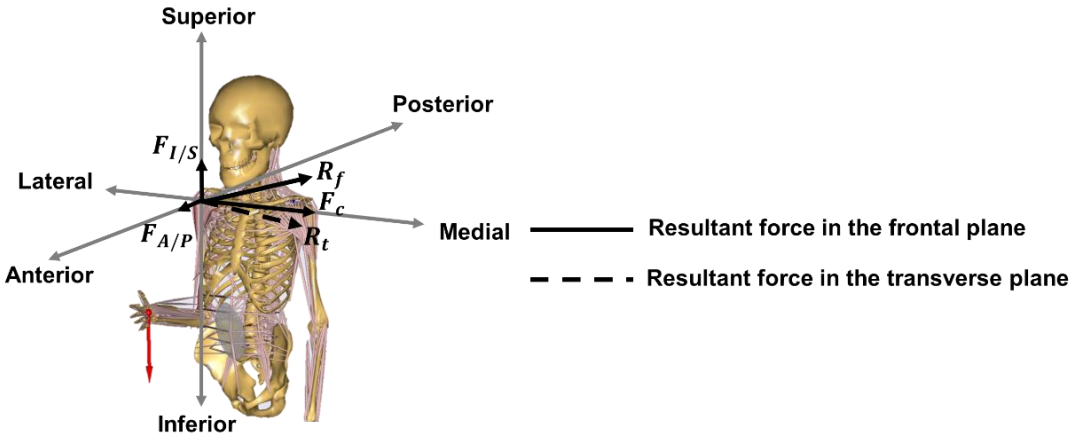

Figure 5: The joint reaction forces to stabilize the shoulder joint

The resultant of the compressive force and the translational force in the inferior-superior direction ($F_{I/S}$) is directed in the frontal plane (Figure 6a). Similarly, the resultant of the compressive force and the translational force in the anterior-posterior ($F_{A/P}$) direction is directed in the transverse plane (Figure 6b). The direction of these resultant forces can maximally be directed 45° from the medial direction, as compressive force is always higher than the translational forces in the inferior-superior and anterior-posterior directions.

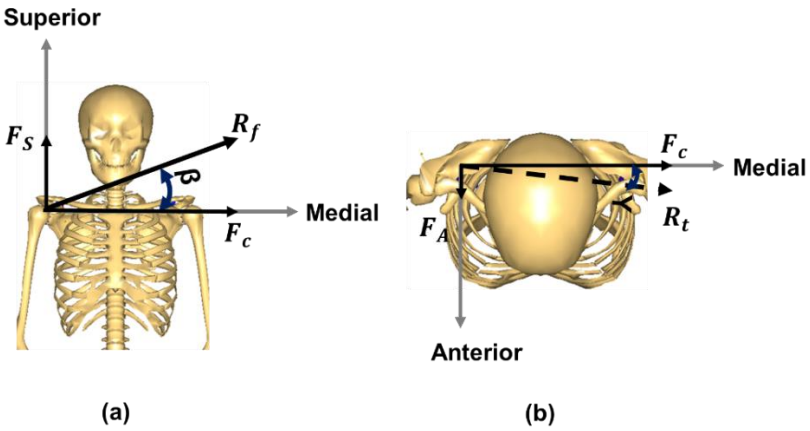

Figure 6: (a) The resultant force in the frontal plane (b) the resultant force in the transverse plane

The magnitudes of the resultant forces in the inferior-superior and anterior-posterior directions were computed using Equation (7) and Equation (8), respectively (Figure 6).

$$R_f = \sqrt{F_c^2 + F_{I/S}^2} \quad (7)$$

$$R_t = \sqrt{F_c^2 + F_{A/P}^2} \quad (8)$$

Where, R_f was the resultant force in the frontal plane.

R_t was the resultant force in the transverse plane.

F_c was the compressive force in the medial direction.

$F_{I/S}$ was the transverse forces in the inferior (I) and superior (S) directions.

$F_{A/P}$ was the transverse forces in the anterior (A) and posterior (P) directions.

R_f and R_t were calculated for the individual tasks as well as for the MVC exertions. The decentralization of the resultant force vector, i.e., angular deviations of the R_f and R_t in the frontal and transverse planes were calculated using Equation (9) and Equation (10), respectively.

$$\beta = tan^{-1}\left(\frac{F_{I/S}}{F_C}\right) \quad (9)$$

$$\gamma = tan^{-1}\left(\frac{F_{A/P}}{F_C}\right) \quad (10)$$

Where, β was the angular deviation of the resultant force in the frontal plane

γ was the angular deviation of the resultant force in the transverse plane

To standardize R_f and R_t between the participants, normalizations were performed using Equation (11) and Equation (12), respectively.

$$N_f = \left(\frac{R_f}{R_{f-MVC}}\right) \quad (11)$$

$$N_t = \left(\frac{R_t}{R_{t-MVC}}\right) \quad (12)$$

Where, N_f was the normalized force in the frontal plane.

N_t was the normalized force in the transverse plane.

R_{f-MVC} was the resultant forces during MVC exertion in the frontal plane.

R_{t-MVC} was the resultant forces during MVC exertion in the transverse plane.

Similarly, the angular deviations of the resultant forces were normalized by the maximum angular deviation of 45° using Equation (13) and Equation (14), respectively.

$$A_f = \left(\frac{\beta}{45}\right) \tag{13}$$

$$A_t = \left(\frac{\gamma}{45}\right) \tag{14}$$

Where, A_f was the normalized resultant force direction in the frontal plane.

A_t was the normalized resultant force direction in the transverse plane.

The strain index (I_f) in the frontal plane was estimated by multiplying the normalized force and the normalized direction in the frontal plane (Equation 15).

$$I_f = \left(N_f \times A_f\right) \times 100 \tag{15}$$

Similarly, the strain index (I_t) in the transverse plane is estimated by multiplying the normalized force and the normalized direction in the transverse plane (Equation 16).

$$I_t = (N_t \times A_t) \times 100 \tag{16}$$

To change the scale of the variable, Equation (15) and Equation (16) are multiplied by 100. Based on the direction of the resultant forces, the values of the angular deviations could be positive or negative. In Anybody modeling software, the posterior and the superior directions are positive. Therefore, a negative value of the strain index (I_f) in the frontal plane signifies that the translational force is directing towards the inferior direction. Similarly, a negative value of the strain index (I_t) in the transverse plane signifies that the translational force is directing towards the anterior direction. The strain index for a task was calculated by summing the absolute values of the two strain indices (Equation 17).

$$I = |I_f| + |I_t| \tag{17}$$

The possible value of the strain index (I) ranges from 0 to 100. Higher value of the strain index (I) indicates higher strain on the shoulder complex.

3.3.3 Participants

Eight healthy male participants were recruited to participate in this study. The primary inclusion criteria used in this study required that the participants to be free from any type of musculoskeletal, degenerative or neurological disorders and have no history of neck, back, and shoulder injury or notable pain. The Physical Activity Readiness Questionnaire (PAR-Q, Canadian Society for Exercise Physiology) was used to screen participants for cardiac and other health problems (e.g., dizziness, chest pain, heart trouble) (Appendix A). Participants who met the inclusion criteria were asked to read and to sign a consent form approved by the local Institutional Review Board (Appendix B).

Based on the findings of our preliminary study, statistical power and sample size calculations were made. The number of participants was determined based on the variance of the error (σ) in the strain index values observed for three planes (α =3). The statistical power was estimated using the operating characteristics curves (OC curves) based on the following equation:

$$\varphi = \sqrt{\frac{nD^2}{2a\sigma^2}} \tag{18}$$

Where φ was noncentrality parameter.

N was the number of blocks (participants).

D was maximum differences we want to detect between strain indices values for different planes.

α was the number of planes.

σ^2 was the estimate of the variance.

The numerator and denominator degrees of freedom in Equation (18) are $v_1 = \alpha - 1$ and $v_2 = (\alpha\text{-}1) \times (n\text{-}1)$, respectively. The D and σ^2 values were calculated based on the data recorded during the

preliminary study (n=3) and they were 9.58 and 4.48, respectively. The significance level was set at $\alpha = 0.05$. The β risk and the power (1- β) of the test are provided in Table 1. The calculations showed that a sample size of three provided a β risk of about 0.42. Increasing the sample size to 8 decreased the β risk to 0.018 and the corresponding power of the test became 98.2%. Therefore, eight subjects were sufficient to insure sufficient statistical power.

Table 1: The β risk and sample size calculations for Aim 1.

n	$\nu 1$	$\nu 2$	φ	β	Power (1- β)
3	2	4	1.85	0.420	0.580
6	2	10	2.62	0.080	0.920
7	2	12	2.82	0.035	0.965
8	2	14	3.02	0.018	0.982

3.3.4 Apparatus/Tools

The following pieces of equipment were used in this research:

3.3.4.1 Custom-built workstations

To simulate the material handling tasks a custom-built workstation was used. This workstation consists of two wood structures (Figure 7). First wood structure was placed in the mid-sagittal plane, and the second one was placed such a way that one end was in the frontal plane and the other end was at 45° right to mid-sagittal plane. Height adjustable ropes were used to designate work surfaces. Based on the participants' anthropometry, the ropes were positioned at the shoulder, mid upper arm, elbow, and trochanterion heights during the completion of the experimental tasks. STr

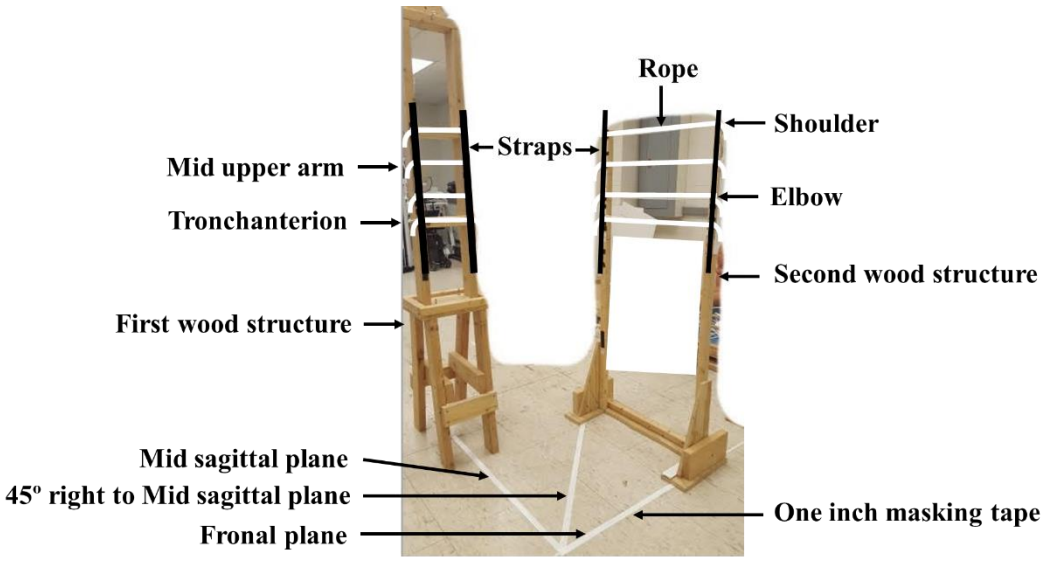

Figure 7: The custom-built material handling workstation.

3.3.4.2 Optical Motion Capture System

Vicon motion capture system (MX-Series, Vicon Motion System, Oxford, UK) was used to capture the motion data during material handling tasks. The system consists of eight optical cameras, retro-reflective markers (14 mm in diameter), and a data-station.

Figure 8: Parts of Vicon motion capture system: (a) infrared camera, (b) data station, and (c) retro-reflective marker

The optical camera with infrared strobes (Figure 8a) emits infrared light which reflects off of the retro-reflective markers (Figure 8b). The cameras capture the reflected light and the locations of the

markers are recorded in 3D space. The data-station (Figure 8c) collects the data from the cameras and sends it to the computer. The marker data were sampled at 100 Hz.

3.3.4.3 Pulling exertion device

A custom-made isometric force exertion device was used to exert the maximum voluntary contraction. The device consists of a 2 inches wide slotted steel bar attached to Lidolift work set and an advanced digital force gauge (Mark-10 Corporation, NY, USA) with a single handle attachment (Figure 9). The force gauge and single-handle attachment connected with the slotted steel bar using an ergonomic padded attachment. The vertical height of the steel bar can vertically be adjusted in the Lidolift work set and can be locked at any vertical position.

Figure 9: Custom made pulling exertion device: (a) subject exerting maximum force, (b) Mark 10 hand dynamometer, and (c) padded attachment

3.3.4.4 Motion analysis software

The Vicon Nexus 1.8.1 software (Vicon Motion Labs, Oxford, UK) was used for recording and processing the marker data to compute three dimensional coordinates. A total of twenty retro-reflective markers were used to model the hand, arm, shoulder, and trunk segments. A three-dimensional representation of the markers is shown in Figure 10. After capturing the data, the software was used to

label the markers. Each marker had its' unique name to represent where it was located on the body. For example, the marker located on the lateral side of the right elbow area was named as RLELB.

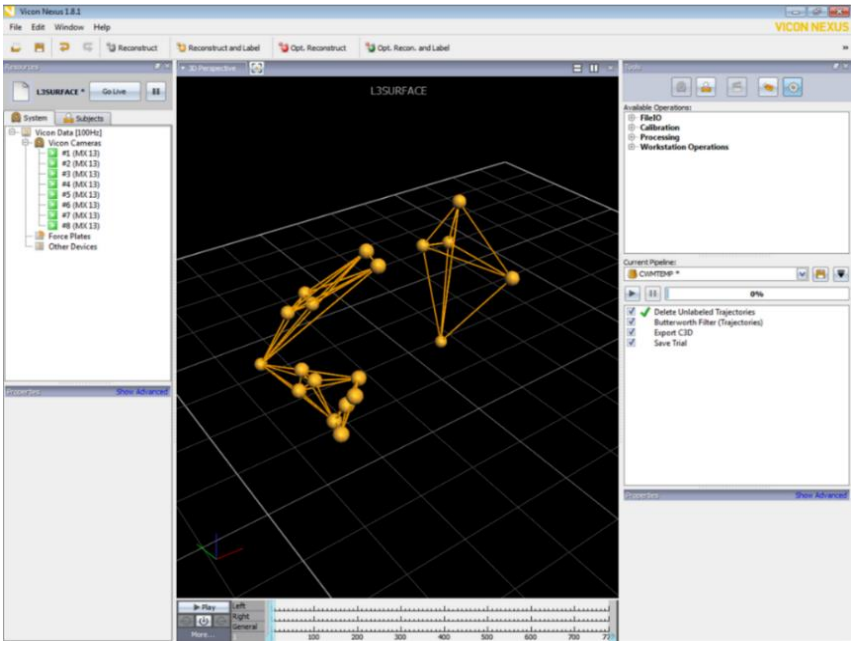

Figure 10: Real-time 3D perspective view in Nexus 1.8.1 software. This view can be panned, zoomed, and rotated in any direction.

After labeling the markers, the software was used for performing additional processing steps such as gap filling and filtering. Finally, the trajectory data of each trial was exported and saved as .c3d files.

3.3.4.5 Kinematic computation software

Visual3D 4.89 (C-Motion Inc, Germantown, MD, USA) software was used to model and to analyze the three-dimensional marker data. The hand, arm, shoulder, and trunk of each trial were modeled as rigid segments. In-built functionality of this software allowed the computation of 3D anatomical joint angles by calculating Euler rotations between the local coordinate frames of the relevant segments.

3.3.4.6 Biomechanical modeling software

The resultant reaction forces acting at the shoulder joint during the material handling task was estimated using the AnyBody Modeling System™ (version 5.0, AnyBody Technology, Aalborg, Denmark). This is an object oriented full-body biomechanical modeling system where models are formulated using AnyScript modeling script to define and model bones, joints, and muscle-tendon units. The model can be driven by experimentally obtained kinematic data from motion capture systems and kinetic data from force plates. The model can handle body model for a given environment. The environment is defined in terms of external forces, geometric boundary conditions and even mechanical elements of a product/machine it interacts with. Any kind of posture or motion for the human and environment – either from scratch or from a set recorded motion data can be imposed to calculate mechanical and dynamical properties for the body-environment system (AnyBody, 2015). The model allows the user to simulate the unique anthropometric characteristics of each participant. Moreover, one can obtain results on individual muscle forces, joint force and moments, metabolism, elastic energy in tendons, antagonistic muscle actions and so on (AnyBody, 2016).

Many other available software packages deal with modeling of the body. Many of these are merely geometric models, occasionally referred to as digital manikins such as Jack and eM-Human by UGS, Human Builder by Safework, and Ramsis by Human Solutions. On contrary, musculoskeletal modeling capabilities are only found in a limited number of available systems. As for example, SIMM/FIT by Musculographics Inc., BRG.LifeModeler by Biomechanics Research Group, Inc. and Armo by G-sport, Inc, and AnyBody by AnyBody Technology. All of them provide similar muscle recruitment analysis, however AnyBody modeling system provide more model building interfaces than others (Damsgaard, Rasmussen, Christensen, Surma, & De Zee, 2006). Moreover, it is also capable of estimating both

individual and total muscle forces using the inverse dynamic analysis and resolving the fundamental indeterminacy of the muscle configuration.

The AnyBody models assumed the musculoskeletal system to be a rigid-body system, allowing standard methods of multibody dynamics to be applied. However, the muscles consist of soft tissue and hence, the model neglects effects such as the wobbly masses of soft tissues (Damsgaard et al., 2006). Moreover, the muscles are activated by the central nervous system by mechanism, which are not considered for detailed modeling in AnyBody modeling system. On contrary, AnyBody modeling is based on some kind of optimality conditions. The problem is that there are more muscles than necessary to drive the degrees of freedom of the musculoskeletal system, which suggest that infinitely many muscle recruitment patterns are possible from a dynamical point of view. In AnyBody modeling system, four muscle recruitment strategies such as linear, quadratic, polynomial and min-max are used to operate the muscle activation. In this study, quadratic muscle recruitment strategy was considered to estimate the joint reaction forces at the right shoulder joint.

A biomechanical model of the shoulder complex was used to quantify the loading placed on the shoulder joint. This model is a part of the public-domain model repository provided by the AnyBody Modeling System™ (Figure 11). It consists of 118 muscle fascicles on each side of the body (left and right) and defined the three main shoulder complex joints: the glenohumeral joint, the acromioclavicular joint, and the sternoclavicular joint (Cutlip, 2014). The muscle forces required to generate motion or sustain body posture are computed using inverse-dynamic methods by solving a multi-body dynamics problem where the unknown internal forces were computed using known external motion and forces (Damsgaard et al., 2006).

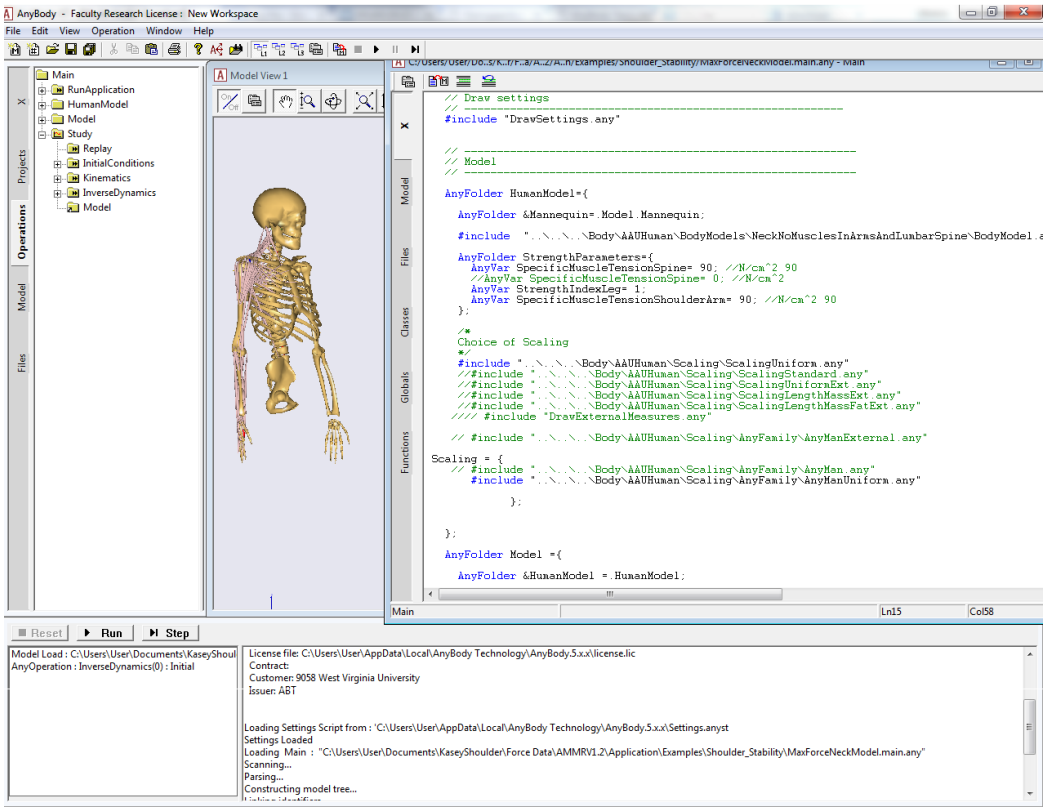

Figure 11: AnyBody biomechanical modeling software interface.

3.3.5 Experimental Design

After studying material handling activities commonly found in different industries (Figure 12), thirty tasks within the right hand reach volume were finalized. These tasks involve transferring (handling) material between a work surface at 30% of the thumb-tip reach (close to body) and another work surface at 100% of the thumb-tip reach (Figure 13). The work surfaces were maintained at four vertical positions – shoulder, elbow, mid upper arm, and trochanterion heights, in three different planes – mid-sagittal plane, frontal plane, and 45 degree right to mid-sagittal plane (Figure 13). All the tasks were performed using a 2 lb dumbbell. The rationale for simulating multiple material handling tasks was that the tasks can be compared with each other using the strain index values. To run the biomechanical model, joint kinematics recorded during the material handling tasks were required as inputs. Considering the simplistic nature of motion involved during these tasks, very little variation was expected between the same tasks. Therefore, each task was performed only once and

the joint kinematics were recorded. The order of the material handling tasks was randomized between the participants.

Figure 12: Material handling tasks common in different industries

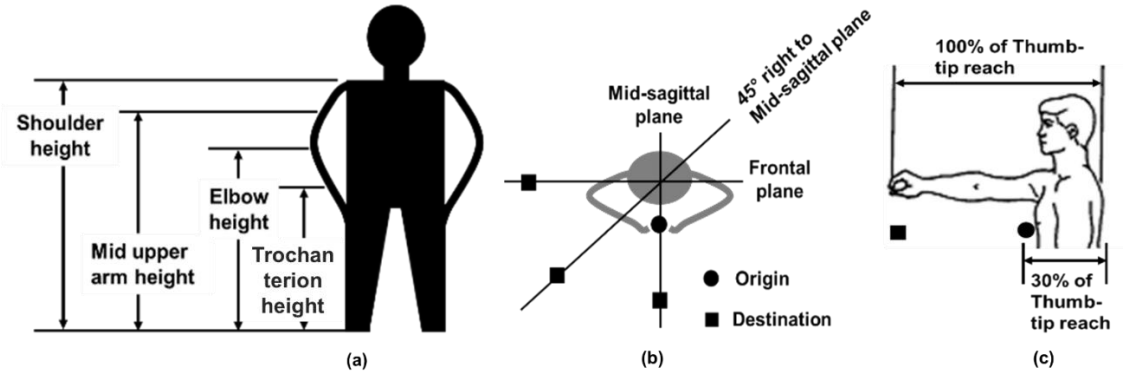

Figure 13: (a) Vertical positions (task heights), (b) task planes, and (c) horizontal positions (thumb-tip reach)

3.3.6 Experimental Procedure

Each eligible participant was provided information on the equipment and experimental tasks. After obtaining their consent, the demographic (race, ethnicity, and age) and anthropometric measurements

(height and weight) were recorded. The other anthropometric measurements included shoulder, mid upper arm, elbow, and trochanterion heights. The work surfaces were adjusted according to a participants' anthropometry. To track the shoulder kinematics, a total of twenty markers were affixed to specific landmarks of the body – five in hand segment, five in lower arm segment, five in upper arm segment, and five markers were placed in trunk segment (Figure 14). Once all the markers were placed on the participant, a 5 second static calibration trial was recorded. One general warm-up trial was then performed for each task.

Figure 14: Retroreflective markers placed on a participant.

Next, the participant was asked to complete the material handling tasks. Individual material handling task consisted of transferring material from a work surface close to the body (at 30% of thumb-tip reach) to a work surface at the farthest away from the body (at 100% of thumb-tip reach) and back to the work surface close to the body. The tasks were performed between the work surfaces at the same height level or from low to high height levels (trochanterion to elbow or elbow to shoulder) (Figure 15 & Table 2). To ensure the work surfaces close to the body, the participants were asked to place their left hand at the corresponding vertical heights (Figure 15).

(a) At same height level

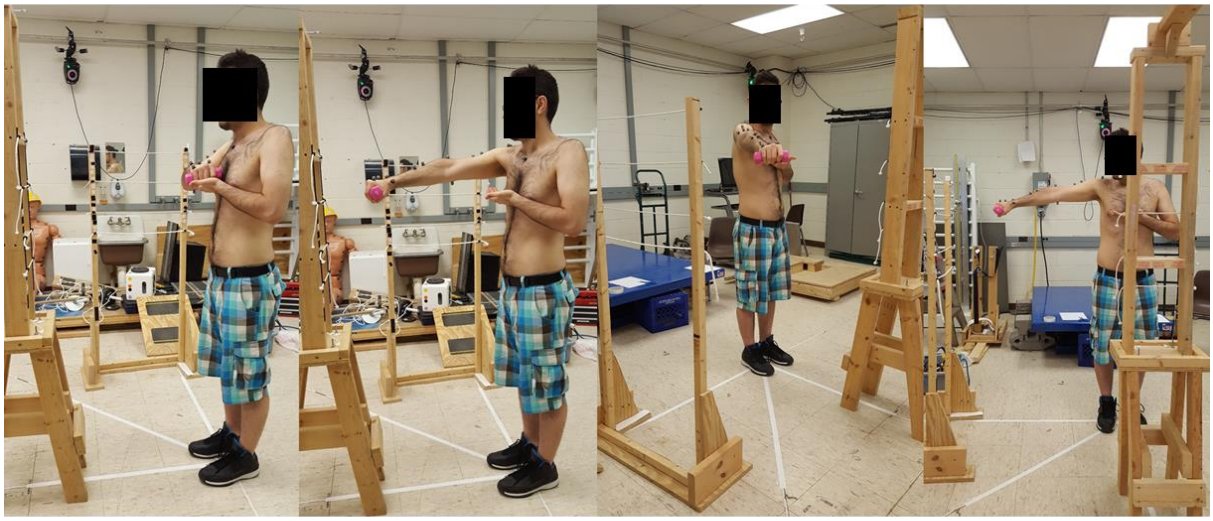

(b) From low to high height level

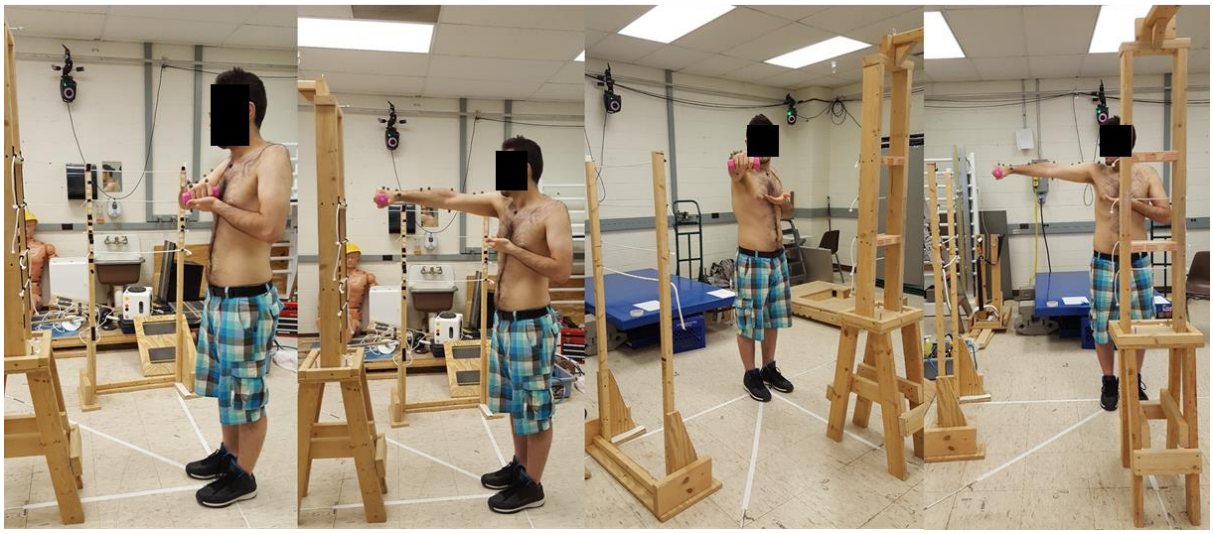

Figure 15: Schematic representation of the material handling tasks during motion data collection: (a) tasks performed at same height level, and (b) tasks performed from low to high height levels.

Table 2: Material handling tasks performed in different planes. At each plane, 10 tasks were performed. The check (√) symbol denotes heights of work surfaces for different tasks.

		Ending height			
Starting height		Mid-sagittal plane			
		Trochanterion	Elbow	Mid-upper arm	Shoulder
Mid-sagittal plane	Trochanterion	√	√	√	√
	Elbow		√	√	√
	Mid-upper arm			√	√
	Shoulder				√
		45° right to mid-sagittal plane			
Mid-sagittal plane	Trochanterion	√	√	√	√
	Elbow		√	√	√
	Mid-upper arm			√	√
	Shoulder				√
		Frontal plane			
Mid-sagittal plane	Trochanterion	√	√	√	√
	Elbow		√	√	√
	Mid-upper arm			√	√
	Shoulder				√

Then, the participants were asked to exert a maximum voluntary exertion (MVC) using Mark-10 hand dynamometer. During the MVC exertion, participants were asked to maintain least amount of abduction and elbow flexion, but shoulder flexion of 90º and hand pronation at 45º.

3.3.7 Data Analysis

3.3.7.1 Motion data

The marker data of each task cycle were processed by first labeling the markers with its unique identifier (i.e. RELB for right elbow) in Vicon nexus software. After all the markers were labeled, gaps in the marker data were filled by selecting one of the following gap filling algorithms: pattern-fill, split-fill and Woltring gap-filling. While the pattern-fill and split-fill algorithms are used to fill one gap at a time, the Woltring gap-filling algorithms can fill longer (up to 5 frame limit) gaps. The marker data was then exported as XYZ coordinates to use in further analysis.

The processed 3D marker data was exported to Visual 3D software to calculate the joint kinematics. Three rigid segments – lower arm, upper arm, and trunk were modeled using the marker data. The elbow rotation was measured by calculating Euler rotations of the lower arm with respect to the upper arm segment. Similarly, the upper arm and the trunk rotations were calculated from the Euler rotations respect to the trunk segment and the Lab coordinates, respectively. The Euler rotations of the lower arm provided elbow flexion, and elbow pronation /supination. The Euler rotation of the upper arm provided flexion/ extension, internal/external rotation, and adduction/abduction of the shoulder. Similarly, the Euler rotation of the trunk segment provided flexion/extension, left/right lateral bending, and left/right rotation of the trunk segments. The kinematic data was exported to the AnyBody software to run the biomechanical model.

3.3.7.2 Anybody biomechanical modeling

The biomechanical model was scaled using the individual anthropometrical data. The force and joint kinematics recorded during the tasks were provided as inputs to the biomechanical model. The quadratic muscle recruitment was used in the inverse dynamics process, because it agrees more precisely with the experimental measurements of muscle activity compared to other muscle recruitment procedures provided by AnyBody Modeling System (AnyBody, 2015). The outcomes of the biomechanical analysis included the reaction forces acting on the right shoulder joint in the following anatomical directions: distraction (medial-lateral), inferior-superior, and anterior-posterior.

3.3.7.3 Strain index calculation:

The strain index (I) was calculated at each data point (t) of the entire task cycle (t = 1…n). The mean strain index (I_{avg}) was also determined by averaging the strain indices of the entire task cycle.

$$I_{avg} = \frac{1}{n} \sum_{t=1}^{t=n} I_t \quad (19)$$

3.3.8 Statistical Analysis

The descriptive statistics such as average and standard deviation of the strain index were calculated across the participants. Based on the average values of the strain index, tasks were categorized into three categories - high, medium, and low strenuous tasks. The lower and higher ends of the range were categorized as low and high strenuous tasks, respectively. The 68-rule in statistics were used to determine the lower and higher ends of the range. The lower end was determined by calculating the mean and subtracting one standard deviation of the range. Similarly, the higher end was determined by adding one standard deviation with the mean of the range. Tasks resulted in strain index values around the median of the range were categorized as the medium strenuous tasks. Data failed to follow normal distribution, and hence, the Mann-Whitney non-parametric statistic was computed to test

whether the selected tasks of low, medium and high strain index values were significantly different from each other. A P-value ≤ 0.05 was considered to be statistically significant. All statistical analyses were performed using Minitab 17 (Minitab Inc., PA, USA).

3.4 Results

As explained in the experimental protocol (section 3.3.5) and the procedures (section 3.3.6), eight participants performed thirty different material handling tasks using a weight of 2 lbs. The demographic and the anthropometric measurements of the participant appear in Table 3. The individual demographic and physical measurement are provided in Appendix C. The units of age, weight, and height were years, pounds (lb) and inch (in), respectively. All the values are reported as mean (±standard deviation). Error bars in the figures represent associated standard deviation value.

Table 3: The demographic and physical measurement data for Aim 1.

Age	28.50 (±3.55)
Weight	165.13 (±17.01)
Height	69.25 (±1.49)
Tronchanterion	38.13 (±1.73)
Elbow	43.81 (±1.60)
Mid upper arm	51.00 (±1.46)
Shoulder	58.19 (±1.49)

Please refer to Appendix D for the mean strain index values of the individual participants. The mean strain index values of the individual tasks ranged from 11.16 to 22.29 (Table 3). Using the 68-rule, tasks with strain index less than 14.82 were categorized as low strain tasks, and with index values higher

than 20.46 were categorized as high strain task. The median strain index value was 17.00. Tasks with index value around the median values were categorized as the medium strain tasks.

Table 4: Mean strain index of the tasks. Dagger (†) denoted low strain tasks and double dagger (‡) represented high strain tasks.

Vertical positions	Mid-sagittal plane	45° right to mid-sagittal plane	Frontal plane
Trochanterion to trochanterion	12.63 (±4.36)†	11.16 (±4.20) †	10.82 (±4.02) †
Elbow to elbow	14.95 (±5.35)	14.47 (±4.39) †	15.22 (±3.35)
Mid upper arm to mid upper arm	19.63 (±3.65)	18.08 (±4.09)	18.75 (±4.15)
Shoulder to shoulder	20.43 (±4.16) ‡	19.43 (±3.92)	20.36 (±4.23) ‡
Trochanterion to elbow	16.75 (±4.62)	15.70 (±5.56)	16.05 (±5.09)
Trochanterion to mid upper arm	17.86 (±5.18)	17.29 (±5.77)	17.31 (±5.14)
Trochanterion to shoulder	18.86 (±4.94)	17.87 (±3.62)	17.50 (±3.96)
Elbow to mid upper arm	21.23 (±5.05) ‡	19.67 (±4.73)	19.59 (±3.75)
Elbow to shoulder	18.69 (±3.54)	17.76 (±3.64)	17.75 (±2.91)
Mid upper arm to shoulder	22.29 (±3.96)‡	19.97 (±4.00)	21.10 (±3.67) ‡

Three tasks were selected such a way that the tasks were significantly different from each other across the participants. The tasks performed between the work surfaces from the mid upper arm height to shoulder height in the mid-sagittal plane (I_{avg} = 22.29) was selected as a high strain task. The task performed between the work surfaces from the tronchanterion height to elbow height in the frontal plane (I_{avg} = 16.05) was selected as medium strain task. The task performed between the work surfaces from the tronchanterion height to tronchanterion height in the 45° right to mid-sagittal plane (I_{avg} = 11.16) was

selected as low strain task. The nonparametric test using Mann-Whitney demonstrated that high strain tasks were significantly higher than medium ($p = 0.012$) and low strain ($p = 0.001$) tasks, respectively. The medium strain task was also significantly higher than the low strain task ($p = 0.026$) (Appendix E).

3.5 Discussion

In Aim 1, a strain index was developed to quantify the concavity compression of the shoulder joint during dynamic exertions. The biomechanical measurements such as magnitude and direction of the resultant joint forces were used in the formulation of the strain index. The index was then utilized to classify different material handling tasks into low, medium and high strain tasks.

The strain index is an estimation of shoulder muscle loading. A high strain index value signified either high magnitude or high angular deviation or both for the resultant reaction forces in the shoulder joint. The resultant reaction forces are the direct measures of the loading on the shoulder muscles as they attempt to stabilize the joint against the translation caused by external loading. Several previous studies have observed that the joint forces are directly associated with the risk of shoulder injury (C. R. Dickerson, Martin, & Chaffin, 2006; Favre, Jacob, & Gerber, 2009; Nimbarte et al., 2013). In a reaching task study, Dickerson et al. (2006) observed that shoulder torque values were significantly related to increased load. Similarly, Nimbarte et al.(2013) observed higher compressive forces at the shoulder joint with the increase in the external load for the cart pushing tasks. The results obtained from the strain index value of the present study not only supported the findings of these studies but also provided important additional insight as it incorporated the magnitude and direction of both compressive and translational forces.

The hand reach position influenced the strain index values, i.e. concavity compression of the shoulder joint. In this study, the minimum and the maximum strain index values across the tasks were observed when the hand position was close to the body (at 30% of thumb-tip reach) and far away from

the body (100% of thumb-tip reach), respectively. In general, the shoulder angle, i.e. abduction or flexion or rotation increases if the hand position moves away from the body. As shoulder angles increase, the moment arm also increases (Lim, Jung, & Kong, 2011). To counteract the increasing moment arm, muscles work duress to stabilize the shoulder joint. As a result, the magnitudes of both compressive and translational forces increased as the hand moved away from the body. Results obtained in the present study are consistent with recent experimental studies though they have used entirely different methodologies (Anton et al., 2001; C. Dickerson et al., 2007; Hall & Dickerson, 2010). Dickerson et al. (2007) estimated the shoulder loading using a 3-D mathematical model of the human shoulder during several reaching tasks. They observed that the resultant dynamic torque experienced at the shoulder complex were higher for far reaching targets than near reaching targets. In another study, Hall and Dickerson (2010) measured shoulder moment using inverse dynamic biomechanical shoulder model and observed higher shoulder moments during load displacement tasks at 90% of arm reach than 60% and 30% of arm reach.

Increase in the vertical heights also affected the strain index values. As for example, the mean strain index value of the tasks performed at shoulder height were 9.24%, 18.37%, and 36.12% higher than the mean strain index values of the tasks performed at mid upper arm, elbow, and tronchanterion heights, respectively. This is most likely due to increases in shoulder angles i.e. abduction or flexion or both while elevating the arm vertically. While the arm was abducted or flexed or both, the effect of both gravity and external loading resulted in adducting or extending or both moments around the shoulder joint. These external moments pushed the humeral head further away from the glenoid center line. Consequently, the shoulder muscles are required to produce a higher compressive force to achieve the concavity compression of the shoulder joint. A higher compressive force is achieved through activating a few other adductors (e.g. teres major, pectoralis major) or extensors (e.g. teres major, posterior deltoid, infraspinatus) or co-

activating the surrounding musculatures to reinforce the stiffness of the shoulder joint (Granata & Orishimo, 2001; Veeger & Van Der Helm, 2007). The results are consistent with the previous studies. Blache et al. (2015) observed that the greater the humeral elevation the greater the superficial shoulder muscles co-activation. In the studies to evaluate the effects of shoulder joint angles on the shoulder loading, both Lim et al. (2011) and Garg et al. (2006) observed significantly higher shoulder muscle activities and perceived discomforts with the increase in shoulder joint angles. Similarly, Brookham et al. (2010) also observed a general increment in shoulder muscle forces with the increase in humeral elevation.

To summarize, in this aim, a biomechanical modeling system was used to estimate the compressive and translational forces in the shoulder joint during sub-maximal material handling tasks. Using these forces and the concept of concavity compression mechanism, a strain index was formulated. To validate the strain index, the tasks were classified as low, medium and high strain tasks. In the next chapter, formulation of global fatigue index is discussed. Global fatigue index is used to validate strain index.

CHAPTER FOUR: FORMULATION OF A GLOBAL FATIGUE INDEX (AIM 2)

4.1 Background

Muscle fatigue has generally been defined as an acute impairment of physical performance due to an increase in the perceived effort necessary to exert force, regardless of whether a subject can perform the task successfully or not (Bigland-Ritchie, Rice, Garland, & Walsh, 1995). Vollestad (1997) defined neuromuscular fatigue as the reduction of force generating capacity of the muscular system, usually seen as a failure to maintain or to develop a certain expected force or power. In the scientific literature, researchers have used the following five assessment methods to quantify neuromuscular fatigue: 1) changes in the maximum voluntary contraction (MVC), 2) changes in the endurance time, 3) changes in the metabolite concentration, 4) near-infrared spectroscopy, and 5) electromyography (EMG). Among these methods, surface electromyography (SEMG) is a preferred method due to its high precision, non-invasiveness, and unobtrusiveness. Previous studies have used SEMG based measures to investigate the muscle fatigue associated with various occupational tasks. In SEMG, surface electrodes are placed on the muscle of interest over the skin to record spatial-temporal summation of action potential trains generated by the motor units of a contracting muscle (De Luca, 1979; Masuda, Masuda, Sadoyama, Inaki, & Katsuta, 1999)

Several data processing methods have been developed to describe fatigue measurement using the SEMG signal. The most commonly used methods include: 1) increases in the time domain parameters i.e. integrated EMG (IEMG), root mean square (RMS) and mean absolute value (MAV), and 2) a decrease in the spectral domain parameters i.e. median frequency (MDF) and the mean frequency (MPF) (Calder, Stashuk, & McLean, 2008; Dedering, Oddsson, Harms-Ringdahl, & Németh, 2002; Mathur, Eng, & MacIntyre, 2005; Roman-Liu, Tokarski, & Wójcik, 2004; Sbriccoli et al., 2003). Increase in the time domain amplitude values during fatiguing contraction have been attributed to recruitment of additional

motor units to maintain the required force output constant (Maton, 1981). Decreases in the spectral parameters, i.e., leftward shift in the spectrum towards the lower frequency during fatiguing contraction have been attributed to decrease in the recruitment of high frequency fast-twitch fibers and a compensatory increase in the recruitment of low frequency slow twitch fibers (Suman Kanti Chowdhury, Nimbarte, Jaridi, & Creese, 2013; S. Kumar & Narayan, 1999). Many previous ergonomic studies have used these time domain and frequency domain parameters to evaluate the localized muscle fatigue. Seghers and Spaepen (2004) studied two different types of loading on medial biceps brachii, medial brachioradialis, and medial triceps muscles during 20 minutes of two elbow flexion tasks. The first task was low intermittent task (25% of the MVC) and the second task was high intermittent task (50% of the MVC). The muscle fatigue was evaluated by determining the RMS of the SEMG data. Results showed a significant increase in the RMS values for the high force intermittent task. In another study, Yassierli and Nussbaum (2008) also evaluated isometric shoulder abduction tasks at 15% and 30% of MVC levels until exhaustion. They collected the SEMG signals from middle deltoid muscle of the shoulder region. Results showed that rate of MVC have declined, rating of perceived discomfort increased, and endurance time declined for shoulder abduction task at 30% of MVC. The SEMG based indices such as RMS, MPF, and MDF also showed an increased level of muscle fatigue for shoulder abduction task at 30% of MVC compared to shoulder abduction task at 15% of MVC.

The aforementioned time and frequency domain parameters have been shown to be affected by the task intensity and duration, and the muscles involved (Basmaijan & De Luca, 1985). Some isometric studies have found the expected trend of increase in the time domain parameters and decrease in the spectral domain parameters with the development of fatigue (Iridiastadi et al., 2008; Nussbaum, 2008; Søgaard et al., 2003; Tucker, Falla, Graven-Nielsen, & Farina, 2009). Whereas some other isometric studies did not observe the expected trend (Åström, Lindkvist, Burström, Sundelin, & Karlsson, 2009;

Clancy et al., 2008; Piscione & Gamet, 2006; Strimpakos et al., 2005). Moreover, many dynamic studies found these traditional fatigue parameters to be insensitive to fatigue related changes during dynamic sub-maximal contractions (Tim Bosch et al., 2012; Tim Bosch, Mathiassen, Visser, Looze, & Dieën, 2011; El Falou et al., 2003; Nussbaum, 2001; Sood et al., 2007).

During dynamic exertion, the magnitude and direction of force application as well as body posture changes continuously. The SEMG signal recorded under such conditions may not satisfy the stationarity assumption (Roberto Merletti, A Rainoldi, & D Farina, 2004). The fast Fourier transform (FFT) algorithm used in the frequency domain analysis assumes that the signal under investigation is stationary (Bilodeau, Cincera, Arsenault, & Gravel, 1997; Oppenheim, Schafer, & Buck, 1989). In one of our previous studies, we researched the suitability of discrete wavelet transform (DWT) algorithm in performing fatigue estimation during sub-maximal repetitive exertions (Suman Kanti Chowdhury et al., 2013). In this study, we have compared commonly used wavelet functions to identify the most appropriate one for analyzing neuromuscular fatigue of neck and shoulder muscles generated by repetitive exertions. Additionally, we have identified the frequency bands that show characteristic changes with the development of fatigue and recovery. In a different study, we have compared FFT algorithm with the DWT algorithm in assessing muscle fatigue during sub-maximal repetitive dynamic exertions. Less variability and higher statistical significance was observed for the spectral trend computed using the DWT algorithm compared to the FFT algorithm (S K Chowdhury & Nimbarte, 2015).

Thus, the result of our previous studies indicated that DWT algorithm provides a better data processing method when analyzing sub-maximal repetitive exertions. In our previous studies or similar other FFT studies, the efficacy of data processing algorithms was tested using a few representative muscles (mostly one or two). The challenge is when SEMG data from several muscles that stabilize a joint is used for estimating the joint fatigue. To our knowledge, no such method exists.

4.2 Objectives

There are two objectives in this aim:

Objective 1: The main objective in Aim 2 was to develop a global fatigue index.

Objective 2: To evaluate the global fatigue index under different muscle loading conditions.

Several factors in addition to the muscle activation pattern were used to develop the global fatigue index. These factors include the anatomical characteristics of the muscles, load sharing pattern, and co contraction between the muscle groups. Larger muscles typically exert more forces but may fatigue differently due to the difference between the fiber compositions. Generally, muscle fibers can be divided into three types: slow-twitch fibers (Type I) with small force generation capability and slow conduction velocity, but a very high fatigue resistance; fast-twitch-fatigable fibers (type IIb) with high force capacity, but fast fatigability; fast-twitch fibers (type IIa) with moderate force capacity and moderate fatigue resistance. Higher percentage of slow-twitch fibers are present in the muscles that primarily maintain posture against gravity such as back and leg muscles. Greater percentage of fast-twitch fibers are present in the shoulder and forearm muscles that produce powerful and rapid strength movements.

In additional to the anatomical characteristics, the load sharing pattern is another important factor when evaluating joint fatigue. Muscle with higher load sharing may fatigue faster independent of their size and fiber composition. This can affect the activation required by other supporting muscles and their temporal and spatial recruitment. Moreover, co-contraction of the agonist and antagonist muscles have also been studied to demonstrate temporal change in the muscle activation with the development of fatigue.

4.3 Methods

4.3.1 Approach

A global fatigue index was developed by incorporating the activation pattern, load sharing pattern, and co-activation pattern of the shoulder muscles. Human subjects were recruited to record surface electromyography (SEMG) data during fatiguing exertions. The SEMG data were used to validate the global fatigue index.

4.3.2 Global Fatigue Index Formulation

The following criterions were used in the development of global fatigue index:

1) Muscle sharing higher amount of external load is more vulnerable to fatigue than the muscle sharing low amount of external load.
2) As a muscle fatigues there is simultaneous occurrence of a shift in the SEMG power spectrum to the low frequency and an increase in the amplitude of the SEMG. These changes are attributed to a decrease in muscle fiber conduction velocity and firing rates during fatiguing contractions (Basmaijan & De Luca, 1985).
3) Muscle with higher proportion of type II fibers fatigues faster
4) Coactivation between the antagonistic muscle groups are reduced with the progression of muscle fatigue

Based on these criterions the following multipliers were included in the global fatigue index:

4.3.2.1 Muscle activation and load sharing multiplier

The maximum force a muscle can exert is directly proportional to its cross-sectional area (Knuttgen, 1976). Muscle activation recorded during Maximum Voluntary contraction (MVC) is a

surrogate measure of muscle cross sectional area. Therefore, muscle activation normalized with respect to MVC was used to understand individual muscle's contribution.

The integrated EMG (IEMG) is calculated to reflect the degree of muscle activation (Bigland-Ritchie & Woods, 1983). In this study, mean absolute value (MAV) was used as a muscle activation and load sharing multiplier.

$$MAV_i(n) = \frac{IEMG_i(n)}{\tau_i(n)} \times 100 \quad (20)$$

Where, MAV_i was the mean absolute value of muscle i at nth repetitive exertion.

τ_i was the contraction duration of muscle i at nth repetitive exertion.

$IEMG_i$ was the integrated EMG of muscle i at nth repetitive exertion (see section 4.3.8).

4.3.2.2 Spectral multiplier

Results of our previous studies indicated that the power of low frequency bands (level 6 (12 – 23 Hz) and level 5 (23 – 46 Hz)) increases with the development of fatigue (Suman Kanti Chowdhury et al., 2013). Combining this finding with findings of other studies that indicated that the power ratio of low to high frequency bands showed a characteristic change with the development of fatigue (Allison & Fujiwara, 2002; Cardozo et al., 2011), the following spectral measurement was included in the global fatigue index:

$$Fre_i(n) = \left(\frac{P_{lf}(n)}{P_{hf}(n)}\right)_i \times 100 \quad (21)$$

Where, P_{lf} was power of low frequency bands at nth repetitive exertion (Please refer to section 4.3.8 for exact frequency content)

P_{hf} was power of high frequency bands at nth repetitive exertion (Please refer to section 4.3.8 for exact frequency content)

Based on the findings of our previous study, DWT with Rbio3.1 wavelet function was used to estimate the powers of different frequency bands (Suman Kanti Chowdhury et al., 2013).

4.3.2.3 Muscle fiber types multiplier

The relative proportion of the muscle fiber types determine the contractile force, twitch speed, and susceptibility to fatigue of a muscle (Kuo & Clamann, 1981). It is generally accepted that relatively more force is allocated to the slow-twitch muscles than to the fast-twitch muscles, since slow twitch muscles are more fatigue-resistant (Smith, Edgerton, Betts, & Collatos, 1977; Walmsley, Hodgson, & Burke, 1978). The contractile properties of each of the muscles were calculated by dividing the percentages of the fast twitch fiber type of a muscle by the slow twitch fiber type.

$$F_i = \frac{f_i}{s_i} \tag{22}$$

Where, f_i – Fast twitch fiber of muscle i

s_i – Slow twitch fiber of muscle i

Table 5 shows the relative proportion of muscle fiber types of several shoulder muscles (Karlsson, 1992). The percentages of the muscle fiber types varied considerably between the muscles. In this study, this variation was controlled by regularizing the percentages of the slow twitch fiber type (Equation 23).

$$FSF_i = s_i \times \frac{1}{m}\sum_{i=1}^{m} s_i \tag{23}$$

Where, m – Total number of muscle $i = 1 \ldots m$

FSF_i – Fiber standardizing factor of muscle i

Then, the contractile properties of each of the muscles was standardized by multiplying Equation (23) by the fiber standardizing factor.

$$F_i = \frac{f_i}{s_i} \times FSF_i \tag{24}$$

4.3.2.4 Coactivation multiplier

Muscle coactivation is defined as the simultaneous activation of agonist and antagonist muscles around a joint. The antagonist muscle groups produce forces in opposite directions to the agonist muscle groups to facilitate exertion of controlled torque and to maintain stiffness of the joint separately (Basmaijan & De Luca, 1985). When both agonist and antagonist muscles are coactivated, the net torque of the joint is low, but the stiffness is high (Basmaijan & De Luca, 1985). The coactivation of the opposing muscle groups requires additional muscular activation. Thus, it could be decreased during fatiguing contraction in order to minimize energy expenditure when energy reserve is decreasing (Missenard, Mottet, & Perrey, 2008; Selen, Beek, & van Dieën, 2007). Missenard et al. (2008) has studied the effect of fatigue on coactivation during elbow extensions aimed at a target, before and after a fatigue protocol. They have observed a decrease in muscle coactivation with the progression of muscle fatigue. In this study, coactivation index (CI) for a pair of antagonistic muscle group (c) was calculated using the formulation suggested by Unnithan et al. (1996).

$$CI_c(n) = \frac{1}{k-l}\sum_{t=l}^{t=k} \frac{Min\left(EMG_{agonist}EMG_{antagonist}\right)_t}{Max\left(EMG_{agonist}EMG_{antagonist}\right)_t} \tag{25}$$

Where, $EMG_{agonist}$ – SEMG amplitude of agonist muscle group at time *t* of nth repetitive exertion.

$EMG_{antagonist}$ – SEMG amplitude of antagonist muscle group at time *t* of nth repetitive exertion.

Coactivation multiplier was calculated for all the possible antagonistic muscle groups (c).

Table 5: Fiber type compositions in the shoulder muscles

Muscles	Short twitch fiber (Type I)	Fast twitch fiber (Type II)
Infraspinatus	0.45	0.55
Teres major	0.48	0.52
Supraspinatus	0.59	0.41
Medial deltoid	0.60	0.40
Anterior deltoid	0.60	0.40
Posterior deltoid	0.60	0.40
Medial biceps	0.42	0.58
Medial triceps	0.34	0.66

Thus, the final equation for the global fatigue index (GFI) can be expressed mathematically as:

$$GFI\ (n) = \left\{\frac{1}{m}\left[\sum_{i=1}^{m}\{MAV_i(n)\} \times Fre_i(n) \times \left(\frac{f_i}{s_i} \times SF_i\right)\right] + \frac{1}{c}\left[\sum_c \frac{1}{CI_c}\right]\right\} \times SF \quad (26)$$

In Equation (26), $SF = \left[\frac{1}{10\times\left(\frac{1}{m}\sum_{i=1}^{m} FSF_i\right)}\right]$ was the scaling term to make the magnitude of the GFI values to range between 0 and 1000.

4.3.3 Participants

Eight healthy male participants were recruited to participate in this study. The primary inclusion criteria used in this study required that the participants to be free from any type of musculoskeletal, degenerative or neurological disorders and have no history of neck, back, and shoulder injury or notable pain. The Physical Activity Readiness Questionnaire (PAR-Q, Canadian Society for Exercise Physiology) was used to screen participants for cardiac and other health problems (e.g., dizziness, chest pain, heart

trouble) (Appendix A). Participants who met the inclusion criteria were asked to read and to sign a consent form approved by the local Institutional Review Board (Appendix B).

4.3.4 Apparatus/Tools

4.3.4.1 Custom-built workstations

The custom-built workstation was discussed in section 3.3.4.1

4.3.4.2 Electromyography (EMG) system

A Bagnoli-16 desktop EMG system (Delsys Inc., Boston, USA) was used to collect the muscle activation data of the shoulder muscles (Figure 16). The system mainly consisted of EMG sensors (Figure 16 a), a main amplifier unit (Figure 16 b), input modules (Figure 16 c), input cable (Figure 16 d), power supply (Figure 16 e), and other peripheral cables.

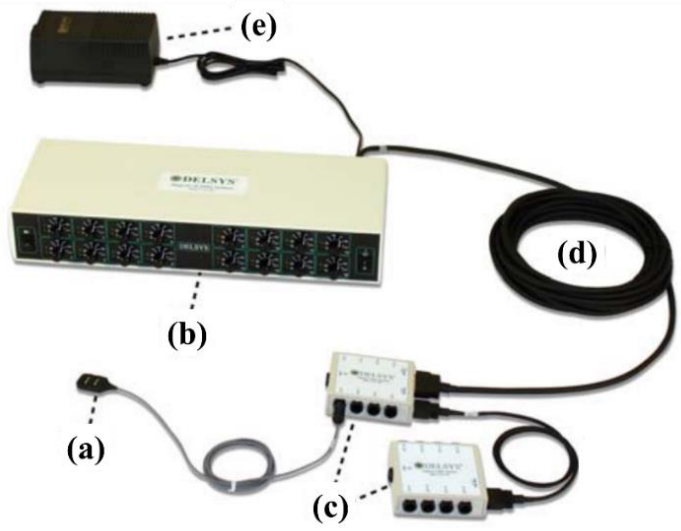

Figure 16: Parts of the Bagnoli -16 EMG system: (a) EMG sensor, (b) main amplifier (desktop) unit, (c) input models, (d) Input module cable, and (e) power supply (Delsys, 2012).

The Bagnoli-16 used two input modules. Each input module can carry up to eight electrodes. A belt clip on one side of the input module facilitates its mounting on to waist belts or other articles of

clothing. The main amplifier unit receives and conditions the signals transmitted by the input modules. It has a band pass filter of 20 to 450 Hz, and a mechanism to check for excessive amounts of line interference. Each channel of the main amplifier unit has a selectable gain which can be set to a factor of 100, 1000 or 10000. In this study, the gain was set to 1000. The input module cable connected the input module with the main amplifier. The analog channel outputs from the amplifier unit are sent directly to the optical motion capture (Vicon Nexus) software using an analog to digital (A/D) acquisition system.

The EMG sensors used for data acquisition are parallel bar single differential surface electrodes (DE-2.1 EMG Sensors, Delsys Inc., Boston, USA). The sensor housing is constructed from durable polycarbonate and completely waterproof. The electrode bars are made from 99.9% pure silver (Ag) measuring 10mm in length, 1mm in diameter. The inter-electrode distance is 10 mm (Figure 17 a). The resultant SEMG signal is the potential difference between these two electrodes (V_1 and V_2) on the skin surface with respect to the reference electrode (Figure 17 b). The reference electrode is usually placed away from the EMG muscle location. The reference electrode has a tip connector to connect with the input module. The common mode rejection ratio (CMRR) for the sensors is 92 dB with input impedance greater than $10^{15}\,\Omega$. A frequency of 2096 Hz was used to collect the EMG data.

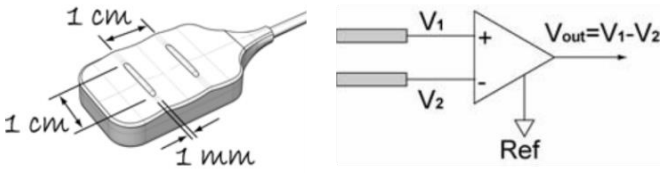

(a) (b)

Figure 17: (a) Single differential SEMG sensor, and (b) electrical circuit diagram of the resultant SEMG signal.

4.3.4.3 Weights

Two dumbbell weights of 2 lb and 6lb were used. The gripping diameter of 2 and 6 lb weights were 1.25 and 1.5 inches, respectively (Figure 18).

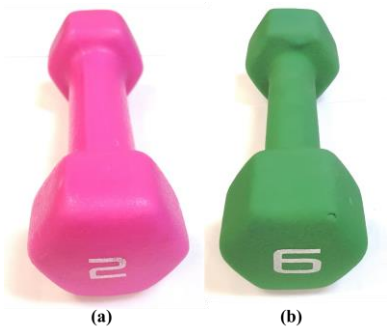

Figure 18: Two dumbbells: (a) 2 lb and (b) 6 lb.

4.3.3.4 MVC exertion device

The MVC contractions of each muscle were measured using isokinetic dynamometry (HUMAC NORM, Computer Sports Medicine (CSMi), Stoughton, MA). The system consists of movable dynamometry set up and adjustable chair (Figure 19). The sophisticated design chair provides safe placement of the participant, seating at different positions. It has four straps to secure the upper back of the participant. It also consists of headrest cushion, seat back cushion, lab/shoulder belt assembly, and seat cushion assembly. The whole HUMAC system comes with a variety of adapters and devices that are quickly and easily installed or removed by the retaining clips. These adapters and devices could be precisely regulated according to its' software calibration. The input adapters and accessories used in this study are Elbow/Shoulder assembly, Wrist/Shoulder assembly, and Elbow support subassembly (Figure 19).

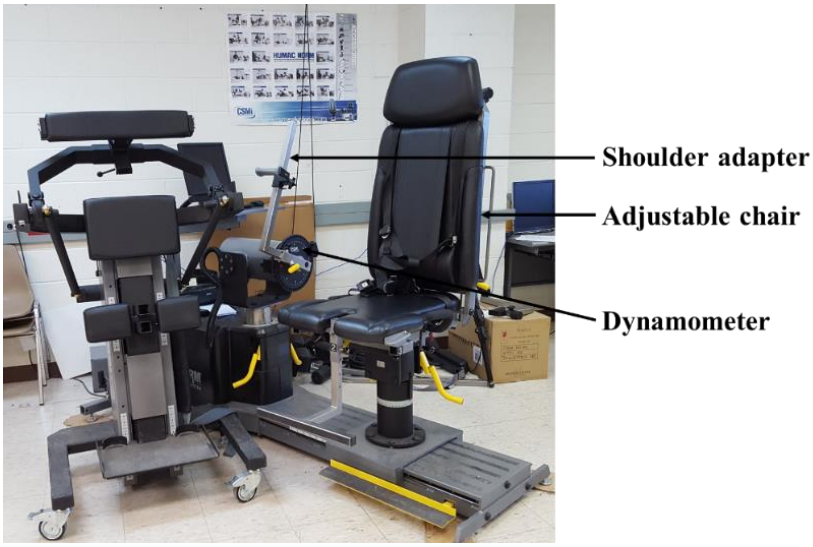

Figure 19: Humac norm set up to perform MVC exertions during SEMG data collection.

4.3.5 Experimental Design

To test the appropriateness of the global fatigue index, eight participants performed fatiguing exertions under both static and dynamic conditions. The static exertion involved holding a weight with right arm at shoulder flexion of 90°. There was no elbow flexion and shoulder abduction. The dynamic exertion involved repetitive exertions from elbow height to mid upper arm height. The starting and ending point of the exertions were 30% and 100% of thumb-tip reach at mid-sagittal plane, respectively. Both the static and dynamic exertions were performed using two different weights of 2 and 6 lb. The tasks were randomly selected for each participant. There were a total of eight experimental conditions.

4.3.6 Muscle Selection

SEMG signal can only record activity of the superficial muscles. Therefore, eight superficial shoulder muscles that stabilize shoulder joint during physical exertion were selected for data collection. All of these muscles were inserted into the glenohumeral joint and their actions are described in Table 6. The insertions and actions of these muscles were described in Cram et al. (Cram, Kasman, & Holtz, 1997).

Table 6: The selected shoulder muscles with their actions and insertions.

Muscles	Insertion	Action
Supraspinatous	Arise from supraspinatus fossa and insert on the greater tubercle of the humerus.	Abduction of the arm; controls head of the humerus
Infraspinatus	Arise from infraspinatus fossa, below the spine of the scapula and insert on the greater tubercle of the humerus.	Lateral rotation of the joint, along with stabilization of the head of the humerus in the glenoid cavity.
Anterior deltoid	Arise from lateral third of the clavicle and inserts on deltoid tuberosity of the humerus	Forward flexion, medial rotation, and abduction of the arm.
Middle deltoid	Arise from the acromion and inserts on the deltoid tuberosity of the humerus	Abduction of the arm
Posterior deltoid	Arise from the lower border of the spine of the scapula and inserts on the deltoid tuberosity of the humerus	Extension, lateral rotation, and abduction of the arm.
Biceps – Brachium (medial)	The biceps arises from the superior margin of the supra glenoid tubercle of the scapula and passes over the head of the humerus.	Forearm flexion, supination, and shoulder flexion.
Triceps (medial)	The medial triceps arise from the medial aspects of the radial groove of the humerus.	Adduction and extension of the shoulder.
Teres major	Originate at lateral side of inferior angle of scapula below teres minor and inserted into medial lip of bicipital groove of humerus.	Medially rotates and adducts arm. Stabilizes shoulder joint.

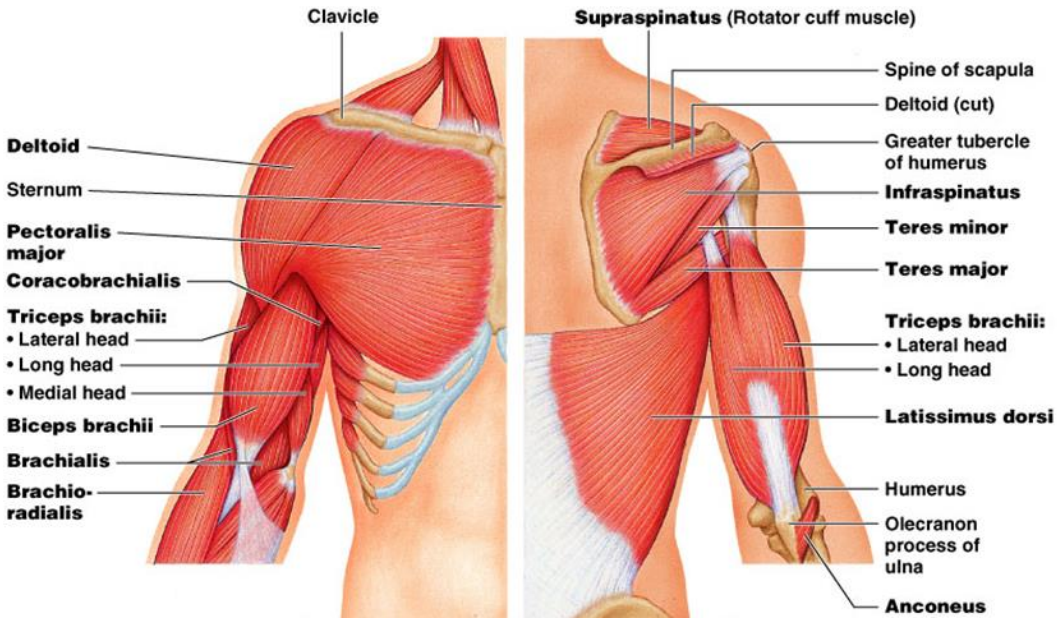

Figure 20: Major shoulder muscles around glenohumeral joint.

4.3.7 Experimental Procedure

Upon arrival, participants were explained the specifics of the experimental tasks and subsequently their signatures were obtained on the consent form. Prior to the placement of the SEMG electrodes, the skin underneath the anatomical landmarks was shaved, and cleaned with 70% alcohol. The locations of the surface electrodes for the selected muscles are described in Table 7. The placement of the electrodes was checked for accuracy and cross talk. At the beginning, the participant was asked to perform two consecutive maximum voluntary contractions (MVC) for each muscle. The MVC procedure of each muscle is provided in Table 8. During maximal effort (MVC), a standard set of verbal prompting were given to each participant using the words "push, push, push" beginning after 1 second and continuing until 5 seconds. To reduce any effect of fatigue, a rest period of two minutes was provided between the maximal efforts (MVC) of the muscles. It may take around one hour to complete subject preparation and the MVC exertions. After the MVC data collection, participant was permitted to elapse a rest period of ten minutes prior to beginning the repetitive exertions of the tasks.

Table 7: Electrode locations of the selected shoulder muscles

Muscles	Electrode placement
Infraspinatus	At 3.5 cm medial to border of scapula and 3 cm below the spine of scapula (Nussbaum, 2001)
Supraspinatus	At midpoint of supraspinous fossa and 2 finger breadths anterior to the scapular spine (Cram et al., 1997)
Middle deltoid	At midway between the acromion and the deltoid insertion (Nussbaum, 2001).
Anterior deltoid	At two to three finger-breadths below the acromion process, over the muscle belly, in line with the fibers (Pontillo et al., 2007).
Posterior deltoid	Over the muscle belly at three finger-widths behind the angle of the acromion, in line with the fibers. (Pontillo et al., 2007)
Medial biceps	Over the belly of the medial head of the triceps (Cram et al., 1997).
Triceps	Over the middle of the muscle belly along the (Cram et al., 1997).
Teres Majors	Over the middle of the muscle belly (Meskers, de Groot, Arwert, Rozendaal, & Rozing, 2004).

Table 8: The MVC procedures for the shoulder muscles

Muscle	MVC posture	MVC action
Infraspinatus	Arm abduction at 50° in frontal plane; elbow flexion at 90°; and hand pronation at 90°.	Arm will resist the external shoulder rotation.
Supraspinatus	Arm abduction at 20° in frontal plane; elbow flexion at 90°; and no shoulder flexion.	Arm will resist the abduction,
Medial deltoid	Arm abduction at 90° in frontal plane; elbow flexion at 90°; and no shoulder flexion.	Arm will resist the abduction.
Anterior deltoid	Arm abduction at 20° in frontal plane; elbow flexion at 90°; and no shoulder flexion.	Arm resisting the horizontal flexion.
Posterior deltoid	Arm abduction at 20° in frontal plane; elbow flexion at 90°; and no shoulder flexion.	Arm will resist the horizontal extension.
Medial biceps	No shoulder abduction; elbow flexion at 90°; and hands supination at 90°.	Arm will resist the vertical flexion.
Triceps (long head)	No shoulder abduction; elbow flexion at 90°; and hands supination at 90°.	Arm will resist the vertical extension.
Teres major	Arm abduction at 50° in frontal plane; elbow flexion at 90°; and hand pronation at 90°.	Arm will resist the internal shoulder rotation.

Next, the participant was asked to perform fatiguing exertions under both static and dynamic conditions. During dynamic exertion, participants were allowed to choose the pace of the repetitive exertions. However, they were asked to maintain the same pace throughout the experiment. The pace were also controlled using a metronome. Both the static and dynamic exertions were performed using two

different weights of 2 and 6 lb. The participants were asked to perform both the static and dynamic exertions for 1.5 minutes. A rest period of 3 minutes was provided between the tasks. SEMG data were recorded continuously during the tasks. At the beginning and at the end of each task, the participants were asked to rate their self-perceived shoulder discomfort on a 0 – 10 Borg CR-10 scale (Borg, 1982).

4.3.8 Data Processing

The data processing involved to obtain various parameters used in the estimation of the fatigue index multipliers is explained in this section.

The SEMG signal could be offset during data collection. To avoid such uncertainty, it is always better to demean the SEMG data. Demean will be performed by subtracting the mean SEMG signal from each point of the recorded SEMG signal.

$$Demeaned\ signal, X_{i,j}^{d}(n) = X_{i,j} - \bar{X} \quad (27)$$

Where X_i, and $\bar{X}$ were the instantaneous and mean of the SEMG signal at nth repetition, respectively.

j was the task of interest.

Though, amplifier of the SEMG equipment has a band pass filter of 20-450 Hz, however, a complete noise-free recording is practically impossible to record. That's why, it is better to perform a frequency distribution analysis using fast Fourier transformation (FFT) to check for movement artifacts, low and high frequency noises, and baseline equipment noise of 60 Hz. In this study, the SEMG data were filtered with a cut off frequency between 10 Hz to 400 Hz. The 60 Hz equipment noise and its harmonics were efficiently attenuated by using a notch filter. The filtered signals ($X_{i,j}^{f}$) were then be analyzed in both time and time-frequency domains to retrieve the essential information.

4.3.3.1 Time domain analysis

The filtered signal was full-wave rectified by converting all negative amplitudes into positive amplitudes. Smoothing algorithm was applied to minimize the SEMG burst or steep amplitude spikes. The rectified signal ($X_{i,j}^{r}$) was then smoothed ($X_{i,j}^{s}$) using an eight order Butterworth low pass filter with a cut off frequency of 10Hz.

All SEMG signals, including the MVC trials (M_i) were filtered, full wave rectified, and smoothed. The SEMG signals recorded during repetitive tasks were normalized with respect to the peak of the MVC signal to minimize between-subject or between-muscle errors. The equation that was used to normalize the SEMG signal is given below –

$$Normalized\ SEMG, X_{i,j}^{N}(n) = \frac{X_{i,j}^{s}(n)}{max(M_i)} \times 100\ ; \quad \text{for } i = 1, \dots, 8 \text{ and } j = 1, \dots 27 \tag{28}$$

Where, *i* is the muscle of interest and j is the task of interest.

The integrated EMG ($IEMG_{i,j}$) was calculated for the muscle contraction duration (t = l…k). Then, the degree of muscle activation and load sharing multiplier were estimated using Equation (28). The equation that was used to calculate IEMG signal is given below –

$$IEMG, X_{i,j}^{E}(n) = \sum_{t=l}^{t=k} \left(X_{i,j}^{N}(n)\right)_t ; \quad \text{for } i = 1, \dots, 8 \text{ and } j = 1, \dots 27 \tag{29}$$

During repetitive dynamic exertion, a period of muscle contraction is characteristically followed by a period of muscle relaxation when the muscle is returned to its original resting position. The muscle contraction duration was defined as the onset and the termination of the electrical activation of the muscle. The onset of the muscle activation was determined as a point corresponding to instantaneous amplitude of two standard deviations above the mean. The termination of the muscle activation was determined as a point corresponding to instantaneous amplitude of two standard deviations below the mean. The mean

($\bar{\mu}$) and standard deviation (σ) were calculated using a moving window size of 25 ms. The moving window was slid at the starting point during the nth repetitive exertion to determine the onset of the muscle activation, whereas the moving window was slid from the ending point of the nth repetitive exertion to determine the termination of the muscle activation.

To search for agonist-antagonist muscle group, a cross correlation calculation was performed between the muscles. The cross correlation was performed at each time instance of a repetition. The cross-correlation of two filtered, smoothed, and full wave rectified signals - $x(t)$, and $y(t)$ at nth repetition is –

$$r_{xy}\,(n) = E[(x(t) - \bar{x})(y(t+\tau) - \bar{y})]/(\sigma_x \sigma_y) \quad (30)$$

Where, $\bar{x}$ and $\bar{y}$ are the mean, and σ_x and σ_y are the standard deviation of the signals - $x(t)$, and $y(t)$, respectively. A negative correlation value indicated that the two signals are antagonistic muscle group. A higher positive correlation value between two muscles indicated that the two signals are firing in a synergistic manner. Then, muscle co-activation multiplier was calculated using Equation (25).

4.3.3.2 Time-frequency analysis

Dynamic SEMG signals are usually non stationary, Fourier transform is not suitable for such signals. To extract information from dynamic signals, the spectral analysis was performed on the filtered SEMG signal ($X_{i,j}^{f}$) with the use of discrete wavelet transform (DWT) algorithm.

According to Nyquist's theory, the maximum frequency in a signal is half of its sampling frequency (f_s). Based on the sampling frequency of 2000 Hz, the maximum frequency (f_{max}) in this study was 1000 Hz (Samar et al., 1999). The relationship between a decomposition level (L) and the corresponding frequency bandwidth (B) were estimated using the following equation (Cong et al., 2012):

$$B = \frac{f_s}{2^{L+1}} \quad (31)$$

In this study, the sampling frequency was selected as 2000 Hz. To accommodate level 5 and level 6 (lower frequency bands of 15 – 62 Hz), which were described as the fatigued frequency bands (S.K. Chowdhury, Nimbarte, Jaridi, & Creese, 2012; Dolan, Mannion, & Adams, 1995) , seven levels of decomposition were used (Figure 21). The DWT decomposition was conducted using reverse Biorthogonal with scale of 3.1 (Rbio3.1) based on the finding of our previous study (Suman Kanti Chowdhury et al., 2013). The values of the frequency bands were obtained from the detail coefficients of the DWT algorithm. The power (P_{jk}) of each frequency band was calculated using the following equation:

$$P_{ijk} = \sum_{l=1}^{l=b} (C_l)^2 \; ; \qquad \text{for i = 1,…8, j = 1,…27, and k = 1, …, 7} \tag{32}$$

Where, k is the decomposition levels

C_l are the detail coefficients at k^{th} decomposition level

b is the number of coefficient specific to the decomposition level, k

Spectral multiplier in Equation 21 was calculated by estimating ratio of the power of level 5 and 6 (low frequency bands of 15.75 – 62.5 Hz), and power of level 4 and 3 (high frequency bands of 62.5 – 250 Hz).

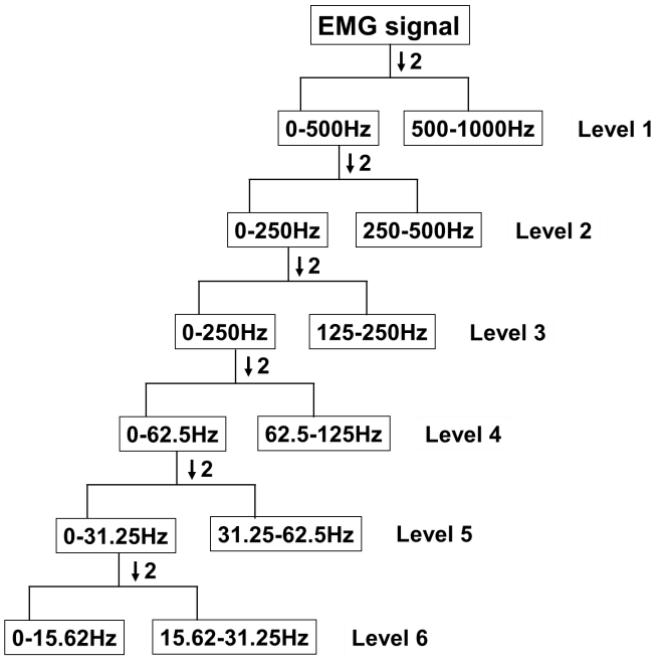

Figure 21: The DWT decomposition into six levels. The frequency bands were calculated based on a sampling

4.3.9 Data Analysis

The SEMG signal was processed using a custom-built Matlab script in MATLAB (R2011a, Math Works Inc) software. The Matlab scripts are presented in Appendix F. Global fatigue index was estimated at first three repetitive exertions and last three repetitive exertions of the dynamic task. The values of the global fatigue index were then averaged across three consecutive repetitions for dynamic tasks. For static exertion signals, global fatigue index was calculated at first and last three seconds. Changes in muscle fatigue were calculated between the first and last time instances for all eight experimental conditions (j = 1… 8) using the following equations.

$$Change\ in\ muscle\ fatigue_j = \left(\frac{\overline{GFI}_{j,last} - \overline{GFI}_{j,first}}{\overline{GFI}_{j,first}}\right) \times 100\% \quad (33)$$

Where, $\overline{GFI}_{j,last}$ – Mean global fatigue index value at last time instances.

$\overline{GFI}_{j,first}$ – Mean global fatigue index value at first time instances.

4.3.10 Statistical Analysis

In total, each subject performed eight randomized experimental runs (2 types of exertion × 2 exertion levels × 2 repetitions) during the experiment. Two repetitions were averaged together for the statistical analysis.

4.3.10.1 Statistical model

A two-factor complete block design was used in this experiment. The linear statistical model of this design is –

$$Y_{ijk} = \mu + \alpha_i + \beta_j + \delta_k + \epsilon_{ijk} \quad (34)$$

Where,

μ denoted the overall mean of all observations.

α_i denoted the effect of exertion type at two levels (i = 1 and 2).

β_j denoted the effect of exertion level at two levels (j = 1 and 2).

δ_k denoted the effect of the block, represents the number of subjects (k = 1, …, 10).

ϵ_{ijk} was a random error term.

Y_{ijk} represented the percent change in global fatigue index values.

The exertion type (α_i) and exertion level (β_j) were treated as fixed variables and subjects (δ_k) were treated as a random block. The random error term, ϵ_{ijk} was assumed to follow normally and independently distributed (NID) (0, $\boldsymbol{\sigma}^2$) in the model. The dependent variable was the percent change in global fatigue index for each task. The appropriate F tests were applied to test the model significance and the individual effect of the factors and their interactions. The level of significance, α = 0.05 was chosen for hypothesis testing. The hypotheses of interests were:

H_{10}: $\alpha_i = 0$;

H_{1A}: at least one $\alpha_i \neq 0$.

H_{20}: $\beta_j = 0$;

H_{2A}: at least one $\beta_j \neq 0$.

All statistical analyses were performed in statistical analysis software (SAS) version 9.4. The expected mean square table, F –value and P-value of the statistical model were recalculated using appropriate expected mean squared error equations (Montgomery, 2008).

4.3.10.2 Data transformation

Prior to conducting the statistical analysis, the normality of data was tested using Shapiro-Wilk, Kolmogorov-Smirnov, Cramer-vonMises and Anderson-Darling tests. The equality of variance (homogeneity of variance) was also tested using the Levene's test.

If the data failed to achieve normal distribution, it was transformed in order to achieve normality assumption. Several commonly used transforms such as square root, logarithmic, power, and reciprocal transformations are utilized to achieve normality. Among these techniques, log transformation has been widely used as a normality and variance stabilizing transformation. The transformed data are provided in Appendix G.

4.3.10.2 Data normality and equality of variance tests

The Shapiro-Wilk, Kolmogorov-Smirnov, Cramer-vonMises and Anderson-Darling tests for normality showed that the logarithmic transformed data of global fatigue index data followed a normal distribution ($p<0.05$), respectively. The normality test results are presented in Appendix H. For the transformed data, Levene's test also showed that the assumption of the homoscedasticity condition was valid (Appendix H).

4.3.11 Results

The individual demographic and physical measurement are provided in Appendix C. All the values are reported as mean (±standard deviation). The global fatigue index values for the individual participants are provided in Appendix G. Please refer to Appendix H for all statistical test results. An increase in the global fatigue index was seen for both static and dynamic tasks (Table 9). For both weight conditions, the static tasks showed significantly (P=0.0232) higher level of muscle fatigue comparted to dynamic tasks. Similarly, repetitive tasks using 6 lb weight showed significantly higher level of muscle fatigue than tasks using 2 lb weight (Table 9). The correlation analysis showed significant linear correlation (0.66) between percent change in global fatigue index and perceived exertion scores (Figure 22). Static task using 6 lb weight showed significantly (P=0.0006) higher (P<0.001) increases in both muscle fatigue and discomfort ratings compared to dynamic task using 2 lb weight (Figure 22).

Table 9: Main effects on global fatigue index.

Source	GFI	F-value	P-value
Type of exertion		5.957	0.0232
Static	55.96 (±33.92)		
Dynamic	37.27 (±23.75)		
Weight		15.585	0.0006
2 lb	32.28 (±21.55)		
6 lb	60.95 (±31.95)		

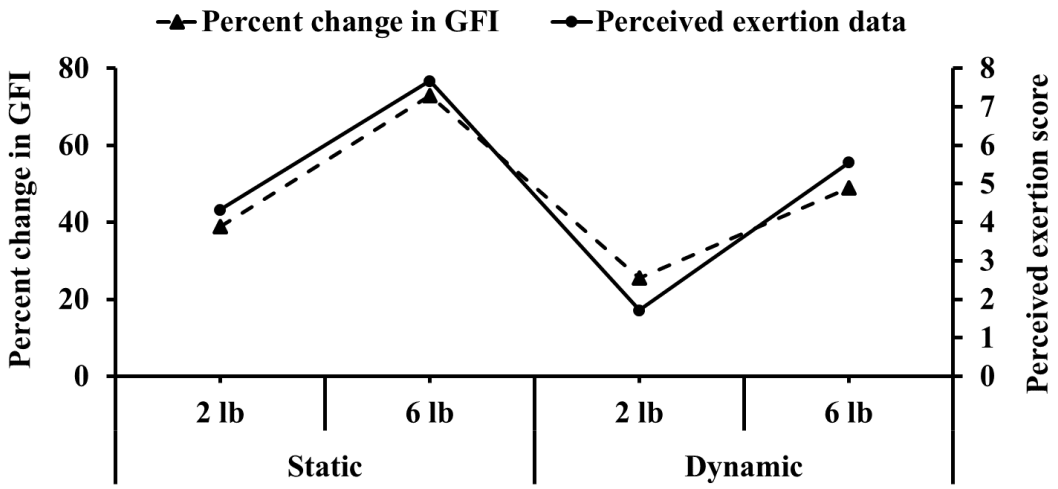

Figure 22: The relationship between global fatigue index and perceived exertion scores for the effect of type of exertion and weight level. Global fatigue index is abbreviated as GFI in the Figure.

4.3.12 Discussion

In Aim 2, a global fatigue index was formulated to quantitatively assess shoulder muscle fatigue generated by both dynamic and static arm exertions. The exertions were performed using two different weight conditions – 2 lb and 6 lb. SEMG data from eight surrounding shoulder muscles were analyzed to calculate the global fatigue index. In addition, subjective perceived ratings were also recorded for each task. With the increase in the weight level, progressively higher objective (global fatigue index value) and subjective (perceived exertion scores) fatigue were observed. Moreover, static exertion tasks resulted in higher objective and subjective fatigue than dynamic exertion tasks.

Onset and development of muscle fatigue showed characteristics changes in the global fatigue index value. If the global fatigue index value increased during a task, it indicated either increased power of lower frequency bands in the SEMG power spectrum or increment in the amplitude of the SEMG signal or both. The increment in the amplitude of the SEMG signal was primarily due to the increased firing rate of motor units (Von Tscharner, Goepfert, & Nigg, 2003). The increases in the power of the lower

frequency bands could be attributed to the decline in firing rates and conduction velocity of muscle fibers due to lack of calcium (Ca^{2+}) release from the sarcoplasmic reticulum and accumulation of lactic acid (Broman, Bilotto, & De Luca, 1985; Vukova et al., 2008). In our previous study, we found significant increase in the power of lower frequency band (6 – 46 Hz) when SEMG signal from fatigued and non-fatigued upper trapezius muscle were compared during dynamic shoulder exertion tasks (Suman Kanti Chowdhury et al., 2013). Walker et al. (2012) observed increases in the SEMG amplitude with the onset of muscle fatigue during two leg press loading tasks. Increase in the global fatigue index also indicated a reduction in the coactivation between the antagonistic muscle groups. The decline in muscle coactivation could be attributed to the notion that the central nervous system could have chosen to minimize energy expenditure than to task performance during fatigue state (Missenard et al., 2008). Missenard et al. (2008) observed a decrease in muscle coactivation with the progression of muscle fatigue during elbow extension tasks. The results obtained from the global fatigue index not only supported the findings of these studies but also provided important additional insights regarding muscle fatigue as it incorporated muscle fiber characteristics, simultaneous occurrence in the shifts of amplitude and power spectrum, and muscle co-activation between the antagonistic muscle groups.

Higher level of exertion generates higher muscle forces and therefore can be expected to lead to higher rates of muscle fatigue. In this study, exertions using 6 lb (27% of MVC) weight led to 80% and 88% greater localized muscle fatigue than exertions using 2 lb (9% of MVC) weight for static and dynamic exertions, respectively. The subjective fatigue data also showed that subjects perceived 77% and 222% greater discomforts during exertions using 6 lb than exertions using 2 lb for static and dynamic tasks, respectively. Rashedi and Nussbaum (2016) also observed higher localized muscle fatigue for 25% of MVC exertion than 15% of MVC exertion during a 1-h trials of intermittent isometric index finger abduction task.

It is well established that static task is more tiring than the dynamic tasks (Chen & Lee, 1998; Enoka, 1995; Korshøj et al., 2016; Luger et al., 2016). During static task, muscles remain contracted for a period of time and squeezed against the surrounding blood vessels. As the blood flow is restricted, it cut down the delivery of oxygen to the muscles and the removal of lactic acid from the muscles (Enoka, 1995). On contrary, there are rhythmical contractions and relaxations of the muscles during dynamic exertion. As a result, muscles act like a pump for the flow of blood in the blood vessels, allowing the blood to supply more oxygen and take away more lactic acid than the static exertions (Enoka, 1995). Results obtained in this study showed that the objective fatigue in terms of changes in the global fatigue index were 40% and 34% greater during static tasks compared to dynamic task for the weight levels of 2 lb and 6lb, respectively.

In summary, the results of aim 2 study show that the global fatigue index was sensitive to the fatigue-related neuromuscular changes and was able to accurately predict the shoulder joint fatigue. In the next chapter, the global fatigue index is used to validate strain index. The tasks with low, medium and high strain index values were repetitively performed for a sustained duration. The fatigue generated during these tasks were estimated using the global fatigue index.

CHAPTER FIVE: RELATIONSHIP BETWEEN STRAIN INDEX AND GLOBAL FATIGUE INDEX (AIM 3)

5.1 Background

With ongoing efforts of cost reduction, most of the companies in the USA have been leaning towards outsourcing strategy for last two decades. Since then, the workforces in the service providing industries have been increasing rapidly. According to the BLS, the workforce in the service providing sectors will constitute 80.9% of the total workforce by 2022 (BLS, 2013). In 2013, workers in the service providing sector incurred the highest rates of MSDs with 80.3 cases per 10,000 full time workers (BLS, 2014). Majority of the tasks in this sector are characterized as material handling tasks that require low to moderate efforts by the upper extremities.

As noted, in the Aim 1 and 2, certain characteristics of the upper extremity exertions such as force, repetition, posture have been identified as the risk factors for shoulder MSD (T Bosch et al., 2007; Mathiassen, Winkel, Sahlin, & Melin, 1993). If the stress level associated with these factors (for example, increase in the force demand) increases, then the internal shoulder strain have been known to increase (Chiang et al., 1993; Iridiastadi et al., 2008; Piscione & Gamet, 2006; Putz-Anderson et al., 1997; Seghers & Spaepen, 2004; Stenlund et al., 1993). But the underlying physiological mechanism that provides a basis to understand this stress-strain relationship due to increase in the force level is currently not well understood. In Aim 1, we have postulated that concavity compression, a shoulder stabilizing mechanism, may provide physiological basis to understand relationship between stress and strain during physical exertions. In Aim 2, we formulated a global fatigue index to estimate true physiological demand on the shoulder joint. Understanding the relationship between the outcomes of Aim 1 and 2 is essential to validate the appropriateness of concavity compression mechanism in estimating shoulder strain for stressful exertions performed in the workplaces.

5.2 Objective

The objective in Aim 3 was to test our central hypothesis – "the tasks that put higher stabilizing demand on the shoulder muscles would result in higher strain."

The stabilizing demand was measured using strain index and the internal (true) physiological strain was measured using global fatigue index.

5.3 Methods

5.3.1 Approach

A two-factor complete block design was used to test the relationship between strain index and global fatigue index. Human participants performed the repetitive exertions of the three selected material handling tasks (Aim 1) using three different weights of 2, 4, and 6 lb. Rationale for using 3 loads was that it allowed us to test if relationship between strain index and global fatigue index was dependent on the force level. The activities from eight shoulder muscles - supraspinatous, infraspinatous, teres major, middle deltoid, anterior deltoid, posterior deltoid, biceps, and triceps of the right shoulder joint were recorded using SEMG. A percent change in global fatigue index was evaluated by using the SEMG data recorded during the first three and last three repetitive exertions. A correlation between the percent change in the global fatigue index and perceived exertion data was also used to test the central hypothesis. The results of the two-factor complete block design were tested using the following hypotheses:

H_{01}: Percent change in muscle fatigue would not be affected by the tasks

H_{A1}: Percent change in muscle fatigue would be affected by the tasks

H_{02}: Percent change in muscle fatigue would not be affected by the weights

H_{A2}: Percent change in muscle fatigue would not be affected by the weights

H_{03}: Percent change in muscle fatigue would not be affected by the combined effect of task and weight

H_{A3}: Percent change in muscle fatigue would be affected by the combined effect of task and weight

5.3.2 Participants

Ten healthy male participants were recruited to participate in this study. The primary inclusion criteria used in this study required that the participants to be free from any type of musculoskeletal, degenerative or neurological disorders and have no history of neck, back, and shoulder injury or notable pain. The Physical Activity Readiness Questionnaire (PAR-Q, Canadian Society for Exercise Physiology) was used to screen participants for cardiac and other health problems (e.g., dizziness, chest pain, heart trouble) (Appendix A). Participants who met the inclusion criteria were asked to read and sign a consent form approved by the local Institutional Review Board (Appendix B).

Based on the findings of the preliminary study, statistical power and sample size calculations were made. The number for participants were determined based on the variance of the error (σ) in the global fatigue index. The number of participants was for three different weights (α =3). The statistical power was estimated using the operating characteristics curves (OC curves) based on the following equation:

$$\varphi = \sqrt{\frac{nD^2}{2a\sigma^2}} \tag{35}$$

Where, φ: noncentrality parameter

n: blocks or number of participants

D: maximum differences we want to detect between the global fatigue index values

α: number of weights

σ^2: estimate of the variance

There are α-1 (v_1) degrees of freedom and (α-1) × (n-1) degrees of freedom (v_2) in Equation (35). The D and σ^2 values were calculated based on the data recorded during the preliminary study (n=3). The D and σ^2 values calculated from the preliminary study were 20.10 and 14.7, respectively. The significance level was set at α = 0.05. The β risk and the power (1- β) of the test are provided in Table 10. The calculations showed that a sample size of three provides a β risk of about 0.40. Increasing the sample

size to 10 decreases the β risk to 0.012 and the corresponding power is 98.8%. Therefore, ten subjects were sufficient to insure sufficient statistical power.

Table 10: The β risk and sample size calculations for Aim 3.

n	ν1	ν2	φ	β	Power (1-β)
3	2	4	1.675	0.400	0.600
6	2	10	2.369	0.100	0.900
8	2	14	2.736	0.040	0.960
10	2	18	3.060	0.012	0.988

5.3.3 Apparatus/Tools

5.3.3.1 Custom-built workstations

The custom-built workstation was discussed in section 3.3.4.1

5.3.3.2 Surface Electromyography (EMG) system

The SEMG system was discussed in section 4.3.4.2.

5.3.3.3 Weights

Three dumbbell weights of 2 lb, 4lb and 6lb were used. The gripping diameter of 2, 6, and 8 lb weights are 3.0, 3.5 and 3.5 inches, respectively (Figure 23)

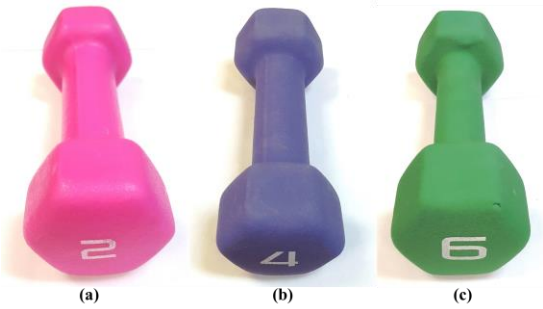

Figure 23: Three dumbbells: (a) 2 lb, (b) 4 lb, and (c) 6 lb.

5.3.3.4 MVC exertion system

The MVC exertion system was discussed in section 4.3.3.4.

5.3.4 Experimental Design

A two-factor complete block design was used. Factor 1, task was treated at three levels: (1) task with low strain index, (2) task with medium strain index, and (3) task with high strain index. These tasks were determined based on the findings of Aim 1. Factor 2, weight was treated at three levels: (1) 2 lb, (2) 4 lb, and (3) 6 lb. The weights represented three different force levels, approximately at 9.4%, 17.4%, and 27.3% of maximum voluntary isometric exertion (MVIE) in the superior direction. The reference force value of the MVIE was chosen from the work of Cutlip (2014). There were a total of nine different experimental conditions (3 tasks x 3weights). Each condition was repeated three times, i.e., a total of 27 conditions. Each task was performed for 1 minute. The rest period between the tasks was 2 minutes. The order of the material handling tasks and their repetitions were randomized for each participant. During each experimental condition, the participants were allowed to select their own pace but were asked to perform the repetitions as fast as they can. The participants were asked to maintain the selected pace throughout all the experimental conditions.

5.3.5 Muscle Selection

Please refer to section 4.3.6.

5.3.6 Experimental Procedure

Upon arrival, participants were explained the specifics of the experimental tasks and subsequently their signatures were obtained on the consent form. Prior to the placement of the SEMG electrodes, the skin underneath the anatomical landmarks was shaved, and cleaned with 70% alcohol. The locations of the surface electrodes for the selected muscles are described in section 4.3.7.

At the beginning, the participant was asked to perform two consecutive maximum voluntary contractions (MVC) for each muscle. The MVC procedure of each muscle is described in section 4.3.7. Almost an hour was spent per participant to complete data collection preparation and the MVC exertions. After the MVC data collection, participant was permitted to elapse a rest period of at least ten minutes prior to beginning the repetitive exertions of the tasks.

Next, the participant was asked to perform the 27 experimental conditions as explained in the experimental design. SEMG data were recorded continuously during the task. At the beginning and at the end of each task, participants were asked to rate their self-perceived shoulder discomfort on a 0 – 10 Borg CR-10 scale (Borg, 1982). The time distribution of the SEMG data collection is provided in Figure 24.

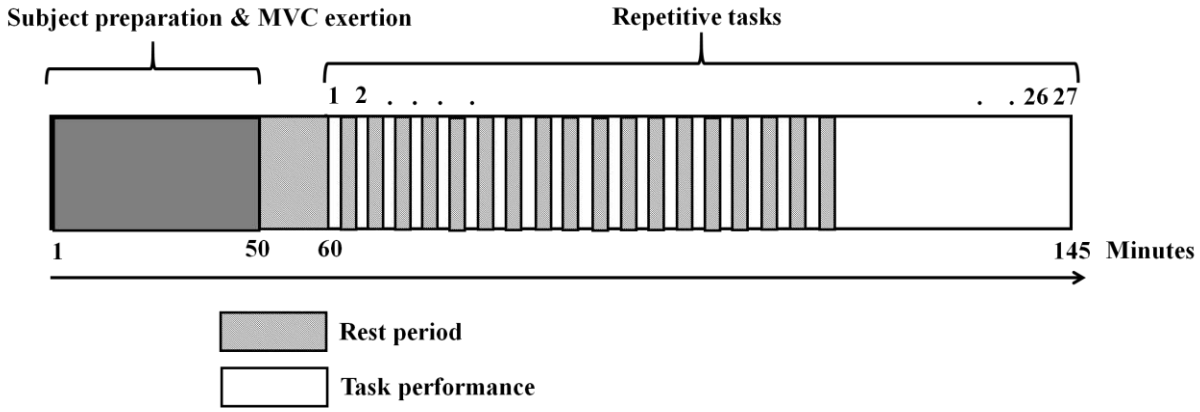

Figure 24: Experimental time distribution

5.3.7 Data Analysis

The SEMG data recorded during first three and last three consecutive exertions (repetitions) of each experimental condition were selected for global fatigue index calculation. The SEMG signals were processed using a custom-built Matlab script (Appendix F). The procedures of the signal processing are described in Section 4.3.8. The global fatigue index was calculated to observe the gradual development of

fatigue for each task (j). The values of the global fatigue index were then averaged across three consecutive repetitions using following equation.

$$\overline{GFI}_j = \frac{1}{3} \sum_{n=1}^{3} GMFI_j\ (n) \tag{36}$$

The mean global fatigue index values at each time instance was calculated for all twenty seven tasks (j = 1,….., 27). To understand the effects of exertions and the concavity compressions of the shoulder joint, changes in muscle fatigue was calculated using the following equation:

$$Change\ in\ muscle\ fatigue_j = \left(\frac{\overline{GFI}_{j,last} - \overline{GFI}_{j,first}}{\overline{GFI}_{j,first}}\right) \times 100\% \tag{37}$$

Where, $\overline{GFI}_{j,last}$ – Mean global fatigue index value for last three consecutive exertions

$\overline{GFI}_{j,first}$ – Mean global fatigue index value for first three consecutive exertions

5.3.8 Statistical Analysis

In total, each subject performed 27 randomized experimental runs (3 tasks × 3 weights × 3 repetitions) during the experiment. The average of three repetitions was used to perform the statistical analysis.

5.3.8.1 Statistical model

The two factors of interest, i.e. tasks and weights and their levels are shown in

Table 11. The response variable was the percent change in global fatigue index for each task. There were 3×3 = 9 treatment combinations. A two-factor complete block design was employed in this experiment. Subjects represented blocks.

Table 11: The factors and their levels

Variables	Levels		
Tasks (strain index values)	Low	Medium	High
Weights (lb)	2	4	6

The linear statistical model of this design is:

$$Y_{ijk} = \mu + \alpha_i + \beta_j + (\alpha\beta)_{ij} + \delta_k + \epsilon_{ijk} \quad (38)$$

Where, μ denoted the overall mean of all observations.

α_i denoted the effect of strain index (tasks) at three levels (i = 1, 2, 3).

β_j denoted the effect of weight at three levels (j = 1, 2, 3).

$(\alpha\beta)_{ij}$ was the effect of interaction between strain index (task) and weight.

δ_k denoted the effect of the block, represents the number of subjects (k = 1, …, 10).

ϵ_{ijk} was a random error term.

Y_{ijk} represented the percent change in global fatigue index values.

The task (α_i) and weight level (β_j) were treated as fixed variables and subjects (δ_k) were treated as a random block. The random error term, ϵ_{ijk} was assumed to follow normally and independently distributed (NID) (0, $\boldsymbol{\sigma}^2$) in the model. The appropriate F tests were applied to test the model significance and the individual effect of the factors and their interactions. The level of significance, α = 0.05 was chosen for hypothesis testing. The following hypothesis tests were employed:

H_{10}: $\alpha_i = 0$; for $i = 1, 2, 3$

H_{1A}: at least one $\alpha_i \neq 0$.

H_{20}: $\beta_j = 0$; for $j = 1, 2, 3$

H_{2A}: at least one $\beta_j \neq 0$.

H_{30}: $(\alpha\beta)_{ij} = 0$; for $i = 1, 2, 3$ and $j = 1, 2, 3$

H_{3A}: at least one $(\alpha\beta)_{ij} \neq 0$.

Similarly, another two-factor block design was chosen to study the significance of the perceived exertion data. The linear statistical model was similar to Equation (38), however the response variable (Y_{ijk}) was the perceived exertion score.

Significant effects on the percent change in the global fatigue index and perceived exertion scores were further evaluated by conducting comparison between means using Tukey's Honestly Significant Difference (HSD) all-pairwise comparison test. All statistical analysis was performed in statistical analysis software (SAS) version 9.4. Nevertheless, F –value and P-value of the statistical model (Equation 38) were recalculated using appropriate expected mean squared error equations (Montgomery, 2008).

5.3.8.1 Data transformation.

Prior to conducting the statistical analysis, the normality of data was tested using Shapiro-Wilk, Kolmogorov-Smirnov, Cramer-vonMises and Anderson-Darling tests. The equality of variance (homogeneity of variance) was also tested using the Levene's test.

If the data failed to achieve normal distribution, it was transformed in order to achieve normality assumption. Several commonly used transforms such as square root, logarithmic, power, and reciprocal transformations were utilized to achieve normality. The log transformation technique has been chosen as a normality and variance stabilizing transformation of global fatigue index data. On contrary, square root technique has been chosen as a normality and variance stabilizing transformation of perceived exertion data. The transformed data are provided in Appendix I.

5.3.8.1 Data normality and equality of variance tests

The Shapiro-Wilk, Kolmogorov-Smirnov, Cramer-vonMises and Anderson-Darling tests for normality showed that the logarithmic and square root transformed data of global fatigue index and perceived exertion data followed a normal distribution ($p<0.05$), respectively. The normality test results are presented in Appendix J. For the transformed data, Levene's test also showed that the assumption of the homoscedasticity condition was valid (Appendix K).

5.4. Results

Ten participants were tested for Aim 3. The demographic and the anthropometric measurements of the participant appear in Table 12. The individual demographic and physical measurements are provided in Appendix L. The units of age, weight, and height were years, pounds (lb) and inch (in), respectively. All the values are reported as mean (±standard deviation). Statistically significant values (*p*-value ≤ 0.05) in the tables are marked with asterisks (*). Error bars in the figures represent associated standard deviation value.

Table 12: The demographic and physical measurement data for Aim 3.

Age	27.70 (±3.62)
Weight	165.90 (±15.15)
Height	68.90 (±1.91)
Tronchanterion	38.30 (±1.64)
Elbow	43.70 (±1.55)
Mid upper arm	51.30 (±2.76)
Shoulder	56.95 (±2.96)

5.4.1 Percent Change in global fatigue index

The percent change in global fatigue index are presented in Table 13. Please refer to Appendix M for the percent change in global fatigue index for the individual participants. The statistical analysis indicated significant ($p<0.0001$) increases in the global fatigue index due to the main effects of task and weight. However, the two-way interaction between the task and weight was observed to be insignificant ($p = 0.1376$). Post hoc analysis indicated that high strain task resulted in significantly higher muscle fatigue than medium and low strain tasks. It also indicated significantly higher muscle fatigue during medium strain task than low strain task (Appendix N). Significantly higher muscle fatigue was observed for the tasks performed using 6 lb weight than tasks performed using 4 lb and 2 lb weights.

Table 13: Main and interaction effects table.

Source	GFI	F-value	P-value
Task		27.538	<0.0001
Low strain	9.93 (±4.40)		
Medium strain	15.58 (±7.61)		
High strain	24.24 (±9.46)		
Weight		18.453	<0.0001
2 lb	10.63 (±3.80)		
4 lb	16.03 (±8.32)		
6 lb	23.09 (±10.60)		
Task × Weight		1.803	0.1376

5.4.1 Percent Change in Perceived Exertion Ratings

The individual perceived exertion data are provided in Appendix O. The mean of perceived exertion scores showed increasing trend in response to the increase in either weight or task difficulty levels

(Table 14). The statistical analysis indicated significant ($p<0.0001$) main effect and insignificant ($p=0.0732$) interaction effect, complementing the results obtained from global fatigue index analysis (Appendix P). Post-hoc analysis of perceived exertion data also indicated that subjects experienced significantly higher discomforts if the task difficulty level or weight level increased (Appendix P).

Table 14: Perceived exertion data.

Source	Perceived exertion data	F-value	P-value
Task		31.327	<0.0001
Low strain	2.26 (±1.10)		
Medium strain	2.75 (±1.05)		
High strain	3.81 (±1.50)		
Weight		94.794	<0.0001
2 lb	1.64 (±0.96)		
4 lb	2.96 (±1.10)		
6 lb	4.23 (±1.63)		
Task × Weight		2.239	0.0732

5.4.3 The Relationship between global fatigue index and Perceived Exertion Ratings

The trend between the global fatigue index and the perceived discomfort data showed that changes in global fatigue index data followed a pattern similar to the perceived discomfort data (Figure 25). The correlation analysis also displayed a significant correlation (0.62) between perceived exertion data and global fatigue index data. The highest percent change in the global fatigue index occurred for the high strain task using 6 lb weight and was accompanied by the highest perceived exertion score. Similarly, the lowest percent change in the GFI value was observed for the low strain task using 2 lb weight and was

complemented by the lowest perceived exertion score. Additionally, as the weight level increased, both the percent change in the global fatigue index and perceived exertion rating increased in response.

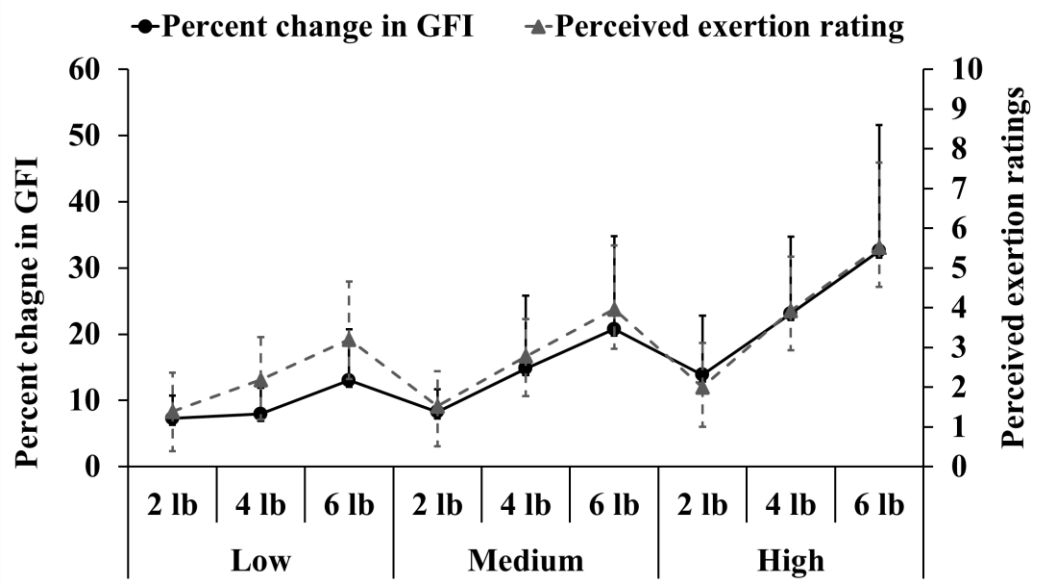

Figure 25: The relationship between global fatigue index and perceived exertion scores for different repetitive exertion tasks. Global fatigue index is abbreviated as GFI in the Figure.

5.5 Discussion

The objective of Aim 3 was the scientific validation of concavity compression mechanism. This was achieved by recording muscle activity data during repetitive exertions of low, medium and high strain tasks (Aim 1) using 2, 4 and 6 lb weights. The joint fatigue due to muscular demand during these tasks were estimated using the global fatigue index (Aim 2). The results indicated that both task and weight had significant effects on percent change in global fatigue index.

The task level influenced both subjective (change in perceived exertion data) and objective (percent change in global fatigue index) muscle fatigue. High strain task was found to exhibit the highest amount of muscle fatigue. As noted in Aim 1, the surrounding shoulder muscles had to produce relatively larger compressive force to limit the humeral translation. It was observed that high strain task required

significantly higher concavity compression than medium and low strain tasks. The repetitive exertions of this task led to 56% and 144% greater amount of objective fatigue, and 39% and 69% higher amount of subjective fatigue compared to medium and low strain tasks, respectively (Table 13 & Table 14). The knowledge gained from Aim 3 demonstrated that the strain index based on the concavity compression mechanism could reasonably predict the stressful exertions in the shoulder joint during repetitive submaximal tasks.

The muscles actively support mobility and stability of the shoulder joint. Depending on the shoulder posture, some muscles contribute more to mobility, i.e. translation of the humeral head, and some other muscles contribute more into stability, i.e. compression of the humeral head (Labriola, Lee, Debski, & McMahon, 2005). For example, deltoid muscles increases shoulder joint stability at 60° of shoulder abduction in the scapular plane (Blasier, Guldberg, & Rothman, 1992). The very same muscle led to shoulder joint destabilization at 60° of shoulder abduction in the frontal plane. In a bench-pressing task, Arciero and Cruser (1997) observed that eccentric contraction of the pectoralis muscle had led to anterior shoulder joint dislocation and rotator cuff muscles – infraspinatus and teres minor counteracted the anterior dislocation of the joint. Nevertheless, it is widely accepted that the rotator cuff muscles i.e. supraspinatus, infraspinatus, and teres major are ideally aligned to move the humerus and simultaneously prevent shoulder dislocation (Labriola et al., 2005).

Previous studies suggested that awkward shoulder angles promote the tendency for a higher dislocation of the humeral head (Moor, Bouaicha, Rothenfluh, Sukthankar, & Gerber, 2013; Viehöfer, Gerber, Favre, Bachmann, & Snedeker, 2015). During high strain task (mean shoulder angles of 75° abduction, 60° flexion and 4° external rotation), the anterior deltoid muscle showed higher muscle activation due to higher horizontal abduction and flexion than other medium and low strain tasks. This might have led to anterosuperior translation of the humeral head. To counteract this translation, the

infraspinatus muscles showed 79% and 86%, and teres major muscle showed 216% and 243% greater muscle activation during high strain task than medium and low strain tasks, respectively. Similarly, during medium strain task (mean shoulder angles of 41° abduction, 2.1° flexion and 8° external rotation), supraspinatus and posterior deltoid muscles exhibited comparatively greater muscle activations than high and low strain tasks to counteract superior and lateral (external) translations of the shoulder joint, respectively.

In general, it was observed that the flexor and abductor muscles in the shoulder joint showed comparatively higher muscle activation when the task was performed at mid-sagittal plane (high strain task) and frontal plane (medium strain task), respectively. A possible explanation is that the abductor and flexor muscles were required to provide the maximum amount of moment arms in the frontal (~ 0 flexion) and the mid-sagittal (~ 0 abduction) planes, respectively. During low strain task (mean shoulder angles of 26° abduction, 16° flexion and 14° internal rotation) at 45° right to mid-sagittal plane, the abductor and flexor muscles did not require to provide the maximum moment arms. As a result, both subjective and objective measures of muscle fatigue were observed to be least during low strain task.

The weight level also affected both subjective and objective muscle fatigue. Higher weight level contributed to higher internal moments in the shoulder joint and therefore can be expected to lead to higher rates of shoulder muscle fatigue. Tasks performed using 6 lb weight resulted in 44% and 144% higher objective muscle fatigue, and 43% and 158% higher subjective muscle fatigue than the tasks using 4 lb and 2 lb weights, respectively (Table 13 & Table 14). The results are consistent with the previous studies (Blache et al., 2015; Rashedi & Nussbaum, 2016; Yung et al., 2012). Yung et al. (2012) evaluated muscle fatigue at middle deltoid and upper trapezius muscles for five elbow and shoulder flexion protocols. They observed significantly higher amount of muscle fatigue as the force level was increased from 0 to 30% of MVC. Blache et al. (2015) also studied the effect of weight levels (6 kg, 12 kg and 18 kg) on shoulder

muscle fatigue and observed higher superficial shoulder muscle fatigue with the increased level of weights.

The interactions of weight and task were insignificant. It indicated that task level influenced muscle fatigue irrespective of weight level and vice versa. It also suggested that certain weight or task, as well as their combination might place high strain in the shoulder joint. Garg et al. (2006) recommended a perceived exertion limit of 3.5 on the Borg CR-10 scale to limit the risk of injury. The perceived exertion data showed that only high strain tasks using 4 lb and 6 lb weights and medium strain task using 6 lb weight resulted in perceived discomforts of more than 3.5. Based on this finding, it could be deduced that if a task requiring higher concavity compression of the shoulder joint is performed using higher weight level, muscles had to work harder to create higher compressive force to prevent translational strain. Cumulative exposures of such task may lead to muscle fatigue, and hence, it may increase the possibility for excessive translational instability at the shoulder joint.

CHAPTER 6: CONCLUSIONS AND FUTURE WORKS

6.1 Conclusions

The shoulder joint represents a perfect balance of stability and mobility. Both mobility and stability are primarily ensured by coordinated muscular action, which provides concavity compression. In Aim 1, a strain index was formulated from the magnitude and direction of the resultant of compressive and translational forces at the shoulder joint during sub-maximal material handling tasks. The forces were measured using AnyBody biomechanical system. Three tasks were selected to validate the notion of concavity compression mechanism using real physiological data.

In Aim 2, a global fatigue index was developed by incorporating the activation pattern, load sharing pattern, and co-activation pattern of the shoulder muscles. The results showed that fatigue assessment method using global fatigue index could precisely predict joint fatigue under different muscle loading patterns.

In Aim 3, the relationship between strain index and global fatigue index was evaluated using three different exertion levels. Global fatigue index was found to increase with the increase in task difficulty level (strain index value). The increment in weight level also increased global fatigue index and was found to differ between the tasks. Based on the findings in Aim 3, it was concluded that if a task with high strain index value is performed using a high weight level, it will lead to muscle fatigue. The repetitive exertions of the task increase the possibility of excessive translational instability at the shoulder joint. The chronic instability may lead to inflammation and risk of injury.

The overall results of this study conclude that a shoulder strain index based on the concept of concavity compression mechanism can predict the stabilizing demand and thus the shoulder muscle fatigue during dynamic physical exertions.

6.2 Practical and Theoretical Implications

Normal function and stability of the shoulder joint is essential for completing most tasks in the workplaces. Identifying the tasks that are stressful for shoulder complex are important for designing safe work conditions. The successful completion of this study suggest that concavity compression mechanism provides a sound physiological basis to understand the stress and strain relationship during physical exertions performed by the shoulder complex. The strain index detailed in this study is a first step towards developing a workplace ergonomic assessment/evaluation tool. Additionally, we believe that the global fatigue index is an important theoretical contribution as no previous study has provided an index that estimate joint fatigue due to muscular demand. The global fatigue index could be directly applicable in evaluating shoulder joint fatigue during both submaximal repetitive exertions and sustained arm exertions. The submaximal repetitive tasks are very common in various industries such as metal, packaging, warehousing, automobile, garments, and transportation. The sustained exertions are very common in various industries such as construction, transportation, stock clerk, nursing, janitorial works, etc.

6.3 Study Limitations

There are a few limitations of this study that need to be acknowledged. First, the findings of this study are a function of the experimental conditions investigated. The tasks tested were performed in standard neutral standing posture at a fixed speed and frequency. The workplace tasks are not always performed under such conditions. Second, participation was voluntary and the participant pool was limited to university-aged students with little to no manual materials handling experience. Experienced workers may exhibit different material handling and muscle recruitment strategies. Third, to control the effect of gender, only female participants were recruited. Female workers, although at a lower percent, are hired to perform manual materials handling tasks in the several occupational setting. Fourth, AnyBody modeling system was used in the formulation of strain index. Like any other biomechanical modeling system,

AnyBody modeling system makes some assumptions regarding muscle recruitment. The model implemented muscle recruitment may not truly represent the muscle activation strategies used by the central nervous system. Therefore, output of a biomechanical model may not truly, capture subtle inter subject differences. It is also likely that different biomechanical modeling (e.g. OpenSim) systems due to differences in the muscle recruitment protocols may show different strain index values. However, we expect that the trend in terms of low, medium and high strain for different exertions will be the same independent of the biomechanical modelling software. Six, in Aim 3, the duration of the repetitive exertions was kept for one minute in order to reduce the risk of injury or discomfort to the participants. A longer duration may yield different results.

6.4 Future Works

Repetition was considered as one of the most significant risk factors for shoulder MSD. In the occupational settings, some repetitive tasks are performed more frequently than other repetitive tasks. Moreover, the speed or acceleration of the repetitive exertions are widely varied across the industries. In both cases, the internal shoulder strain has been known to increase. Therefore, future studies should look at the effect of changes in both frequency and acceleration of repetitive exertion on both strain index (stabilizing demand) and global fatigue index (real physiological strain).

In this study, the compressive-translational force relationship in terms of strain index values provided mixed evidence for the tasks performed at different vertical heights. In general, the strain index values were observed to be higher for the tasks performed at higher vertical heights compared to the tasks performed at lower vertical heights. On the other hand, tasks performed from the elbow to mid upper arm heights showed consistently higher strain index values across the participants than the tasks performed from elbow to shoulder heights. A possible explanation for this is that the muscle co-activation of the surrounding musculatures produced relatively higher torque while the arm was at mid-reach distance of

the mid upper arm height. Further studies are required to investigate these two tasks in more detail to understand the muscle activation pattern and shoulder joint movements.

Physical motion during the repetitive tasks in Aim 3 was not studied. A better understanding of the actual motion during sub-maximal repetitive tasks could provide additional cues about the shoulder stabilization process. Future study should be performed using motion capture data in addition to the EMG data to investigate the effect of muscle fatigue on shoulder stabilization process.

The risk of shoulder joint injury increases with aging since muscles become less toned and less able to contract because of changes in the muscle tissue (Tsai & Hsu, 2015). According to the BLS, civilian labor force of age 55 and older will constitute 39.4% by 2024 (BLS, 2015a). Therefore, future studies should investigate the shoulder stabilizing demand for different age groups under different muscle loading patterns.

The long-term goal of this research is to aid in the development of workplace assessment/evaluation tool. There are several such tools (e.g. NIOSH, REBA, RULA, etc.) available but no tool exists specifically for the evaluation and prevention of shoulder MSD. The results from this dissertation provide some promise in using concavity compression based strain index in developing such tool. However, several future studies are warranted in order to completely develop such tool. Firstly, strain index should be validated for the forceful exertions performed in the other five anatomical directions and at various working heights. Note that exertions performed only in the vertical directions were studied in this dissertation. There is also a need of thorough investigation of the effect of gender and personal factors on the strain index values under different physical and psychologically stressful exertions. Furthermore, a validation of strain index in the real industrial setting is also necessary to see its applicability to different occupations.

REFERENCES

Alizadehkhaiyat, O., Fisher, A., Kemp, G., Vishwanathan, K., & Frostick, S. (2011). Shoulder muscle activation and fatigue during a controlled forceful hand grip task. *Journal of Electromyography and Kinesiology, 21*(3), 478-482.

Allison, G., & Fujiwara, T. (2002). The relationship between EMG median frequency and low frequency band amplitude changes at different levels of muscle capacity. *Clinical Biomechanics, 17*(6), 464-469.

Andrews, J. R., Wilk, K. E., & Reinold, M. M. (2008). *The athlete's shoulder*: Elsevier Health Sciences.

Andrzejewska, R., Jaskólski, A., Jaskólska, A., Gobbo, M., & Orizio, C. (2014). Electromyogram features during linear torque decrement and their changes with fatigue. *European journal of applied physiology*, 1-13.

Anton, D., Shibley, L. D., Fethke, N. B., Hess, J., Cook, T. M., & Rosecrance, J. (2001). The effect of overhead drilling position on shoulder moment and electromyography. *Ergonomics, 44*(5), 489-501.

AnyBody. (2015). Quadratic Muscle Recruitment. Retrieved from http://www.anybodytech.com/fileadmin/AnyBody/Docs/Tutorials/chapX_MuscleRecruitment/lesson3.html

AnyBody. (2016). The AnyBody Modeling System. Retrieved from http://www.anybodytech.com/index.php?id=26

Arciero, R. A., & Cruser, D. L. (1997). Pectoralis major rupture with simultaneous anterior dislocation of the shoulder. *Journal of Shoulder and Elbow Surgery, 6*(3), 318-320.

Åström, C., Lindkvist, M., Burström, L., Sundelin, G., & Karlsson, J. S. (2009). Changes in EMG activity in the upper trapezius muscle due to local vibration exposure. *Journal of Electromyography and Kinesiology, 19*(3), 407-415.

Basmaijan, J., & De Luca, C. J. (1985). *Muscles alive: their functions revealed by electromyography*: Baltimore: Williams and Wilkins.

Bernard, B. P., Putz-Anderson, V., & Burt, S. (1997). A critical review of epidemiologic evidence for work-related musculoskeletal disorders of the neck, upper extremity, and low back. *Cincinnati: Centers for Disease Control and Prevention National Institute for Occupational Safety and Health publication*, 97-141.

Bigland-Ritchie, B., Rice, C., Garland, S., & Walsh, M. (1995). *Task-dependent factors in fatigue of human voluntary contractions.* Paper presented at the Fatigue.

Bigland-Ritchie, B., & Woods, J. (1983). Changes in muscle contractile properties and neural control during human muscular fatigue. *Muscle & nerve*, *7*(9), 691-699.

Bilodeau, M., Cincera, M., Arsenault, A. B., & Gravel, D. (1997). Normality and stationarity of EMG signals of elbow flexor muscles during ramp and step isometric contractions. *Journal of Electromyography and Kinesiology*, *7*(2), 87-96.

Bjelle, A., Hagberg, M., & Michaelson, G. (1981). Occupational and individual factors in acute shoulder-neck disorders among industrial workers. *British journal of industrial medicine*, *38*(4), 356-363.

Blache, Y., Dal Maso, F., Desmoulins, L., Plamondon, A., & Begon, M. (2015). Superficial shoulder muscle co-activations during lifting tasks: Influence of lifting height, weight and phase. *Journal of Electromyography and Kinesiology*, *25*(2), 355-362.

Blasier, R. B., Guldberg, R. E., & Rothman, E. D. (1992). Anterior shoulder stability: contributions of rotator cuff forces and the capsular ligaments in a cadaver model. *Journal of Shoulder and Elbow Surgery*, *1*(3), 140-150.

BLS. (2013). Industry employment and output projections to 2022. Retrieved October 1, from Bureau of Labor Statistics http://www.bls.gov/emp/ep_table_201.htm

BLS. (2014). Nonfatal occupational injuries and illnesses requiring days away from work, 2013. from Bureau of Labor Statistics http://www.bls.gov/news.release/pdf/osh2.pdf

BLS. (2015a, December 8, 2015). Civilian labor force participation rate by age, gender, race, and ethnicity. Retrieved from http://www.bls.gov/emp/ep_table_303.htm

BLS. (2015b). Nonfatal occupational injuries and illnesses requiring days away from work, 2014. from Bureau of Labor Statistics http://www.bls.gov/news.release/pdf/osh2.pdf

Borg, G. A. (1982). Psychophysical bases of perceived exertion. *Med sci sports exerc, 14*(5), 377-381.

Bosch, T., De Looze, M., & Van Dieen, J. (2007). Development of fatigue and discomfort in the upper trapezius muscle during light manual work. *Ergonomics, 50*(2), 161-177.

Bosch, T., Mathiassen, S. E., Hallman, D., de Looze, M., Lyskov, E., Visser, B., & van Dieën, J. (2012). Temporal strategy and performance during a fatiguing short-cycle repetitive task. *Ergonomics, 55*(8), 863-873.

Bosch, T., Mathiassen, S. E., Visser, B., Looze, M. d., & Dieën, J. v. (2011). The effect of work pace on workload, motor variability and fatigue during simulated light assembly work. *Ergonomics, 54*(2), 154-168.

Broman, H., Bilotto, G., & De Luca, C. J. (1985). Myoelectric signal conduction velocity and spectral parameters: influence of force and time. *Journal of Applied Physiology, 58*(5), 1428-1437.

Brookham, R. L., Wong, J. M., & Dickerson, C. R. (2010). Upper limb posture and submaximal hand tasks influence shoulder muscle activity. *International journal of industrial ergonomics, 40*(3), 337-344.

Burdorf, A., Derksen, J., Naaktgeboren, B., & van Riel, M. (1992). Measurement of trunk bending during work by direct observation and continuous measurement. *Applied ergonomics, 23*(4), 263-267.

Cady, E., Jones, D., Lynn, J., & Newham, D. (1989). Changes in force and intracellular metabolites during fatigue of human skeletal muscle. *The Journal of physiology, 418*(1), 311.

Calder, K. M., Stashuk, D. W., & McLean, L. (2008). Physiological characteristics of motor units in the brachioradialis muscle across fatiguing low-level isometric contractions. *Journal of Electromyography and Kinesiology, 18*(1), 2-15.

Cardozo, A. C., Gonçalves, M., & Dolan, P. (2011). Back extensor muscle fatigue at submaximal workloads assessed using frequency banding of the electromyographic signal. *Clinical Biomechanics, 26*(10), 971-976.

Chen, Y.-L., & Lee, Y.-H. (1998). Effect of combined dynamic and static workload on heart rate recovery cost. *Ergonomics, 41*(1), 29-38.

Chiang, H.-C., Ko, Y.-C., Chen, S.-S., Yu, H.-S., Wu, T.-N., & Chang, P.-Y. (1993). Prevalence of shoulder and upper-limb disorders among workers in the fish-processing industry. *Scandinavian journal of work, environment & health*, 126-131.

Chopp, J. N., O'Neill, J. M., Hurley, K., & Dickerson, C. R. (2010). Superior humeral head migration occurs after a protocol designed to fatigue the rotator cuff: a radiographic analysis. *Journal of Shoulder and Elbow Surgery, 19*(8), 1137-1144.

Chowdhury, S. K., & Nimbarte, A. D. (2015). Comparison of Fourier and wavelet analysis for fatigue assessment during repetitive dynamic exertion. *Journal of Electromyography and Kinesiology, 25*(2), 205-213.

Chowdhury, S. K., Nimbarte, A. D., Jaridi, M., & Creese, R. C. (2012). *Assessment of neck and shoulder muscle fatigue using discrete wavelet transforms of surface electromyography.* Paper presented at the Proceedings of the Human Factors and Ergonomics Society Annual Meeting.

Chowdhury, S. K., Nimbarte, A. D., Jaridi, M., & Creese, R. C. (2013). Discrete wavelet transform analysis of surface electromyography for the fatigue assessment of neck and shoulder muscles. *Journal of Electromyography and Kinesiology, 23*(5), 995-1003. doi:http://dx.doi.org/10.1016/j.jelekin.2013.05.001

Christmansson, M. (1994). *The HAMA-method: a new method for analysis of upper limb movements and risk for work-related musculoskeletal disorders.* Paper presented at the Proceedings of the 12th Triennial Congress of the International Ergonomics Association/Human Factors Association of Canada, August, Toronto.

Clancy, E. A., Bertolina, M. V., Merletti, R., & Farina, D. (2008). Time-and frequency-domain monitoring of the myoelectric signal during a long-duration, cyclic, force-varying, fatiguing hand-grip task. *Journal of Electromyography and Kinesiology, 18*(5), 789-797.

Cong, F., Huang, Y., Kalyakin, I., Li, H., Huttunen-Scott, T., Lyytinen, H., & Ristaniemi, T. (2012). Frequency-response-based Wavelet Decomposition for Extracting Children's Mismatch Negativity Elicited by Uninterrupted Sound. *Journal of Medical and Biological Engineering, 32*(3), 205-213.

Cram, J., Kasman, G., & Holtz, J. (1997). Introduction to surface electromyography. 1998. *Gaithersburg, Marland: Aspen publishers Inc*.

Culham, E., & Peat, M. (1993). Functional-anatomy of the shoulder complex. *Journal of Orthopaedic & Sports Physical Therapy, 18*(1), 342-350.

Cutlip, K. (2014). *Stability of the Shoulder Complex During Manual Exertions.* West Virginia University.

Damsgaard, M., Rasmussen, J., Christensen, S. T., Surma, E., & De Zee, M. (2006). Analysis of musculoskeletal systems in the AnyBody Modeling System. *Simulation Modelling Practice and Theory, 14*(8), 1100-1111.

Daubechies, I. (1990). The wavelet transform, time-frequency localization and signal analysis. *Information Theory, IEEE Transactions on, 36*(5), 961-1005.

De Looze, M., Van Greuningen, K., Rebel, J., Kingma, I., & Kuijer, P. (2000). Force direction and physical load in dynamic pushing and pulling. *Ergonomics, 43*(3), 377-390.

De Luca, C. J. (1979). Physiology and mathematics of myoelectric signals. *Biomedical Engineering, IEEE Transactions on*(6), 313-325.

Dedering, Å., Németh, G., & Harms-Ringdahl, K. (1999). Correlation between electromyographic spectral changes and subjective assessment of lumbar muscle fatigue in subjects without pain from the lower back. *Clinical Biomechanics, 14*(2), 103-111.

Dedering, Å., Oddsson, L., Harms-Ringdahl, K., & Németh, G. (2002). Electromyography and ratings of lumbar muscle fatigue using a four-level staircase protocol. *Clinical Biomechanics, 17*(3), 171-176.

Delsys. (2012). Bagnoli EMG system. Retrieved from https://www.delsys.com/Attachments_pdf/Bagnoli%20Users%20Guide%20(MAN-004-1-3).pdf

Dickerson, C., Martin, B., & Chaffin, D. B. (2007). Predictors of perceived effort in the shoulder during load transfer tasks. *Ergonomics, 50*(7), 1004-1016.

Dickerson, C. R., Martin, B. J., & Chaffin, D. B. (2006). The relationship between shoulder torques and the perception of muscular effort in loaded reaches. *Ergonomics, 49*(11), 1036-1051.

Dingwell, J. B., Joubert, J. E., Diefenthaeler, F., & Trinity, J. D. (2008). Changes in muscle activity and kinematics of highly trained cyclists during fatigue. *Biomedical Engineering, IEEE Transactions on, 55*(11), 2666-2674.

Dolan, P., Mannion, A., & Adams, M. (1995). Fatigue of the erector spinae muscles: A quantitative assessment using" frequency banding" of the surface electromyography signal. *Spine, 20*(2), 149.

Dubowsky, S. R., Rasmussen, J., Sisto, S. A., & Langrana, N. A. (2008). Validation of a musculoskeletal model of wheelchair propulsion and its application to minimizing shoulder joint forces. *Journal of biomechanics, 41*(14), 2981-2988.

Dunning, K. K., Davis, K. G., Cook, C., Kotowski, S. E., Hamrick, C., Jewell, G., & Lockey, J. (2010). Costs by industry and diagnosis among musculoskeletal claims in a state workers compensation system: 1999–2004. *American journal of industrial medicine, 53*(3), 276-284.

Ebaugh, D. D., McClure, P. W., & Karduna, A. R. (2006). Effects of shoulder muscle fatigue caused by repetitive overhead activities on scapulothoracic and glenohumeral kinematics. *Journal of Electromyography and Kinesiology, 16*(3), 224-235.

El Falou, W., Duchêne, J., Grabisch, M., Hewson, D., Langeron, Y., & Lino, F. (2003). Evaluation of driver discomfort during long-duration car driving. *Applied ergonomics, 34*(3), 249-255.

Engin, A., & Chen, S.-M. (1986). Statistical data base for the biomechanical properties of the human shoulder complex—I: Kinematics of the shoulder complex. *Journal of biomechanical engineering, 108*(3), 215-221.

Enoka, R. M. (1995). Mechanisms of muscle fatigue: central factors and task dependency. *Journal of Electromyography and Kinesiology, 5*(3), 141-149.

Favre, P., Jacob, H. A., & Gerber, C. (2009). Changes in shoulder muscle function with humeral position: a graphical description. *Journal of Shoulder and Elbow Surgery, 18*(1), 114-121.

Fischer, S. L., Brenneman, E. C., Wells, R. P., & Dickerson, C. R. (2012). Relationships between psychophysically acceptable and maximum voluntary hand force capacity in the context of underlying biomechanical limitations. *Applied ergonomics, 43*(5), 813-820.

Fuller, J. R., Lomond, K. V., Fung, J., & Côté, J. N. (2009). Posture-movement changes following repetitive motion-induced shoulder muscle fatigue. *Journal of Electromyography and Kinesiology*, *19*(6), 1043-1052.

Gallagher, S., & Heberger, J. R. (2013). Examining the Interaction of Force and Repetition on Musculoskeletal Disorder Risk A Systematic Literature Review. *Human Factors: The Journal of the Human Factors and Ergonomics Society*, *55*(1), 108-124.

Garg, A., Hegmann, K., & Kapellusch, J. (2006). Short-cycle overhead work and shoulder girdle muscle fatigue. *International journal of industrial ergonomics*, *36*(6), 581-597.

Garg, A., Hegmann, K. T., Schwoerer, B. J., & Kapellusch, J. M. (2002). The effect of maximum voluntary contraction on endurance times for the shoulder girdle. *International journal of industrial ergonomics*, *30*(2), 103-113.

Georgakis, A., Stergioulas, L. K., & Giakas, G. (2003). Fatigue analysis of the surface EMG signal in isometric constant force contractions using the averaged instantaneous frequency. *Biomedical Engineering, IEEE Transactions on*, *50*(2), 262-265.

Granata, K. P., & Orishimo, K. F. (2001). Response of trunk muscle coactivation to changes in spinal stability. *Journal of biomechanics*, *34*(9), 1117-1123.

Grieve, J. R., & Dickerson, C. R. (2008). Overhead work: Identification of evidence-based exposure guidelines. *Occupational Ergonomics*, *8*(1), 53-66.

Grooten, W. J. A., Mulder, M., Josephson, M., Alfredsson, L., & Wiktorin, C. (2007). The influence of work-related exposures on the prognosis of neck/shoulder pain. *European spine journal*, *16*(12), 2083-2091.

Hägg, G. M., Luttmann, A., & Jäger, M. (2000). Methodologies for evaluating electromyographic field data in ergonomics. *Journal of Electromyography and Kinesiology*, *10*(5), 301-312.

Hall, L. C., & Dickerson, C. R. (2010). Perceived shoulder moment load during load transfer tasks following a novel moment-based perception training program. *International journal of industrial ergonomics, 40*(4), 402-405.

Harkness, E., Macfarlane, G., Nahit, E., Silman, A., & McBeth, J. (2003). Mechanical and psychosocial factors predict new onset shoulder pain: a prospective cohort study of newly employed workers. *Occupational and environmental medicine, 60*(11), 850-857.

Haslegrave, C. M., Tracy, M. F., & Corlett, E. N. (1997). Force exertion in awkward working postures-strength capability while twisting or working overhead. *Ergonomics, 40*(12), 1335-1356.

Hoozemans, M., Kuijer, P., Kingma, I., van Dieen, J., de Vries, W., van der Woude, L., . . . Frings-Dresen, M. (2004). Mechanical loading of the low back and shoulders during pushing and pulling activities. *Ergonomics, 47*(1), 1-18. doi:10.1080/00140130310001593577

Hoozemans, M. J., Kuijer, P. P. F., Kingma, I., van Dieën, J. H., de Vries, W. H., van der Woude, L. H., . . . Frings-Dresen, M. H. (2004). Mechanical loading of the low back and shoulders during pushing and pulling activities. *Ergonomics, 47*(1), 1-18.

Hummel, A., Läubli, T., Pozzo, M., Schenk, P., Spillmann, S., & Klipstein, A. (2005). Relationship between perceived exertion and mean power frequency of the EMG signal from the upper trapezius muscle during isometric shoulder elevation. *European journal of applied physiology, 95*(4), 321-326.

Hussain, M., Reaz, M., Mohd Yasin, F., & Ibrahimy, M. (2009). Electromyography signal analysis using wavelet transform and higher order statistics to determine muscle contraction. *Expert Systems, 26*(1), 35-48.

Inbar, G., Paiss, O., Allin, J., & Kranz, H. (1986). Monitoring surface EMG spectral changes by the zero crossing rate. *Medical and Biological Engineering and Computing, 24*(1), 10-18.

Iridiastadi, H., Nussbaum, M. A., & van Dieën, J. H. (2008). Muscular load characterization during isometric shoulder abductions with varying force. *Journal of Electromyography and Kinesiology, 18*(4), 695-703.

Kanoun, S., & Ali, N. (2009, 14-16 Dec. 2009). *A new digital signal processing technique for the estimation of motor unit action potential templates.* Paper presented at the Computer Engineering & Systems, 2009. ICCES 2009. International Conference on.

Karhu, O., Härkönen, R., Sorvali, P., & Vepsäläinen, P. (1981). Observing working postures in industry: Examples of OWAS application. *Applied ergonomics, 12*(1), 13-17.

Karhu, O., Kansi, P., & Kuorinka, I. (1977). Correcting working postures in industry: a practical method for analysis. *Applied ergonomics, 8*(4), 199-201.

Karlsson, D. (1992). *Force distributions in the human shoulder*: Chalmers University of Technology.

Keyserling, W. M. (1986). Postural analysis of the trunk and shoulders in simulated real time. *Ergonomics, 29*(4), 569-583.

Khezri, M., & Jahed, M. (2008, 20-25 Aug. 2008). *Surface Electromyogram signal estimation based on wavelet thresholding technique.* Paper presented at the Engineering in Medicine and Biology Society, 2008. EMBS 2008. 30th Annual International Conference of the IEEE.

Kilbom, Å. (1994). Assessment of physical exposure in relation to work-related musculoskeletal disorders-what information can be obtained from systematic observations. *Scandinavian journal of work, environment & health,* 30-45.

Kilby, J., & Hosseini, G. (2004). *Wavelet analysis of surface electromyography signals*.

Knuttgen, H. (1976). Development of muscular strength and endurance. *Neuromuscular mechanisms for therapeutic and conditioning exercise*, 97-118.

Konrad, G. G., Jolly, J. T., Labriola, J. E., McMahon, P. J., & Debski, R. E. (2006). Thoracohumeral muscle activity alters glenohumeral joint biomechanics during active abduction. *Journal of Orthopaedic Research, 24*(4), 748-756.

Korshøj, M., Clays, E., Lidegaard, M., Skotte, J. H., Holtermann, A., Krustrup, P., & Søgaard, K. (2016). Is aerobic workload positively related to ambulatory blood pressure? A cross-sectional field study among cleaners. *European journal of applied physiology, 116*(1), 145-152.

Kumar, D. K., Pah, N. D., & Bradley, A. (2003). Wavelet analysis of surface electromyography. *Neural Systems and Rehabilitation Engineering, IEEE Transactions on, 11*(4), 400-406.

Kumar, S., & Narayan, Y. (1999). EMG spectral characteristics of spinal muscles during isometric axial rotation. *Journal of Electromyography and Kinesiology, 9*(1), 21-38.

Kuo, K. H., & Clamann, H. (1981). Coactivation of synergistic muscles of different fiber types in fast and slow contractions. *American Journal of Physical Medicine & Rehabilitation, 60*(5), 219-238.

Labriola, J. E., Lee, T. Q., Debski, R. E., & McMahon, P. J. (2005). Stability and instability of the glenohumeral joint: The role of shoulder muscles. *Journal of Shoulder and Elbow Surgery, 14*(1, Supplement), S32-S38.

Leclerc, A., Chastang, J., Niedhammer, I., Landre, M., & Roquelaure, Y. (2004). Incidence of shoulder pain in repetitive work. *Occupational and environmental medicine, 61*(1), 39-44.

Li, G., & Buckle, P. (1998). The development of a practical method for the exposure assessment of risks to work-related musculoskeletal disorders. *General report to the HSE (Contract No. R3408), Robens Centre for Health Ergonomics, European Institute of Health and Medical Sciences, University of Surrey*.

Lim, C.-M., Jung, M.-C., & Kong, Y.-K. (2011). Evaluation of upper-limb body postures based on the effects of back and shoulder flexion angles on subjective discomfort ratings, heart rates and muscle activities. *Ergonomics, 54*(9), 849-857.

Lin, H.-T., Ko, H.-T., Lee, K.-C., Chen, Y.-C., & Wang, D.-C. (2015). The changes in shoulder rotation strength ratio for various shoulder positions and speeds in the scapular plane between baseball players and non-players. *Journal of physical therapy science, 27*(5), 1559.

Lippitt, S., & Matsen, F. (1993). Mechanisms of glenohumeral joint stability. *Clinical orthopaedics and related research, 291*, 20-28.

Lippitt, S. B., Vanderhooft, J. E., Harris, S. L., Sidles, J. A., Harryman, D. T., & Matsen, F. A. (1993). Glenohumeral stability from concavity-compression: a quantitative analysis. *Journal of Shoulder and Elbow Surgery, 2*(1), 27-35.

Lötters, F., Meerding, W.-J., & Burdorf, A. (2005). Reduced productivity after sickness absence due to musculoskeletal disorders and its relation to health outcomes. *Scandinavian journal of work, environment & health*, 367-374.

Luger, T., Bosch, T., Hoozemans, M. J., Veeger, D. H., & de Looze, M. P. (2016). Is rotating between static and dynamic work beneficial for our fatigue state? *Journal of Electromyography and Kinesiology, 28*, 104-113.

Mallat, S. G. (1989). A theory for multiresolution signal decomposition: The wavelet representation. *Pattern Analysis and Machine Intelligence, IEEE Transactions on, 11*(7), 674-693.

Masuda, K., Masuda, T., Sadoyama, T., Inaki, M., & Katsuta, S. (1999). Changes in surface EMG parameters during static and dynamic fatiguing contractions. *Journal of Electromyography and Kinesiology, 9*(1), 39-46.

Mathiassen, S. E., Winkel, J., Sahlin, K., & Melin, E. (1993). Biochemical indicators of hazardous shoulder-neck loads in light industry. *Journal of Occupational and Environmental Medicine, 35*(4), 404-407.

Mathur, S., Eng, J., & MacIntyre, D. (2005). Reliability of surface EMG during sustained contractions of the quadriceps. *Journal of Electromyography and Kinesiology, 15*(1), 102-110.

Maton, B. (1981). Human motor unit activity during the onset of muscle fatigue in submaximal isometric isotonic contraction. *European journal of applied physiology and occupational physiology, 46*(3), 271-281.

McAtamney, L., & Corlett, E. N. (1993). RULA: a survey method for the investigation of work-related upper limb disorders. *Applied ergonomics, 24*(2), 91-99.

McAtamney, L., & Hignett, S. (1995). REBA: a rapid entire body assessment method for investigating work related musculoskeletal disorders. *Proceedings of the Ergonomics Society of Australia, Adelaide*, 45-51.

McCluskey III, G. M., & Getz, B. A. (2000). Pathophysiology of anterior shoulder instability. *Journal of athletic training, 35*(3), 268.

McMahon, P. J., & Lee, T. Q. (2002). Muscles may contribute to shoulder dislocation and stability. *Clinical orthopaedics and related research, 403*, S18-S25.

Medicine. (2013). Mechanics of Glenohueral Instability. Retrieved from http://www.orthop.washington.edu/?q=patient-care/articles/shoulder/mechanics-of-glenohumeral-instability.html

Merletti, R., & Parker, P. A. (2004). *Electromyography: Physiology, engineering, and noninvasive applications*: Wiley-IEEE Press.

Merletti, R., Rainoldi, A., & Farina, D. (2004). Myoelectric manifestations of muscle fatigue.

Merletti, R., Rainoldi, A., & Farina, D. (2004). Myoelectric manifestations of muscle fatigue. *Electromyography: physiology, engineering, and noninvasive applications*, 233-258.

Meskers, C. G., de Groot, J. H., Arwert, H. J., Rozendaal, L. A., & Rozing, P. M. (2004). Reliability of force direction dependent EMG parameters of shoulder muscles for clinical measurements. *Clinical Biomechanics, 19*(9), 913-920.

Miranda, H., Punnett, L., Viikari-Juntura, E., Heliövaara, M., & Knekt, P. (2008). Physical work and chronic shoulder disorder. Results of a prospective population-based study. *Annals of the Rheumatic Diseases, 67*(2), 218-223.

Missenard, O., Mottet, D., & Perrey, S. (2008). The role of cocontraction in the impairment of movement accuracy with fatigue. *Experimental brain research, 185*(1), 151-156.

Montgomery, D. C. (2008). *Design and analysis of experiments*: John Wiley & Sons.

Moon, J., Shin, I., Kang, M., Kim, Y., Lee, K., Park, J., . . . O'sullivan, D. (2013). The effect of shoulder flexion angles on the recruitment of upper-extremity muscles during isometric contraction. *Journal of physical therapy science, 25*(10), 1299.

Moor, B., Bouaicha, S., Rothenfluh, D., Sukthankar, A., & Gerber, C. (2013). Is there an association between the individual anatomy of the scapula and the development of rotator cuff tears or osteoarthritis of the glenohumeral joint? *Bone Joint J, 95*(7), 935-941.

Moshou, D., Hostens, I., Papaioannou, G., & Ramon, H. (2005). Dynamic muscle fatigue detection using self-organizing maps. *Applied soft computing, 5*(4), 391-398.

Naomi, A., Darrin, A., David, B., Ninica, H., & Barbara, S. (2015). Work-Related Musculoskeletal Disorders of the Back, Upper Extremity, and Knee in Washington State, 2002-2010. Retrieved from http://www.lni.wa.gov/safety/research/files/wmsd_techreport2015.pdf

Newham, D., McCarthy, T., & Turner, J. (1991). Voluntary activation of human quadriceps during and after isokinetic exercise. *Journal of Applied Physiology, 71*(6), 2122.

Nikooyan, A. A., Veeger, H., Chadwick, E., Praagman, M., & van der Helm, F. C. (2011). Development of a comprehensive musculoskeletal model of the shoulder and elbow. *Medical & biological engineering & computing, 49*(12), 1425-1435.

Nimbarte, A. D., Sun, Y., Jaridi, M., & Hsiao, H. (2013). Biomechanical loading of the shoulder complex and lumbosacral joints during dynamic cart pushing task. *Applied ergonomics, 44*(5), 841-849.

Nussbaum, M. A. (2001). Static and dynamic myoelectric measures of shoulder muscle fatigue during intermittent dynamic exertions of low to moderate intensity. *European journal of applied physiology, 85*(3-4), 299-309.

Nussbaum, M. A. (2008). Utility of traditional and alternative EMG-based measures of fatigue during low-moderate level isometric efforts. *Journal of Electromyography and Kinesiology, 18*(1), 44-53.

Nussbaum, M. A. (2009). Effects of age, gender, and task parameters on fatigue development during intermittent isokinetic torso extensions. *International journal of industrial ergonomics, 39*(1), 185-191.

Ohisson, K., Attewell, R., Pålsson, B., Karlsson, B., Balogh, I., Johnsson, B., . . . Skerfving, S. (1995). Repetitive industrial work and neck and upper limb disorders in females. *American journal of industrial medicine, 27*(5), 731-747.

Oppenheim, A. V., Schafer, R. W., & Buck, J. R. (1989). *Discrete-time signal processing* (Vol. 2): Prentice hall Englewood Cliffs, NJ:.

Östör, A., Richards, C., Prevost, A., Speed, C., & Hazleman, B. (2005). Diagnosis and relation to general health of shoulder disorders presenting to primary care. *Rheumatology, 44*(6), 800-805.

Parameswariah, C., & Cox, M. (2002). Frequency characteristics of wavelets. *Power Delivery, IEEE Transactions on, 17*(3), 800-804.

Phinyomark, A., & Phukpattaranont, C. L. P. (2009). *Evaluation of wavelet function based on robust emg feature extraction*.

Piscione, J., & Gamet, D. (2006). Effect of mechanical compression due to load carrying on shoulder muscle fatigue during sustained isometric arm abduction: an electromyographic study. *European journal of applied physiology, 97*(5), 573-581.

Polikar, R. (2006). The wavelet tutorial. *Internet Resources: http://engineering. rowan. edu/ polikar/WAVELETS/WTtutorial. html*.

Pontillo, M., Orishimo, K. F., Kremenic, I. J., McHugh, M. P., Mullaney, M. J., & Tyler, T. F. (2007). Shoulder musculature activity and stabilization during upper extremity weight-bearing activities. *North American journal of sports physical therapy: NAJSPT, 2*(2), 90.

Poppen, N., & Walker, P. (1978). Forces at the glenohumeral joint in abduction. *Clinical orthopaedics and related research, 135*, 165-170.

Potvin, J. (1997). Effects of muscle kinematics on surface EMG amplitude and frequency during fatiguing dynamic contractions. *Journal of Applied Physiology, 82*(1), 144.

Putz-Anderson, V., Bernard, B. P., Burt, S. E., Cole, L. L., Fairfield-Estill, C., Fine, L. J., . . . Hurrell Jr, J. J. (1997). Musculoskeletal disorders and workplace factors. *National Institute for Occupational Safety and Health (NIOSH)*.

Ranniger, C. U., & Akin, D. (1997). *EMG mean power frequency determination using wavelet analysis*.

Rashedi, E., & Nussbaum, M. A. (2016). Cycle time influences the development of muscle fatigue at low to moderate levels of intermittent muscle contraction. *Journal of Electromyography and Kinesiology, 28*, 37-45.

Reaz, M. B. I., Hussain, M. S., & Mohd-Yasin, F. (2006, 17-19 Aug. 2006). *EMG analysis using wavelet functions to determine muscle contraction.* Paper presented at the e-Health Networking, Applications and Services, 2006.

Roman-Liu, D., Tokarski, T., & Wójcik, K. (2004). Quantitative assessment of upper limb muscle fatigue depending on the conditions of repetitive task load. *Journal of Electromyography and Kinesiology, 14*(6), 671-682.

Sakakibara, H., Miyao, M., Kondo, T.-A., & Yamada, S. Y. (1995). Overhead work and shoulder-neck pain in orchard farmers harvesting pears and apples. *Ergonomics, 38*(4), 700-706.

Samar, V. J., Bopardikar, A., Rao, R., & Swartz, K. (1999). Wavelet analysis of neuroelectric waveforms: a conceptual tutorial. *Brain and language, 66*(1), 7-60.

Savoie, S. (2015). *Predicting co-contraction with an open source musculoskeletal shoulder model during dynamic and static tasks.*

Sbriccoli, P., Bazzucchi, I., Rosponi, A. e. a., Bernardi, M., De Vito, G., & Felici, F. (2003). Amplitude and spectral characteristics of biceps Brachii sEMG depend upon speed of isometric force generation. *Journal of Electromyography and Kinesiology, 13*(2), 139-147.

Seghers, J., & Spaepen, A. (2004). Muscle fatigue of the elbow flexor muscles during two intermittent exercise protocols with equal mean muscle loading. *Clinical Biomechanics, 19*(1), 24-30.

Sekulic, D., Medved, V., & Rausavljevi, N. (2006). EMG analysis of muscle load during simulation of characteristic postures in dinghy sailing. *Journal of sports medicine and physical fitness, 46*(1), 20-27.

Selen, L., Beek, P., & van Dieën, J. (2007). Fatigue-induced changes of impedance and performance in target tracking. *Experimental brain research, 181*(1), 99-108.

Smith, J. L., Edgerton, V. R., Betts, B., & Collatos, T. (1977). EMG of slow and fast ankle extensors of cat during posture, locomotion, and jumping. *Journal of Neurophysiology, 40*(3), 503-513.

Søgaard, K., Blangsted, A., Jørgensen, L., Madeleine, P., & Sjøgaard, G. (2003). Evidence of long term muscle fatigue following prolonged intermittent contractions based on mechano-and electromyograms. *Journal of Electromyography and Kinesiology, 13*(5), 441-450.

Sommerich, C. M., Joines, S. M., Hermans, V., & Moon, S. D. (2000). Use of surface electromyography to estimate neck muscle activity. *Journal of Electromyography and Kinesiology, 10*(6), 377-398.

Sood, D., Nussbaum, M. A., & Hager, K. (2007). Fatigue during prolonged intermittent overhead work: reliability of measures and effects of working height. *Ergonomics, 50*(4), 497-513.

Sparto, P. J., Parnianpour, M., Barria, E. A., & Jagadeesh, J. M. (2000). Wavelet and short-time Fourier transform analysis of electromyography for detection of back muscle fatigue. *Rehabilitation Engineering, IEEE Transactions on, 8*(3), 433-436.

Stenlund, B., Goldie, I., Hagberg, M., & Hogstedt, C. (1993). Shoulder tendinitis and its relation to heavy manual work and exposure to vibration. *Scandinavian journal of work, environment & health*, 43-49.

Strimpakos, N., Georgios, G., Eleni, K., Vasilios, K., & Jacqueline, O. (2005). Issues in relation to the repeatability of and correlation between EMG and Borg scale assessments of neck muscle fatigue. *Journal of Electromyography and Kinesiology, 15*(5), 452-465.

Torrence, C., & Compo, G. P. (1998). A practical guide to wavelet analysis. *Bulletin of the American Meteorological Society, 79*(1), 61-78.

Tsai, M., & Hsu, A. (2015). The aging effects on the glenohumeral joint stiffness in association with anteroposterior glide mobilization: in vivo robotic testing. *Physiotherapy, 101*, e594.

Tucker, K., Falla, D., Graven-Nielsen, T., & Farina, D. (2009). Electromyographic mapping of the erector spinae muscle with varying load and during sustained contraction. *Journal of Electromyography and Kinesiology, 19*(3), 373-379.

Unnithan, V., Dowling, J., Frost, G., Volpe, A. B., & Bar-Or, O. (1996). Cocontraction and phasic activity during GAIT in children with cerebral palsy. *Electromyography and clinical neurophysiology*, *36*(8), 487-494.

Veeger, H., & Van Der Helm, F. (2007). Shoulder function: the perfect compromise between mobility and stability. *Journal of biomechanics*, *40*(10), 2119-2129.

Viehöfer, A. F., Gerber, C., Favre, P., Bachmann, E., & Snedeker, J. G. (2015). A larger critical shoulder angle requires more rotator cuff activity to preserve joint stability. *Journal of Orthopaedic Research*.

Vøllestad, N. K. (1997). Measurement of human muscle fatigue. *Journal of neuroscience methods*, *74*(2), 219-227.

Von Tscharner, V., Goepfert, B., & Nigg, B. M. (2003). Changes in EMG signals for the muscle tibialis anterior while running barefoot or with shoes resolved by non-linearly scaled wavelets. *Journal of biomechanics*, *36*(8), 1169-1176.

Vukova, T., Vydevska-Chichova, M., & Radicheva, N. (2008). Fatigue-induced changes in muscle fiber action potentials estimated by wavelet analysis. *Journal of Electromyography and Kinesiology*, *18*(3), 397-409.

Walker, S., Davis, L., Avela, J., & Häkkinen, K. (2012). Neuromuscular fatigue during dynamic maximal strength and hypertrophic resistance loadings. *Journal of Electromyography and Kinesiology*, *22*(3), 356-362.

Walmsley, B., Hodgson, J., & Burke, R. (1978). Forces produced by medial gastrocnemius and soleus muscles during locomotion in freely moving cats. *J. Neurophysiol*, *41*(5), 1203-1216.

Wang, D., Dai, F., & Ning, X. (2015). Risk Assessment of Work-Related Musculoskeletal Disorders in Construction: State-of-the-Art Review. *Journal of Construction Engineering and Management*, *141*(6), 04015008.

Werner, C., Favre, P., & Gerber, C. (2007). The role of the subscapularis in preventing anterior glenohumeral subluxation in the abducted, externally rotated position of the arm. *Clinical Biomechanics, 22*(5), 495-501.

Wiker, S. F., Chaffin, D. B., & Langolf, G. D. (1989). Shoulder posture and localized muscle fatigue and discomfort. *Ergonomics, 32*(2), 211-237.

Wiktorin, C., Karlqvist, L., & Winkel, J. (1993). Validity of self-reported exposures to work postures and manual materials handling. *Scandinavian journal of work, environment & health*, 208-214.

Yoshitake, Y., Ue, H., Miyazaki, M., & Moritani, T. (2001). Assessment of lower-back muscle fatigue using electromyography, mechanomyography, and near-infrared spectroscopy. *European journal of applied physiology, 84*(3), 174-179.

Yung, M., Mathiassen, S. E., & Wells, R. P. (2012). Variation of force amplitude and its effects on local fatigue. *European journal of applied physiology, 112*(11), 3865-3879.

APPENDICES

Appendix A: Physical Activity Readiness Questionnaire (PAR-Q)

Physical Activity Readiness Questionnaire (PAR-Q)

For most people physical activity should not pose any problem or hazard. PAR-Q has been designed to identify the small number of adults for whom physical activity might be inappropriate or those who should have medical advice concerning the type of activity most suitable for them.

YES	NO	
☐	☐	1. Has your doctor ever said you have a heart trouble and should only do physical activity recommended by a doctor?
☐	☐	2. Do you frequently suffer from chest pain?
☐	☐	3. Do you often faint or have spells of severe dizziness?
☐	☐	4. Has your doctor ever said your blood pressure was too high?
☐	☐	5. Has your doctor ever told you that you have a bone or joint problem such as arthritis that has been aggravated by, or might be made worse with exercise.
☐	☐	6. Is there any good physical reason why you should not follow an activity program even if you want to?
☐	☐	7. Are you 65 and not accustomed to vigorous exercise?

If you answer "yes" to any question, vigorous exercise or exercise testing should be postponed. Medical clearance may be necessary.

I have read this questionnaire, I understand it does not provide medical assessment in lieu of a physical examination by a physician.

Participant's signature: _____ Date: _____

Investigator's signature: _____ Date: _____

Adapted from PAR-Q validation report, British Columbia department of Health, June 1975.

Reference: BQ Hafen, WWK Hoeger (1994), Wellness: Guidelines for a healthy lifestyle. Englewood, CO: Morton Pub. Co.

Appendix B: IRB Approval

Only Minimal Risk
Consent Information Form (without HIPAA)

Principal Investigator	Dr. Ashish Nimbarte
Department	Industrial and Management Systems Engineering
Protocol Number	1505685703
Study Title	**Evaluation of concavity compression mechanism as a possible predictor of shoulder muscle fatigue**
Co-Investigator(s)	**Suman Chowdhury**
Sponsor (if any)	**None**

Contact Persons

In the event you experience any side effects or injury related to this research, you should contact Dr. Ashish Nimbarte at (304) 293-9473. (After hours contact: Dr. Ashish Nimbarte at (225) 226-8813). If you have any questions, concerns, or complaints about this research, you can contact Dr. Ashish Nimbarte at (304) 293-9473 or at (225) 226-8813) for 24/7.

For information regarding your rights as a research subject, to discuss problems, concerns, or suggestions related to the research, to obtain information or offer input about the research, contact the Office of Research Integrity & Compliance at (304) 293-7073.

In addition if you would like to discuss problems, concerns, have suggestions related to research, or would like to offer input about the research, contact the Office of Research Integrity and Compliance at 304-293-7073.

Introduction

You, _____, have been asked to participate in this research study, which has been explained to you by Suman Chowdhury, Con-Investigator. This study is being conducted by Ergonomics Lab in the Department of Industrial and Management Systems Engineering at West Virginia University.

Purpose(s) of the Study

The purpose of this study is to identify risky shoulder exertions in the workplace.

Description of Procedures

In the first experiment, you will be asked to perform thirty different material handling tasks. At the first step, your demographic information will be recorded. Next, you will perform the material handling tasks using a small weight of 2 lbs. Out of these thirty tasks, three tasks will be selected for the second experiment of the study.

After one week of the first experiment, you will participate in the second experiment. At the first step, you will be explained the details of the experimental tasks. Then, you will be prepared for muscle activity data collection. You will perform two consecutive maximum exertions for a muscle. You will be given a ten minutes of rest after all maximum exertion trials. Next, you will be asked to perform repetitive exertions of the selected three tasks in the first experiment. You will perform the tasks using three different weights of 2, 6, and 8 lbs. The duration of each task is 1 min. You will be allowed to take a rest period of 2 min between any two tasks.

Discomforts

There are no known or expected risks from participating in this study, except for the mild discomfort at the shoulder muscles associated with repetitive exertions for 1 min.

Alternatives

You do not have to participate in this study.

Benefits

You may not receive any direct benefit from this study. The knowledge gained from this study may eventually benefit others.

Financial Considerations

There are no special fees for participating in this study. If student, you will not earn extra credit for participating in this study.

Confidentiality

Any information about you that is obtained as a result of your participation in this research will be kept as confidential as legally possible. Your research records and test results, just like hospital records, may be subpoenaed by court order or may be inspected by the study sponsor or federal regulatory authorities (including the FDA if applicable) without your additional consent.

Voluntary Participation

Participation in this study is voluntary. You are free to withdraw your consent to participate in this study at any time.

Refusal to participate or withdrawal will not affect [your class standing or grades, as appropriate] and will involve no penalty to you. Refusal to participate or withdrawal will not affect your future care, or your employee status at West Virginia University.

In the event new information becomes available that may affect your willingness to participate in this study, this information will be given to you so that you can make an informed decision about whether or not to continue your participation.

You have been given the opportunity to ask questions about the research, and you have received answers concerning areas you did not understand.

Upon signing this form, you will receive a copy.

I willingly consent to participate in this research.

Signatures

Signature of Subject

_____

Printed Name Date Time

_____

The participant has had the opportunity to have questions addressed. The participant willingly agrees to be in the study.

Signature of Investigator or Co-Investigator

_____

Printed Name Date Time

_____

Appendix C: Demographic and Physical Measurements of Individual Participants.

Table 15: Individual demographic and physical measurement data for Aim 1.

	Age	Weight	Height	Tronchanterion	Elbow	Mid upper arm	Shoulder
Subject 1	30	140	69	35	43	50.5	58
Subject 2	32	166	71	38	45	52	59
Subject 3	34	183	71	37.5	45	52.5	60
Subject 4	24	158	70	39	44	51.5	59
Subject 5	30	180	70	39.5	45	51.75	58.5
Subject 6	25	153	68	40	43	50.75	58.5
Subject 7	26	188	67	36.5	40.5	47.75	55
Subject 8	27	153	68	39.5	45	51.25	57.5

Appendix D: Mean Strain Index Values of the Individual Participants.

Table 16: Mean strain index values of the tasks for subject 1.

Vertical positions	Mid-sagittal plane	45° right to mid-sagittal plane	Frontal plane
Trochanterion to trochanterion	10.61	9.27	10.06
Elbow to elbow	8.86	9.28	11.70
Mid upper arm to mid upper arm	16.13	13.62	15.88
Shoulder to shoulder	15.17	16.35	16.33
Trochanterion to elbow	10.96	10.16	11.86
Trochanterion to mid upper arm	11.48	11.31	12.33
Trochanterion to shoulder	11.49	12.89	12.45
Elbow to mid upper arm	13.67	14.25	13.97
Elbow to shoulder	13.43	12.37	13.67
Mid upper arm to shoulder	16.92	15.90	17.07

Table 17: Mean strain index values of the tasks for subject 2.

Vertical positions	Mid-sagittal plane	45° right to mid-sagittal plane	Frontal plane
Trochanterion to trochanterion	9.79	10.50	11.19
Elbow to elbow	10.47	11.34	11.70
Mid upper arm to mid upper arm	17.66	15.74	18.05
Shoulder to shoulder	17.65	18.92	18.30
Trochanterion to elbow	13.39	9.40	12.78
Trochanterion to mid upper arm	13.88	13.41	14.56
Trochanterion to shoulder	14.64	17.23	16.07
Elbow to mid upper arm	15.94	16.52	16.02
Elbow to shoulder	15.54	14.61	15.93
Mid upper arm to shoulder	18.11	17.74	18.61

Table 18: Mean strain index values of the tasks for subject 3.

Vertical positions	Mid-sagittal plane	45° right to mid-sagittal plane	Frontal plane
Trochanterion to trochanterion	16.46	15.61	15.27
Elbow to elbow	19.38	19.11	18.50
Mid upper arm to mid upper arm	22.78	21.01	22.72
Shoulder to shoulder	22.79	20.37	21.72
Trochanterion to elbow	18.80	19.57	19.51
Trochanterion to mid upper arm	23.12	24.44	22.54
Trochanterion to shoulder	23.48	21.37	21.85
Elbow to mid upper arm	23.25	20.85	20.84
Elbow to shoulder	20.53	20.20	19.55
Mid upper arm to shoulder	24.42	24.29	24.29

Table 19: Mean strain index values of the tasks for subject 4.

Vertical positions	Mid-sagittal plane	45° right to mid-sagittal plane	Frontal plane
Trochanterion to trochanterion	19.83	18.27	16.92
Elbow to elbow	22.55	20.68	20.34
Mid upper arm to mid upper arm	26.66	24.61	26.83
Shoulder to shoulder	25.30	24.59	27.16
Trochanterion to elbow	21.85	21.19	22.71
Trochanterion to mid upper arm	27.03	27.57	27.26
Trochanterion to shoulder	26.94	24.30	24.31
Elbow to mid upper arm	28.78	23.61	25.65
Elbow to shoulder	24.67	23.77	22.53
Mid upper arm to shoulder	28.26	26.13	26.15

Table 20: Mean strain index values of the tasks for subject 5.

Vertical positions	Mid-sagittal plane	45° right to mid-sagittal plane	Frontal plane
Trochanterion to trochanterion	12.11	8.55	8.06
Elbow to elbow	15.27	14.11	13.90
Mid upper arm to mid upper arm	17.10	17.65	15.91
Shoulder to shoulder	17.13	15.54	16.67
Trochanterion to elbow	18.51	18.49	16.63
Trochanterion to mid upper arm	16.00	14.38	13.59
Trochanterion to shoulder	17.04	15.53	14.37
Elbow to mid upper arm	20.30	17.19	19.01
Elbow to shoulder	17.23	16.17	15.85
Mid upper arm to shoulder	20.98	17.01	17.55

Table 21: Mean strain index values of the tasks for subject 6.

Vertical positions	Mid-sagittal plane	45° right to mid-sagittal plane	Frontal plane
Trochanterion to trochanterion	13.91	11.40	10.80
Elbow to elbow	19.51	18.02	17.77
Mid upper arm to mid upper arm	21.17	21.84	19.64
Shoulder to shoulder	21.09	19.04	20.44
Trochanterion to elbow	23.41	23.36	21.04
Trochanterion to mid upper arm	20.05	17.98	16.97
Trochanterion to shoulder	21.10	19.15	17.71
Elbow to mid upper arm	25.06	21.10	23.40
Elbow to shoulder	21.36	19.96	19.57
Mid upper arm to shoulder	25.57	20.77	21.43

Table 22: Mean strain index values of the tasks for subject 7.

Vertical positions	Mid-sagittal plane	45° right to mid-sagittal plane	Frontal plane
Trochanterion to trochanterion	12.95	11.02	10.34
Elbow to elbow	15.31	13.79	15.58
Mid upper arm to mid upper arm	16.76	13.04	16.12
Shoulder to shoulder	17.73	15.11	16.56
Trochanterion to elbow	15.22	12.80	16.22
Trochanterion to mid upper arm	16.52	15.75	17.43
Trochanterion to shoulder	16.90	15.61	14.96
Elbow to mid upper arm	18.51	15.54	19.08
Elbow to shoulder	17.43	16.07	15.74
Mid upper arm to shoulder	19.73	15.61	18.53

Table 23: Mean strain index values of the tasks for subject 8.

Vertical positions	Mid-sagittal plane	45° right to mid-sagittal plane	Frontal plane
Trochanterion to trochanterion	5.37	4.65	3.92
Elbow to elbow	8.27	9.47	12.29
Mid upper arm to mid upper arm	18.75	17.12	14.89
Shoulder to shoulder	26.56	25.48	25.71
Trochanterion to elbow	11.83	10.60	7.61
Trochanterion to mid upper arm	14.76	13.51	13.80
Trochanterion to shoulder	19.31	16.90	18.30
Elbow to mid upper arm	24.29	28.34	18.77
Elbow to shoulder	19.31	18.94	19.18
Mid upper arm to shoulder	24.36	22.31	25.19

Appendix E: Mean Strain Index Values for Nonparametric Test.

Table 24: Mean strain index values of the individual participant.

	High strain index	Medium strain index	Low strain index
Subject 1	16.92	11.86	9.27
Subject 2	18.11	12.78	10.50
Subject 3	24.42	19.51	15.61
Subject 4	28.26	22.71	18.27
Subject 5	20.98	16.63	8.55
Subject 6	25.57	21.04	11.40
Subject 7	19.73	16.22	11.02
Subject 8	24.36	7.61	4.65

Table 25: Mann-Whitney test results.

Test	Point Estimate	P
High = Medium High > Medium	5.802	0.012
High = Low High > Low	10.831	0.001
Medium = Low Meidum > Low	5214	0.026

Appendix F : Matlab Scripts

Appendix F1: Matlab Script to Estimate the Maximum of the MVC Exertion Signal

```
clear all;
load('C:\Users\User\Desktop\EMG_Dissertation\Farzad_EMG\Triceps_3.txt');
Raw = Triceps_3;
for i = 1:8
EMG_R = Raw(:,i);% extract each muscle data
fs = 2000; %Sampling frequency
[m,z]=size(EMG_R); %Size of the raw signal
EMG_R = EMG_R - mean(EMG_R); %Demeaned
n= floor(m/fs); %duration in # of full seconds
sn = n*fs;% to get only integer # of data
EMG = EMG_R(1:sn,:);% data length
N = n*fs/2; % number of samples in half of FFT
f = fs*(0:N-1)/2/N; % frequency scaling use for median frequency computation
    X = fft(EMG);
    %Filters 0-12 Hz
    X((n*0+1):(n*(12)+1))=0;
    X(length(X)-(n*(12)-1):length(X)-(n*1-1))=0;  % high pass filtering
    %Filters 59-61 Hz
    X((n*59+1):(n*(61)+1))=0;
    X(length(X)-(n*(61)-1):length(X)-(n*59-1))=0; % Attenuating line interference
    %Filters 119-121 Hz
    X((n*119+1):(n*(121)+1))=0;
    X(length(X)-(n*(121)-1):length(X)-(n*119-1))=0; % Attenuating line interference
    %Filters 179-181 Hz
    X((n*179+1):(n*(181)+1))=0;
    X(length(X)-(n*(181)-1):length(X)-(n*179-1))=0; % Attenuating line interference
    %Filters 239-241 Hz
     X((n*239+1):(n*(241)+1))=0;
     X(length(X)-(n*(241)-1):length(X)-(n*239-1))=0; % Attenuating line
interference
    %Filters 299-301 Hz
    X((n*299+1):(n*(301)+1))=0;
    X(length(X)-(n*(301)-1):length(X)-(n*299-1))=0; % Attenuating line interference
    %Filters 359-361 Hz
```

```
    X((n*359+1):(n*(361)+1))=0;
    X(length(X)-(n*(361)-1):length(X)-(n*359-1))=0; % Attenuating line interference
   % Filters 400-1000 Hz
    X((n*400+1):(n*(1000)+1))=0;
    X(length(X)-(n*(1000)-1):length(X)-(n*400-1))=0;  % low pass filtering
    d2 = real(ifft(X,'symmetric'));%ifft transform
d2_abs = abs(d2); % Full wave rectified
%d2_abs = abs(EMG);
Newd2(:,i) = d2;
New_D2(:,i) = d2_abs;
fc = 10 ;
n_o = 8;
[b,a] = butter(n_o,2*fc/fs);
g_abs = filter(b,a,d2_abs);  % low pass Butterworth smoothed
g_smooth_D2(:,i) = g_abs;
Max_g_smooth_D2(:,i) = max(g_smooth_D2(:,i));
end;
openvar('Max_g_smooth_D2');
```

Appendix F2: Matlab Script to Estimate the Global Muscle Fatigue Index.

```
clearvars -except Max_g_smooth_D2 Sig_fre Sig_amp;
Raw_amp = Sig_amp(87001:110000,:);
Raw_sig = Sig_fre(87001:110000,:);
%A = [5.63 4.29 5.21 3.83 3.87 4.48 2.14 8.87];
S_fiber = [0.60 0.60 0.60 0.59 0.45 0.48 0.423 0.34];
F_fiber = [0.40 0.40 0.40 0.41 0.55 0.52 0.577 0.66];
F = F_fiber./S_fiber;

Avg_S_fiber = mean(S_fiber);
FSF = S_fiber.*Avg_S_fiber;
Fib = F.*FSF;
% Amplitude analysis
[m1,z1] = size(Raw_amp);
flip_Raw_amp = flipud(Raw_amp);

w = 50;
% first find the silent period at the beginning
```

```
Raw_amp_std_data = zeros(m1,1);
Raw_amp_mean_data = zeros(m1,1);
Raw_amp_testdata = zeros (m1,1);
flip_Raw_amp_std_data = zeros(m1,1);
flip_Raw_amp_mean_data = zeros(m1,1);
flip_Raw_amp_testdata = zeros (m1,1);

for i = 1:z1
for Raw_amp_j = w+1:m1-w
Raw_amp_std_data = std(Raw_amp(Raw_amp_j-w:Raw_amp_j+w,i));
Raw_amp_mean_data = mean(Raw_amp(Raw_amp_j-w:Raw_amp_j+w,i));
Raw_amp_testdata(Raw_amp_j-w:Raw_amp_j+w,i) = Raw_amp_mean_data +
2*Raw_amp_std_data ;%mean plus three std dev
for Raw_amp_index = 1:m1
     if Raw_amp(Raw_amp_index ,i)> Raw_amp_testdata(Raw_amp_index ,i)
     %if Raw_amp(Raw_amp_index ,i)> Raw_amp_testdata(:,i)
        Beg_Time = Raw_amp(Raw_amp_index ,i);
        Raw_amp_index;
        break;
    else
        continue;
    end;
end;
end;
Beg_T = Raw_amp_index;

for flip_Raw_amp_j = w+1:m1-w
flip_Raw_amp_std_data = std(flip_Raw_amp(flip_Raw_amp_j-w:flip_Raw_amp_j+w,i));
flip_Raw_amp_mean_data= mean(flip_Raw_amp(flip_Raw_amp_j-w:flip_Raw_amp_j+w,i));
flip_Raw_amp_testdata(flip_Raw_amp_j-w:flip_Raw_amp_j+w,i) = flip_Raw_amp_mean_data
+ 2*flip_Raw_amp_std_data ;%mean plus three std dev

% finding the time-location index for ending of the contraction
for flip_Raw_amp_index = 1:m1
     if flip_Raw_amp(flip_Raw_amp_index ,i)>
flip_Raw_amp_testdata(flip_Raw_amp_index ,i)
      %if flip_Raw_amp(flip_Raw_amp_index ,i)> flip_Raw_amp_testdata(:,i)
```

```
         flip_Beg_T1 = flip_Raw_amp(flip_Raw_amp_index ,i);
        flip_Raw_amp_index;
        break;
    else
        continue;
    end;
end;
end;
End_T = m1 - flip_Raw_amp_index; %Ending time of the contraction
%Lp(:,i) =  Raw_amp_index +  flip_Raw_amp_index; % latent/silent period of the
signal
Cp(:,i) = End_T - Beg_T; %contraction time of the signal
%dc(:,i)= Cp(:,i)/m1; % duty cycle of the task

IEMG = sum(Raw_amp(Beg_T:End_T,i));%Integrated EMG of a muscle
%IEMG = sum(Raw_amp(:,i));
MAV = IEMG/(End_T-Beg_T); % MAV of a muscle
%MAV = IEMG/m1;
m_IEMG(:,i)= IEMG; %IEMG matrix
m_MAV(:,i)= MAV; %MAV matrix
m_Beg_T(:,i) = Beg_T; %Beginning time of all muscles
m_End_T(:,i) = End_T; %Ending time of all muscles

%Frequency calculation
EMG2 = Raw_sig(:,i);
w1 = 'rbio3.1';
[C L] = wavedec(EMG2,7,w1);
D1 = detcoef(C,L,1);
D2 = detcoef(C,L,2);
D3 = detcoef(C,L,3);
D4 = detcoef(C,L,4);
D5 = detcoef(C,L,5);
D6 = detcoef(C,L,6);
D7 = detcoef(C,L,7);
Q1 = sum(D1.^2);
Q2 = sum(D2.^2);
Q3 = sum(D3.^2);
Q4 = sum(D4.^2);
```

```
Q5 = sum(D5.^2);
Q6 = sum(D6.^2);
Q7 = sum(D7.^2);
Wave_Fre_Ratio(:,i) = ((Q5+Q6)/(Q3+Q4))*100;
end;
c = 1;
for i = 1:m1
    if Raw_amp(i,7)<Raw_amp(i,8)
       CI(i,:) = Raw_amp(i,7)/(Raw_amp(i,8)+Raw_amp(i,7));
  else
     CI(i,:) = Raw_amp(i,8)/(Raw_amp(i,8)+Raw_amp(i,7));
    end;
end;
Int_CI = m1/(sum (CI)); %antagonist muscle groups
Int_CI2 = (sum(Raw_amp(:,8))+ sum(Raw_amp(:,7)))/sum(Raw_amp(:,7));
GFI_1stTerm = sum(m_MAV.*Wave_Fre_Ratio.*Fib)/8;
GFI_unscaled = [GFI_1stTerm/10 + (1/c)*(Int_CI)*10];
GFI_scaled = [GFI_unscaled*inv(10*mean(FSF)];
openvar('GFI');
```

Appendix G: Global Fatigue Index Data for the Individual Participants.

Table 26: Percent change in global fatigue index and log transformed data for individual participants.

Subject	Exertion type	Weight	Percent change in global fatigue index	Log transformed data	Subject	Exertion type	Weight	Percent change in global fatigue index	Log transformed data
1	Static	2 lb	16.65	1.22	1	Dynamic	2 lb	12.22	1.09
2	Static	2 lb	56.72	1.75	2	Dynamic	2 lb	38.68	1.59
3	Static	2 lb	20.79	1.32	3	Dynamic	2 lb	29.80	1.47
4	Static	2 lb	15.13	1.18	4	Dynamic	2 lb	50.80	1.71
5	Static	2 lb	36.29	1.56	5	Dynamic	2 lb	16.72	1.22
6	Static	2 lb	65.33	1.82	6	Dynamic	2 lb	9.41	0.97
7	Static	2 lb	82.93	1.92	7	Dynamic	2 lb	31.02	1.49
8	Static	2 lb	17.90	1.25	8	Dynamic	2 lb	16.11	1.21
1	Static	6 lb	46.57	1.67	1	Dynamic	6 lb	33.28	1.52
2	Static	6 lb	93.21	1.97	2	Dynamic	6 lb	56.83	1.75
3	Static	6 lb	99.34	2.00	3	Dynamic	6 lb	44.04	1.64
4	Static	6 lb	25.82	1.41	4	Dynamic	6 lb	100.60	2.00
5	Static	6 lb	66.08	1.82	5	Dynamic	6 lb	29.50	1.47
6	Static	6 lb	87.21	1.94	6	Dynamic	6 lb	55.28	1.74
7	Static	6 lb	123.83	2.09	7	Dynamic	6 lb	59.08	1.77
8	Static	6 lb	41.59	1.62	8	Dynamic	6 lb	12.92	1.11

Appendix H: Statistical Analysis Results for the Effect of Type of Exertion and Weight Level

Dependent variable: Percent change in global fatigue index

Source	DF	Sum of Squares	Mean Square	F Value	Pr > F
Model	9	1.829	0.203	4.172	0.003
Error	22	1.071	0.049		
Corrected Total	31	2.900			

R-Square	Coeff Var	Root MSE	Index Mean
0.630527	14.36815	0.225881	1.572092

Source	DF	Type I SS	Mean Square	Expected Mean Square	F Value	Pr > F
Block	7	0.877	0.125	0.1252	2.572	0.0425
Exertion	1	0.241	0.241	0.290	5.957	0.0232
Weight	1	0.710	0.710	0.759	15.585	0.0006

Source	Type III Expected Mean Square
Block	$\sigma^2 + 7\ \sigma^2_{block}$
Exertion	$\sigma^2 + 2*7*\emptyset_{exertion}$
Weight	$\sigma^2 + 2*7*\emptyset_{weight}$

Levene's Test for Homogeneity of Index Variance for the effect of Weight					
Source	DF	Sum of Squares	Mean Square	F Value	Pr > F
Weight	1	0.000969	0.000969	0.14	0.7101
Error	30	0.2065	0.00688		

Levene's Test for Homogeneity of Index Variance for the effect of Exertion					
Source	DF	Sum of Squares	Mean Square	F Value	Pr > F
Exertion	1	0.000310	0.000310	0.05	0.8296
Error	30	0.1973	0.00658		

Normality test results				
Test	Statistic		p Value	
Shapiro-Wilk	W	0.965434	Pr < W	0.3838
Kolmogorov-Smirnov	D	0.101669	Pr > D	>0.1500
Cramer-von Mises	W-Sq	0.050289	Pr > W-Sq	>0.2500
Anderson-Darling	A-Sq	0.349203	Pr > A-Sq	>0.2500

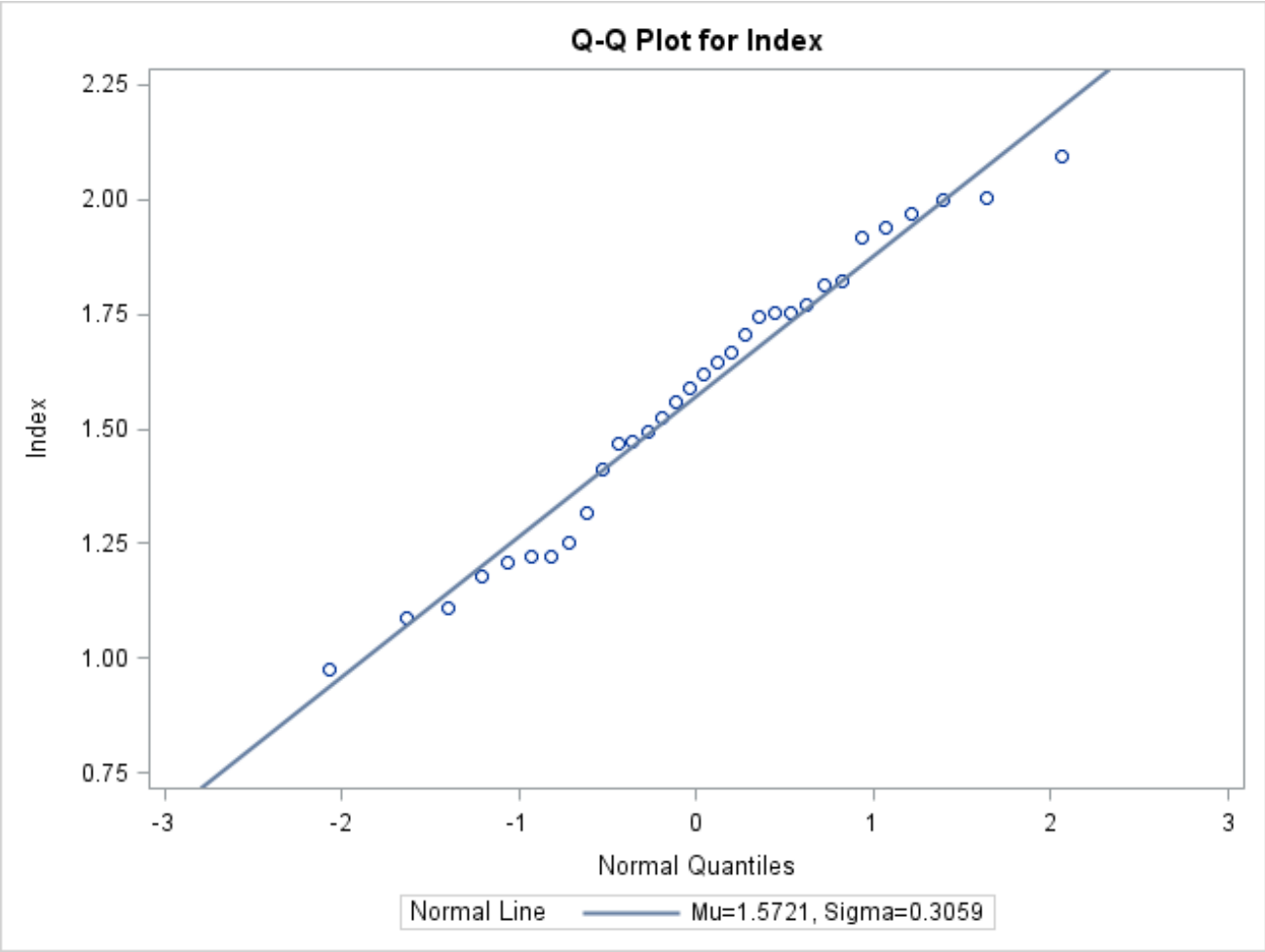

Figure 26: Q-Q plot for the normality test for percent change in global fatigue index in Aim 2.

Appendix I: Log Transformed Data

Appendix I1: Log Transformed Data of Percent Change in Global Fatigue Index.

Table 27: Log transformed data of percent change in global fatigue index for all participants.

Subject	Task	Weight	Percent change in global fatigue index	Transformed data	Subject	Task	Weight	Percent change in global fatigue index	Transformed data
1	Low	2 lb	2.91	0.46	6	Low	2 lb	7.61	0.88
1	Low	4 lb	5.62	0.75	6	Low	4 lb	11.96	1.08
1	Low	6 lb	3.09	0.49	6	Low	6 lb	30.99	1.49
1	Medium	2 lb	5.62	0.75	6	Medium	2 lb	11.01	1.04
1	Medium	4 lb	15.54	1.19	6	Medium	4 lb	37.49	1.57
1	Medium	6 lb	8.21	0.91	6	Medium	6 lb	51.20	1.71
1	High	2 lb	5.13	0.71	6	High	2 lb	31.71	1.50
1	High	4 lb	13.55	1.13	6	High	4 lb	42.21	1.63
1	High	6 lb	22.29	1.35	6	High	6 lb	73.11	1.86
2	Low	2 lb	9.34	0.97	7	Low	2 lb	6.26	0.80
2	Low	4 lb	8.09	0.91	7	Low	4 lb	9.59	0.98
2	Low	6 lb	8.79	0.94	7	Low	6 lb	10.20	1.01
2	Medium	2 lb	11.61	1.06	7	Medium	2 lb	7.26	0.86
2	Medium	4 lb	21.69	1.34	7	Medium	4 lb	19.75	1.30
2	Medium	6 lb	26.47	1.42	7	Medium	6 lb	17.61	1.25
2	High	2 lb	12.46	1.10	7	High	2 lb	14.62	1.16
2	High	4 lb	33.10	1.52	7	High	4 lb	19.69	1.29

Subject	Task	Weight	Percent change in global fatigue index	Transformed data	Subject	Task	Weight	Percent change in global fatigue index	Transformed data
2	High	6 lb	40.91	1.61	7	High	6 lb	35.20	1.55
2	High	6 lb	40.91	1.61	7	High	6 lb	35.20	1.55
3	Low	2 lb	6.77	0.83	8	Low	2 lb	3.71	0.57
3	Low	4 lb	1.98	0.30	8	Low	4 lb	2.98	0.47
3	Low	6 lb	12.32	1.09	8	Low	6 lb	16.67	1.22
3	Medium	2 lb	2.87	0.46	8	Medium	2 lb	8.19	0.91
3	Medium	4 lb	7.75	0.89	8	Medium	4 lb	9.06	0.96
3	Medium	6 lb	6.65	0.82	8	Medium	6 lb	19.60	1.29
3	High	2 lb	10.03	1.00	8	High	2 lb	10.81	1.03
3	High	4 lb	13.57	1.13	8	High	4 lb	31.18	1.49
3	High	6 lb	11.95	1.08	8	High	6 lb	36.38	1.56
4	Low	2 lb	6.68	0.83	9	Low	2 lb	10.68	1.03
4	Low	4 lb	7.16	0.86	9	Low	4 lb	8.14	0.91
4	Low	6 lb	10.00	1.00	9	Low	6 lb	4.11	0.61
4	Medium	2 lb	6.48	0.81	9	Medium	2 lb	6.76	0.83
4	Medium	4 lb	0.74	-0.13	9	Medium	4 lb	7.03	0.85
4	Medium	6 lb	6.38	0.80	9	Medium	6 lb	32.07	1.51
4	High	2 lb	6.51	0.81	9	High	2 lb	11.10	1.05
4	High	4 lb	10.94	1.04	9	High	4 lb	20.76	1.32
4	High	6 lb	20.18	1.30	9	High	6 lb	23.59	1.37
5	Low	2 lb	14.76	1.17	10	Low	2 lb	4.23	0.63
5	Low	4 lb	14.54	1.16	10	Low	4 lb	9.27	0.97

Subject	Task	Weight	Percent change in global fatigue index	Transformed data	Subject	Task	Weight	Percent change in global fatigue index	Transformed data
5	Low	6 lb	18.13	1.26	10	Low	6 lb	15.95	1.20
5	Medium	2 lb	14.53	1.16	10	Medium	2 lb	8.43	0.93
5	Medium	4 lb	18.83	1.27	10	Medium	4 lb	10.31	1.01
5	Medium	6 lb	26.41	1.42	10	Medium	6 lb	13.05	1.12
5	High	2 lb	28.14	1.45	10	High	2 lb	8.25	0.92
5	High	4 lb	35.40	1.55	10	High	4 lb	10.67	1.03
5	High	6 lb	46.83	1.67	10	High	6 lb	15.28	1.18

Appendix I1: Log Transformed Data of Perceived Exertion Score Data.

Table 28: Log transformed data of percent change in global fatigue index for all participants.

Subject	Task	Weight	Discomfort data	Transformed data	Subject	Task	Weight	Discomfort data	Transformed data
1	Low	2 lb	2.00	1.41	6	Low	2 lb	1.00	1.00
1	Low	4 lb	3.67	1.91	6	Low	4 lb	2.33	1.53
1	Low	6 lb	5.67	2.38	6	Low	6 lb	3.00	1.73
1	Medium	2 lb	2.00	1.41	6	Medium	2 lb	1.33	1.15
1	Medium	4 lb	4.00	2.00	6	Medium	4 lb	3.00	1.73
1	Medium	6 lb	6.67	2.58	6	Medium	6 lb	4.00	2.00
1	High	2 lb	2.67	1.63	6	High	2 lb	1.67	1.29
1	High	4 lb	5.33	2.31	6	High	4 lb	4.00	2.00
1	High	6 lb	7.00	2.65	6	High	6 lb	5.67	2.38

Subject	Task	Weight	Discomfort data	Transformed data	Subject	Task	Weight	Discomfort data	Transformed data
2	Low	2 lb	1.00	1.00	7	Low	2 lb	0.67	0.82
2	Low	4 lb	1.67	1.29	7	Low	4 lb	0.83	0.91
2	Low	6 lb	1.83	1.35	7	Low	6 lb	1.00	1.00
2	Medium	2 lb	2.00	1.41	7	Medium	2 lb	0.67	0.82
2	Medium	4 lb	3.00	1.73	7	Medium	4 lb	1.00	1.00
2	Medium	6 lb	3.33	1.83	7	Medium	6 lb	1.33	1.15
2	High	2 lb	2.33	1.53	7	High	2 lb	0.83	0.91
2	High	4 lb	4.00	2.00	7	High	4 lb	1.67	1.29
2	High	6 lb	5.67	2.38	7	High	6 lb	1.67	1.29
3	Low	2 lb	2.00	1.41	8	Low	2 lb	0.33	0.58
3	Low	4 lb	3.00	1.73	8	Low	4 lb	1.67	1.29
3	Low	6 lb	3.67	1.91	8	Low	6 lb	2.67	1.63
3	Medium	2 lb	2.00	1.41	8	Medium	2 lb	0.33	0.58
3	Medium	4 lb	3.33	1.83	8	Medium	4 lb	2.00	1.41
3	Medium	6 lb	5.00	2.24	8	Medium	6 lb	3.00	1.73
3	High	2 lb	3.33	1.83	8	High	2 lb	1.00	1.00
3	High	4 lb	5.00	2.24	8	High	4 lb	3.33	1.83
3	High	6 lb	8.33	2.89	8	High	6 lb	5.00	2.24
4	Low	2 lb	2.33	1.53	9	Low	2 lb	0.67	0.82
4	Low	4 lb	2.00	1.41	9	Low	4 lb	1.00	1.00
4	Low	6 lb	3.33	1.83	9	Low	6 lb	2.67	1.63
4	Medium	2 lb	2.33	1.53	9	Medium	2 lb	0.67	0.82

Subject	Task	Weight	Discomfort data	Transformed data	Subject	Task	Weight	Discomfort data	Transformed data
4	Medium	4 lb	3.00	1.73	9	Medium	4 lb	2.00	1.41
4	Medium	6 lb	3.00	1.73	9	Medium	6 lb	3.67	1.91
4	High	2 lb	2.00	1.41	9	High	2 lb	1.00	1.00
4	High	4 lb	3.33	1.83	9	High	4 lb	2.67	1.63
4	High	6 lb	5.00	2.24	9	High	6 lb	3.33	1.83
5	Low	2 lb	3.00	1.73	10	Low	2 lb	0.33	0.58
5	Low	4 lb	3.67	1.91	10	Low	4 lb	1.67	1.29
5	Low	6 lb	5.00	2.24	10	Low	6 lb	2.67	1.63
5	Medium	2 lb	2.67	1.63	10	Medium	2 lb	0.33	0.58
5	Medium	4 lb	3.67	1.91	10	Medium	4 lb	2.00	1.41
5	Medium	6 lb	5.67	2.38	10	Medium	6 lb	3.00	1.73
5	High	2 lb	3.67	1.91	10	High	2 lb	1.00	1.00
5	High	4 lb	6.00	2.45	10	High	4 lb	3.33	1.83
5	High	6 lb	8.00	2.83	10	High	6 lb	5.00	2.24

Appendix J: Normality Test Results

Table 29: Normality test results for percent changes in global fatigue index.

Test	Statistic		p-Value	
Shapiro-Wilk	W	0.981	Pr < W	0.220
Kolmogorov-Smirnov	D	0.076	Pr > D	>0.150
Cramer-von Mises	W-Sq	0.054	Pr > W-Sq	>0.250
Anderson-Darling	A-Sq	0.386	Pr > A-Sq	>0.250

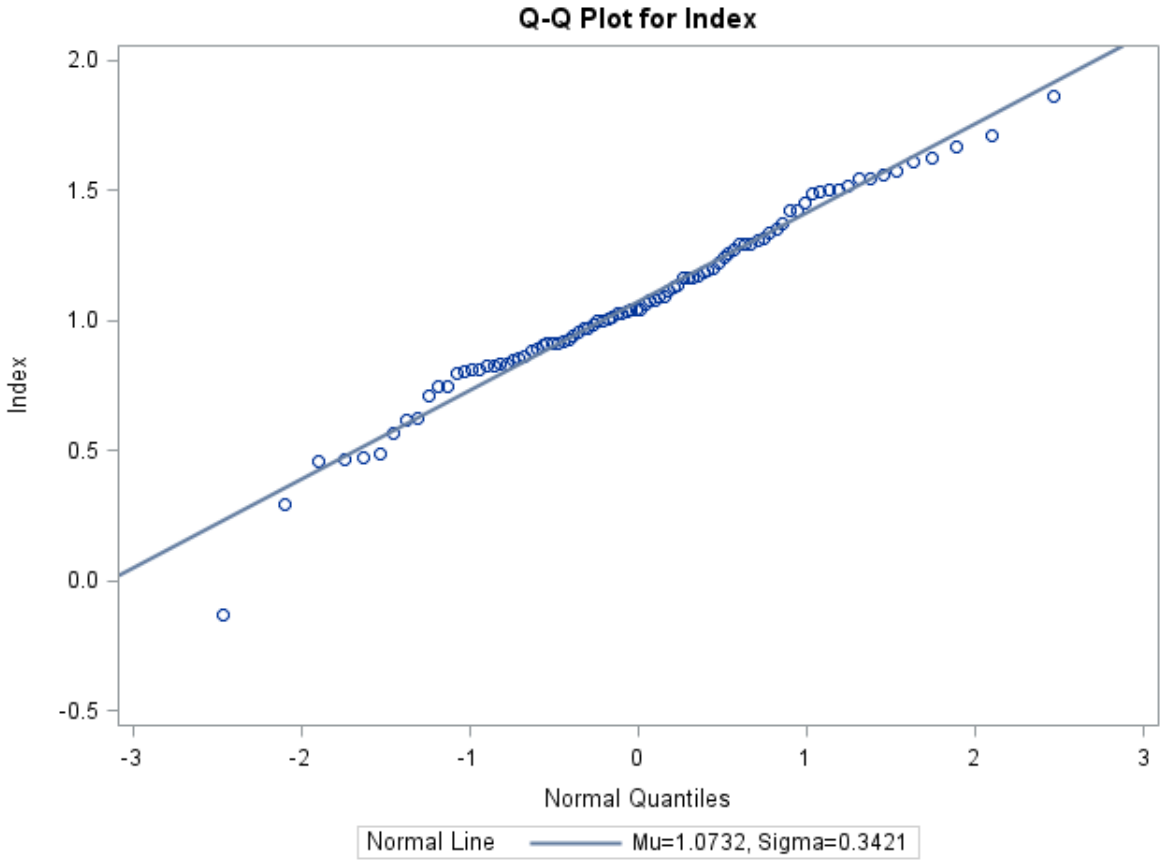

Figure 27: Q-Q plot for the normality test for percent change in global fatigue index in Aim 3.

Table 30: Normality test results for the perceived exertion data.

Test	Statistic		p-Value	
Shapiro-Wilk	W	0.982	Pr < W	0.264
Kolmogorov-Smirnov	D	0.076	Pr > D	>0.150
Cramer-von Mises	W-Sq	0.072	Pr > W-Sq	>0.250
Anderson-Darling	A-Sq	0.466	Pr > A-Sq	>0.250

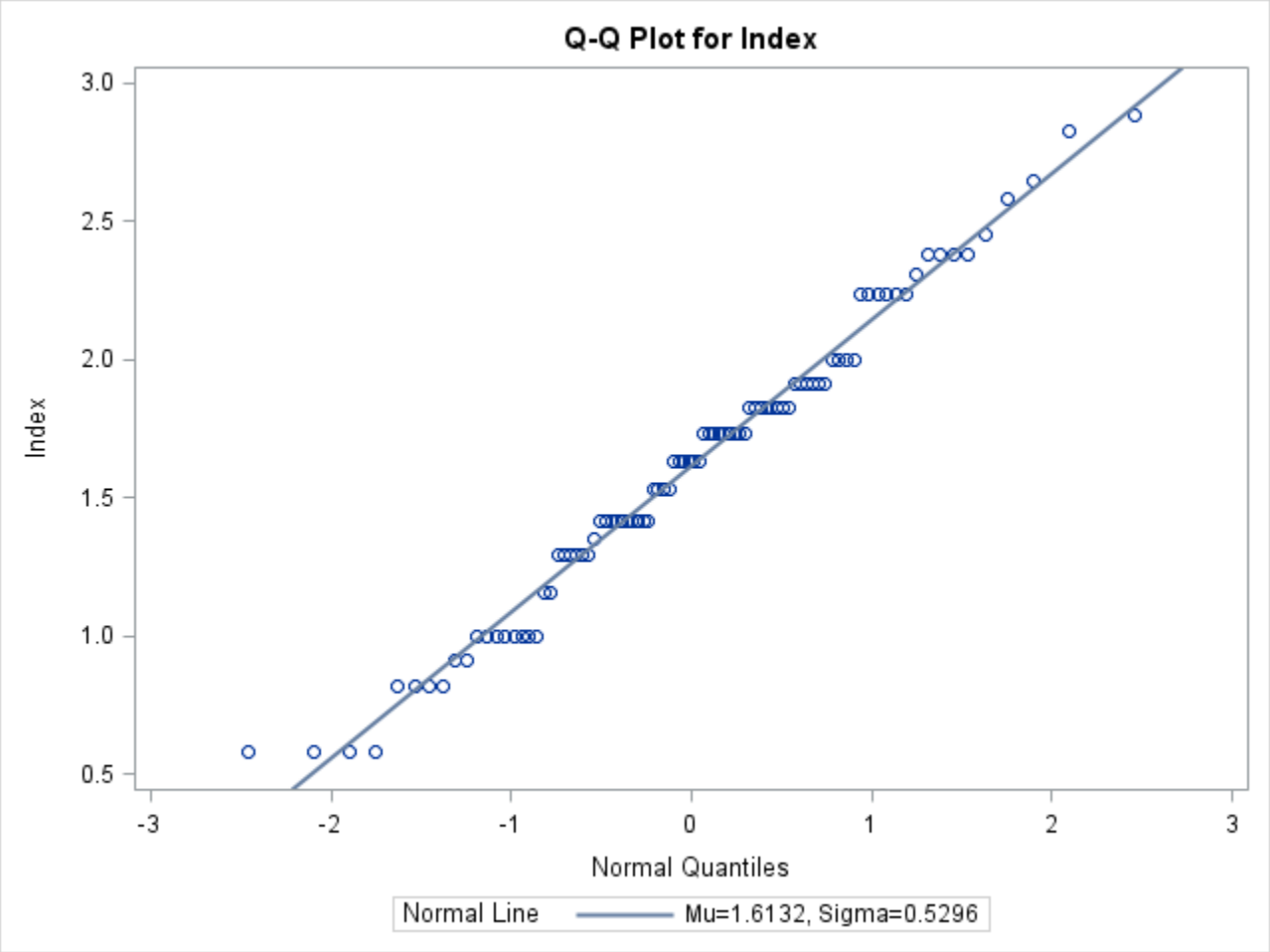

Figure 28: Q-Q plot for the normality test for perceived discomfort data in Aim 3.

Appendix K: Equality of Variance Tests

Table 31: Levene's test for homogeneity of index variance for percent changes in global fatigue index data.

Source	Degrees of freedom	Sum of Squares	Mean Square	F Value	P - value
Weight	2	0.1047	0.0524	1.54	0.221
Error	87	2.9657	0.0341		

Table 32: Levene's test for homogeneity of index variance for perceived exertion data.

Source	Degrees of freedom	Sum of Squares	Mean Square	F Value	P - value
Task	2	0.00189	0.000946	1.94	0.1495
Error	87	0.0424	0.000487		

Appendix L: Individual Demographic and Physical Measurement Data for Aim 3.

Table 33: Individual demographic and physical measurement data for Aim 3.

	Age	Weight	Height	Tronchanterion	Elbow	Mid upper arm	Shoulder
Subject 1	30	140	69	35	43	50.5	58
Subject 2	32	166	71	38	45	52	59
Subject 3	34	183	71	37.5	45	52.5	60
Subject 4	24	158	70	39	44	51.5	59
Subject 5	30	180	70	39.5	45	51.75	58.5
Subject 6	25	153	68	40	43	50.75	58.5
Subject 7	26	188	67	36.5	40.5	47.75	55
Subject 8	27	153	68	39.5	45	51.25	57.5
Subject 9	26	170	70	40	44.5	57.5	51
Subject 10	23	168	65	38	42	47.5	53

Appendix M: Percent Change in Global Fatigue Index Data of All Participants

Table 34: Percent change in global fatigue index data of subject 1.

			Subjects									
Task	Weight	Repetition	1	2	3	4	5	6	7	8	9	10
Low	2 lb	1	-0.96	-2.38	13.18	3.62	20.20	7.35	9.28	-5.07	15.13	4.36
Low	2 lb	2	-0.34	5.75	-0.93	9.53	13.73	3.85	-1.33	16.33	10.90	5.51
Low	2 lb	3	10.04	24.64	8.08	6.90	10.34	11.64	10.85	-0.12	6.02	2.81
Low	4 lb	1	17.74	14.86	-0.52	8.88	17.49	23.43	8.68	-4.67	8.59	8.88
Low	4 lb	2	-4.93	4.21	1.38	10.07	18.14	-5.07	6.39	-0.63	4.39	3.17
Low	4 lb	3	4.04	5.22	5.09	2.54	7.99	17.52	13.71	14.23	11.45	15.75
Low	6 lb	1	2.74	6.50	33.01	19.38	23.87	43.51	3.12	17.50	8.18	19.38
Low	6 lb	2	2.16	-3.11	4.02	-8.75	20.03	20.49	8.99	2.17	5.41	19.66
Low	6 lb	3	4.36	22.97	-0.07	19.37	10.48	28.98	18.48	30.34	-1.27	8.80
Medium	2 lb	1	15.62	11.25	-4.64	12.76	22.72	16.44	6.19	3.52	6.76	6.63
Medium	2 lb	2	2.34	18.15	11.16	3.52	6.82	10.60	-6.76	11.96	0.10	6.78
Medium	2 lb	3	-1.09	5.42	2.09	3.17	14.05	5.98	22.34	9.07	13.42	11.88
Medium	4 lb	1	18.70	11.39	8.21	-11.30	6.13	28.46	9.93	-4.57	-1.89	14.21

			Subjects									
Task	Weight	Repetition	1	2	3	4	5	6	7	8	9	10
Medium	4 lb	2	24.92	38.46	19.47	5.94	22.60	52.02	37.23	14.26	22.97	2.98
Medium	4 lb	3	3.01	15.23	-4.44	7.59	27.77	31.98	12.10	17.49	0.00	13.73
Medium	6 lb	1	12.92	45.69	14.68	9.92	28.72	68.07	26.23	30.13	31.75	10.80
Medium	6 lb	2	13.24	24.70	5.60	1.28	17.37	49.76	25.02	21.56	33.96	15.90
Medium	6 lb	3	-1.52	9.01	-0.32	7.93	33.14	35.76	1.57	7.11	30.50	12.47
High	2 lb	1	8.05	13.05	3.17	2.24	23.01	20.87	4.70	15.69	10.96	11.51
High	2 lb	2	9.10	27.74	15.45	12.11	29.58	34.75	22.79	8.21	19.01	3.25
High	2 lb	3	-1.77	-3.40	11.46	5.18	31.82	39.51	16.38	8.55	3.33	9.99
High	4 lb	1	13.01	36.04	13.07	19.06	45.43	40.68	22.28	20.21	15.78	8.22
High	4 lb	2	6.69	34.33	18.27	18.84	29.58	57.31	14.44	39.69	40.80	8.56
High	4 lb	3	20.96	28.94	9.35	-5.09	31.18	28.63	22.34	33.66	5.71	15.23
High	6 lb	1	1.19	37.15	8.16	18.65	50.32	78.90	33.45	30.06	31.83	17.48
High	6 lb	2	47.71	30.44	7.90	17.69	30.54	47.43	49.03	25.31	18.95	11.35
High	6 lb	3	17.96	55.15	19.79	24.18	59.62	93.00	23.13	53.78	20.00	17.01

Appendix N: SAS Output for Percent Change in Global Fatigue Index in Aim 3

Dependent Variable: Index

Source	DF	Sum of Squares	Mean Square	F Value	Pr > F
Model	17	7.35681584	0.43275387	10.18	<.0001
Error	72	3.06121267	0.04251684		
Corrected Total	89	10.41802850			

R-Square	Coeff Var	Root MSE	Index Mean
0.706162	19.21240	0.206196	1.073245

Source	DF	Type I SS	Mean Square	Expected Mean Square	F Value	Pr > F
Block	9	3.4795	0.3866	0.3866	9.093	<.0001
Task	2	2.2566	1.1283	1.171	27.538	<.0001
Weight	2	1.4841	0.7420	0.785	18.453	<.0001
Task*Weight	4	0.1366	0.0341	0.077	1.803	0.1376

Least Squares Means for effect Task
Pr > |t| for H0: LSMean(i)=LSMean(j)
Dependent Variable: Index

i/j	1	2	3
1		0.0067	<.0001
2	0.0067		<.0001
3	<.0001	<.0001	

Least Squares Means for effect Weight
Pr > |t| for H0: LSMean(i)=LSMean(j)
Dependent Variable: Index

i/j	1	2	3
1		0.0133	<.0001
2	0.0133		0.0013
3	<.0001	0.0013	

Source	Type III Expected Mean Square
Block	$\sigma^2 + 9\ \sigma^2_{block}$
Task	$\sigma^2 + 3*10*\emptyset_{task}$
Weight	$\sigma^2 + 3*10*\emptyset_{weight}$
Task*Weight	$\sigma^2 + 10*\emptyset_{task*weight}$

Appendix O: Individual Perceived Exertion Data

Table 35: Perceived exertion data of all tasks for all participants.

			Subjects									
Task	Weight	Repetition	1	2	3	4	5	6	7	8	9	10
Low	2 lb	1	2	1	3	3	3	1	0.5	1	0	2
Low	2 lb	2	2	1	2	2	3	1	0.5	0	1	1
Low	2 lb	3	2	1	1	2	3	1	1	0	1	2
Low	4 lb	1	3	2	3	2	4	2	0.5	1	1	3
Low	4 lb	2	4	1	4	2	3	2	1	2	1	1
Low	4 lb	3	4	2	2	2	4	3	1	2	1	2
Low	6 lb	1	5	2	3	4	4	3	1	3	3	5
Low	6 lb	2	6	0.5	4	2	6	3	1	2	2	0.5
Low	6 lb	3	6	3	4	4	5	3	1	3	3	4
Medium	2 lb	1	1	2	3	3	3	1	0.5	0	1	1
Medium	2 lb	2	3	2	2	2	3	2	0.5	1	1	2
Medium	2 lb	3	2	2	1	2	2	1	1	0	0	2
Medium	4 lb	1	3	3	4	3	3	3	1	2	2	3

			Subjects									
Task	Weight	Repetition	1	2	3	4	5	6	7	8	9	10
Medium	4 lb	2	5	3	4	3	4	3	1	2	3	3
Medium	4 lb	3	4	3	2	3	4	3	1	2	1	3
Medium	6 lb	1	6	4	5	3	6	5	2	3	5	6
Medium	6 lb	2	7	3	5	3	5	4	1	3	2	3
Medium	6 lb	3	7	3	5	3	6	3	1	3	4	3
High	2 lb	1	2	3	3	2	3	2	0.5	1	1	2
High	2 lb	2	4	3	3	2	4	1	1	1	1	3
High	2 lb	3	2	1	4	2	4	2	1	1	1	2
High	4 lb	1	5	4	5	4	6	5	2	3	2	5
High	4 lb	2	5	4	5	4	6	4	2	4	3	4
High	4 lb	3	6	4	5	2	6	3	1	3	3	4
High	6 lb	1	7	5	8	6	8	5	2	5	4	7
High	6 lb	2	7	5	8	4	8	5	2	4	4	5
High	6 lb	3	7	7	9	5	8	7	1	6	2	4

Appendix P: SAS Output for Perceived Exertion Score Data in Aim 3

Dependent Variable: Perceived Exertion Data

Source	DF	Sum of Squares	Mean Square	F Value	Pr > F
Model	17	22.72444990	1.33673235	26.177	<.0001
Error	72	3.67674912	0.051066		
Corrected Total	89	26.401199			

R-Square	Coeff Var	Root MSE	Index Mean
0.8607	10.92610	0.176255	1.613159

Source	DF	Type I SS	Mean Square	Expected Mean Square	F Value	Pr > F
Block	9	9.7947	1.0883	1.0883	21.312	<.0001
Task	2	3.0974	1.5487	1.600	31.327	<.0001
Weight	2	9.5793	4.7897	4.841	94.794	<.0001
Task*Weight	4	0.2530	0.0633	0.114	2.239	0.0732

Least Squares Means for effect Task Pr > |t| for H0: LSMean(i)=LSMean(j) Dependent Variable: Index			
i/j	1	2	3
1		0.0023	<.0001
2	0.0023		<.0001
3	<.0001	<.0001	

Least Squares Means for effect Weight Pr > |t| for H0: LSMean(i)=LSMean(j) Dependent Variable: Index			
i/j	1	2	3
1		<.0001	<.0001
2	<.0001		<.0001
3	<.0001	<.0001	

Source	Type III Expected Mean Square
Block	$\sigma^2 + 9\ \sigma^2_{block}$
Task	$\sigma^2 + 3*10*\emptyset_{task}$
Weight	$\sigma^2 + 3*10*\emptyset_{weight}$
Task*Weight	$\sigma^2 + 10*\emptyset_{task*weight}$

CURRICULUM VITAE

EDUCATION

PhD in Industrial Engineering — Aug 2016

Area of specialization: Occupational biomechanics and ergonomics

West Virginia University, Morgantown, WV

- **Dissertation:** "*Evaluation of concavity compression mechanism to predict shoulder muscle fatigue during repetitive dynamic exertions*"
- **Advisor:** Professor Ashish Nimbarte

MS in Industrial Engineering — May 2012

West Virginia University, Morgantown, WV

BS in Industrial Engineering — Nov 2006

Bangladesh University of Engineering and Technology, Dhaka, Bangladesh

AWARDS AND HONORS

- *2015 student scholarship award*, 27th Annual International Occupational Ergonomics and Safety Conference, Nashville, Tennessee, USA. — Jun 2015
- *Robert E. Stitzel graduate student travel* fund award, West Virginia University — Oct 2012
- Membership of *Alpha Phi Mu*, West Virginia University — Oct 2010
- *Dean's list scholarship*, Bangladesh University of Engineering and Technology — 2002 – 2003
- *Technical scholarship*, Bangladesh University of Engineering and Technology — 2002 – 2006

RESEARCH INTERESTS

- Ergonomic designs of preventing work related musculoskeletal injuries
- Laboratory methods, and research methods
- Dynamic aspects of human movement
- Slip, fall, and trip preventions
- Sports and occupational biomechanics

TEACHING INTERESTS

- Ergonomics, biomechanics, and human factors system design
- Safety engineering and industrial hygiene

- Research methods, engineering statistics, and design of experiment
- Manufacturing process, and reliability and safety engineering

JOURNAL PUBLICATIONS

[J10] **S. K. Chowdhury**, A. D. Nimbarte, Hongwei Hsiao, Majid Jaridi, Gopalakrishnan Bhaskaran, & Xiaopeng Ning (Under preparation). "Electromyography based global muscle fatigue index formulation." 2016

[J9] **S. K. Chowdhury** & A. D. Nimbarte. (In review). "The effects of fatigue on the stationarity of the surface Electromyography signals." 2015

[J8] A. D. Nimbarte, **S. K. Chowdhury**, M. Chapman, JA Sivak-Callcott, & C. Moore. (In review). "The effects of loupe angle on head-neck posture and activity of neck muscles." 2015

[J7] **S. K. Chowdhury** & A. D. Nimbarte. "Comparison of Fourier and wavelet analysis for fatigue assessment during repetitive dynamic exertion." *Journal of Electromyography and Kinesiology*. 25(2), p. 205 – 213 **2015**

[J6] K. Cutlip, A. D. Nimbarte, **S. K. Chowdhury**, & M. Jaridi. "Evaluation of shoulder stability during forceful arm exertions." *Industrial and Systems Engineering Review*. 3(1), p. 49-58. **2015**

[J5] **S. K. Chowdhury**, C. Moore, & A. D. Nimbarte. (In press). "Effects of lift-assist device on trunk and shoulder kinematics." To be published in *International Journal of Occupational Safety and Health*. 2014

[J4] A. D. Nimbarte, M. M. Zreiqat, & **S. K. Chowdhury**. "Cervical flexion relaxation response to neck muscle fatigue in males and females." *Journal of Electromyography and Kinesiology*. 24 (6), p. 965-971 2014

[J3] **S. K. Chowdhury**, A. D. Nimbarte, M. Jaridi, & R. C. Creese. "Discrete wavelet transforms analysis of surface electromyography for the fatigue assessment of neck and shoulder muscles." *Journal of Electromyography and Kinesiology*. 23 (5), p. 995-1003. 2013

[J2] A. D. Nimbarte, **S. K. Chowdhury**, & E. D. Cartwright. "Empirical evaluation of neck muscle fatigue generated by healthcare related exertions." *Journal of Safety Science*. 57, p. 100–107. 2013

[J1] L. B. Nabatilan, F. Aghazadeh, A. D. Nimbarte, C.C. Harvey, **S. K. Chowdhury**. "Effect of driving experience on visual behavior and driving performance under different driving conditions." *Cognition, Technology & Work*. 14 (4), p. 355-363 2012

CONFERENCE PUBLICATIONS

[C4] **S. K. Chowdhury** & A. D. Nimbarte. "Electromyography Based Global Muscle Fatigue Index Formulation." Presented at *2016 IIE Annual Conference & Expo*. Anaheim, California. May 2016

[C3] **S. K. Chowdhury**. "Evaluation of concavity compression mechanism as a possible predictor of shoulder muscle fatigue during dynamic exertions." *XXIVth Annual International Occupational Ergonomics and Safety Conference*. Nashville, Tennessee, USA. p. 12-17 Jun 2015

[C2] **S. K. Chowdhury**, A. D. Nimbarte, M. Jaridi, & R. C. Creese. "Assessment of neck and shoulder muscle fatigue using discrete wavelet transforms of surface electromyography." Sep 2012

Proceedings of the Human Factors and Ergonomics Society Annual Meeting. Boston, Massachusetts. 56(1). p.1145-1149.

[C1] A. D. Nimbarte, **S. K. Chowdhury**, & E. D. Cartwright. "Impact of Physical and Psychosocial Demand on the Neck and Shoulder Muscle Fatigue." *XXVIth Annual International Occupational Ergonomics and Safety Conference*. Fort Lauderdale, Florida, USA. p. 31-36 — June 2012

INVITED TALKS

[T2] **S. K. Chowdhury**. "Concavity compression mechanism on shoulder joint stability." *Graduate Seminar Talk*, Department of Industrial and Management System Engineering (IMSE), West Virginia University (WVU). — Mar 2015

[T1] **S. K. Chowdhury**. "Discrete wavelet transforms analysis of surface electromyography." *Graduate Seminar Talk*, Department of Industrial and Management System Engineering (IMSE), West Virginia University (WVU). — Feb 2013

RESEARCH AND TEACHING EXPERIENCES

Graduate Instructor — Spring, 2016
Industrial and Management System Engineering, West Virginia University
Class: Engineering Statistics (IENG 360)

- Instructing the class of 123 students with full responsibilities

Graduate Teaching Assistant — 2012 – 2015
Industrial and Management System Engineering, West Virginia University
Class: Human Factors Engineering (IENG 360)

- Assisted with design and implementation of course materials
- Instructed a set of lectures on Biomechanics and Muscle Physiology in IENG 360 class
- Instructed students on how to properly conduct ergonomics research using motion capture and electromyography systems in graduate level Industrial Ergonomics class

Graduate Research Assistant, Ergonomics lab, West Virginia University — 2009 – 2012
Advisor: Professor Dr. Ashish Nimbarte

- Formulated novel ideas through extensive analysis of the existing research and conducted numerous research experiments in a professional manner

PROFESSIONAL EXPERIENCES

Research Analyst, Maxwell Stamp Ltd, Bangladesh — 2009

- Audited small and medium scaled bricks, engineering, and garments industries
- Analyzed data to find the major factors which contributed to low productivity

Senior Executive, Apex Holding Ltd., Bangladesh — 2008

- Scheduled raw materials, work-in-progress, and finished goods
- Introduced lean manufacturing strategies to reduce different types of wastes

Industrial Engineer, Alhaj Group, Bangladesh 2006 – 2007

- Applied 'quality function deployment' technique to design a new jute bag
- Assisted the layout design team with designing plant layout of a new Jute mill

SERVICES TO PROFESSION

- *Reviewer* of Journal of Safety Science 2013 – 2015
- *Reviewer* of IIE Annual Conference 2015 – 2016
- *Speaker and evaluator* of Mountaineer Toastmaster club # 8538 2015
- *Mentoring* Undergraduate and Master's students at
  - West Virginia University, Morgantown, WV, USA 2012 – 2015
  - Bangladesh University of Engineering and Technology, Bangladesh 2003 – 2006
- *Assistant publication secretary* 2005 – 2006
  - An annual periodical publication containing articles illustrating applications of industrial engineering techniques in both service and manufacturing industries.
- *Editorial secretary* 2005
  - First editorial secretary of 'Antasalila' – a campus based Bengali magazine at Bangladesh University of Engineering and Technology, Bangladesh.

VOLUNTEERING ACTIVITIES

- Attained leadership experience by training new research team members voluntarily in Ergonomics lab at West Virginia University 2010 – 2015
- Assisted new graduate students by providing directions in the campus, and moving into their residences at West Virginia University 2011 - 2015
- Event coordinator of Industrial and Production Engineering Symposiums at Bangladesh University of Engineering and Technology 2005 – 2006

AFFILIATIONS

- Member of Human Factors and Ergonomics Society, USA 2012 – present
- Member of Institute of Industrial Engineers (IIE), WVU chapter – USA 2012 – present
- Member of Toastmaster, Mountaineer Toastmaster club # 8538 2015 - present